

GASTROINTESTINAL MOLECULAR IMAGING

A TECHNOLOGISTS' GUIDE

Produced with the kind support of

SIEMENS
Healthineers 

Table of contents

	Foreword	4
	Agata Pietrzak	
	Introduction	6
	Andrea Santos, Luísa Roldão Pereira, Paolo Turco	
Chapter 1	Anatomy, physiology and pathology of the gastrointestinal tract	8
	Erik Rosa-Rizzotto, Diego Caroli, Alessandro Gubbiotti	
Chapter 2	Radiopharmaceuticals for gastrointestinal imaging	28
	Lurdes Gano, Célia Fernandes, António Paulo	
Chapter 3	Salivary gland studies	40
	Carolina Sousa, Ana Geão, Pedro Quaresma	
Chapter 4	Gastrointestinal motility studies	58
	Maryam Jessop	
Chapter 5	Gastrointestinal bleeding and ectopic gastric mucosa	72
	Gracinda Costa, Raquel Silva	
Chapter 6	Hepatobiliary and spleen studies	96
	David Gilmore, Krystle Glasgow, Daniel Tempesta	
Chapter 7	Bile acid malabsorption study	108
	Daniela Teixeira, Raquel Martins	
Chapter 8	Scintigraphy of gastro-oesophageal reflux, pulmonary aspiration and Gastric emptying in children	126
	Zvi Bar-Sever, Laura Drubach	
Chapter 9	Oncological studies (SPECT & PET)	158
	Raquel Massa, Prakash Manoharan	
	Imprint	186

Foreword

Nuclear Medicine (NM) is one of the most rapidly developing disciplines in medicine, science and technology, with multiple advances made each year. These recent developments are indeed fascinating, but the state of the art in existing NM procedures and their performance also deserves detailed discussion. The EANM Technologists Committee (TC) produces an annual edition of the *Technologists' Guide*, providing comprehensive content centred around a specific area of NM interest. This year, the focus of the publication is on *Gastrointestinal Molecular Imaging*.

Molecular imaging of the gastrointestinal (GI) tract deserves special attention due to its significance in detecting and monitoring various GI tract diseases. From salivary gland dysfunctions and ectopic gastric mucosa to hepatobiliary tract studies and GI tract cancer: each of these illnesses can be studied using the molecular imaging techniques of Nuclear Medicine. The crucial element of successful diagnostic management is choosing the appropriate procedure,

specifying the radiopharmaceutical, and – last but not least – defining the characteristics of accurate acquisition protocols. GI molecular imaging calls for a careful and precise approach as well as extensive efforts on the part of the multidisciplinary medical team. Although the clinical standards, guidelines and recommendations pertaining to molecular imaging vary from country to country, the role of Nuclear Medicine Technologists (NMT) remains

constant and relevant across the world. The role of NMTs as study designers and equipment operators is vital to the final outcome. Nevertheless, molecular imaging of the GI tract requires a particular and highly complex set of professional skills, knowledge, and experience that we focus on in this year's edition of the *Technologists' Guide*.

A number of experienced professionals have contributed to this publication, sharing their knowledge and experience of gastrointestinal molecular imaging with readers of the *Technologists' Guide*. I would like to thank all the authors most sincerely for the precious time and effort they have invested in this crucial work on behalf of the *Technologists' Guide* project.

My gratitude also goes to the EANM Committees and their representatives who have actively participated in drafting and reviewing the content of the chapters, as well as to our Society of Nuclear Medicine and Molecular Imaging – Technologists Section

(SNMMI – TS) friends who have been supporting this project for many years now.

I also wish to express my great appreciation to the TC members Andrea Santos (editor-in-chief), Luisa Roldão Pereira and Paolo Turco (co-editors) for the great efforts they have put into this work, and congratulate them on the outstanding result.

A big “thank you” to the EANM office representatives, Sophie Karsai & Núria Serra, for their precious, constant support along the way. And thank you, Angela Parker, for your extensive efforts in the process of language revision.

Finally, I would like to sincerely thank the Technologists Committee and the EANM Board for your help and involvement, and for recognising and acknowledging the importance of the *Technologists' Guide* since the very beginning of the project.

Agata Pietrzak
Chair, EANM Technologists Committee

Introduction

Since the earliest days of the discipline, the study of digestive disorders has historically been a very relevant area of study from the nuclear medicine point of view. The ability to visualise and characterise the varied physiological processes of the gastrointestinal systems without resorting to invasive methods makes nuclear medicine an effective and comparatively easy-to-perform method for evaluating these types of diseases.

The evolution of radiopharmacy and the available molecules, further development of the labelling processes and the routine application of these radiopharmaceuticals has enabled the study of the annexes of the digestive tract, which has also given increased importance to these nuclear medicine procedures.

Gastrointestinal molecular imaging studies have been performed for a long

time now, and their applicability varies according to the different needs of different populations across the globe. To this end, a wide variety of protocols have been developed and harmonisation is a major challenge in this area. Meal composition, imaging protocols, standardisation of results and many other specific challenges arise when these procedures are applied in the clinical setting.

With this in mind, this book provides a summary of the most-performed procedures in molecular gastrointestinal imaging, starting with basic anatomy and physiology and an overview of the available molecules in the radiopharmacy toolkit before going on to discuss a number of the procedures available. The various chapters have been written by authors with a wealth of knowledge and practical expertise in each of the covered topics, who outline the individual procedures together with their applications, the suggested protocols and the expected outcomes.

Last but not least, this edition of the Technologists' Guide provides an overview of gastrointestinal molecular imaging

procedures which have seen growing relevance in recent years. The growth of theranostics has resulted in an increased need to assess the function of some of the digestive organs, such as the liver or the salivary glands.

The editorial team thanks all the authors for their willingness to collaborate and hopes that this book will be useful, both as a guide for those learning how to perform these procedures and as a vehicle for dissemination of best practice in our field.

Andrea Santos, Luísa Roldão Pereira and Paolo Turco
The editorial team

ANATOMY, PHYSIOLOGY AND PATHOLOGY OF THE GASTROINTESTINAL TRACT

*by Erik Rosa-Rizzotto¹
Diego Caroli²
Alessandro Gubbiotti*

*¹Responsible of the Gastroenterology and Digestive Endoscopy Unit,
Azienda Hospital S. Antonio Padova University, Italy*

²Gastroenterology Unit, Azienda Hospital S. Antonio Padova University, Italy

INTRODUCTION

The digestive tract, also called the alimentary canal or gastrointestinal (GI) tract, consists of a long continuous tube that extends from the mouth to the anus. It is composed of the oral cavity, pharynx, oesophagus, stomach, small intestine, and large intestine. The accessory organs are the teeth, tongue, and glandular organs such as salivary glands, liver, gallbladder, and pancreas. The primary purpose of the gastrointestinal tract is to break food down into nutrients which can be absorbed by the body. First, food must be ingested into the mouth to be mechanically processed and moistened. Secondly, digestion occurs mainly in the stomach and small intestine where proteins, fats and carbohydrates are chemically broken down into their basic building blocks. Smaller molecules are then absorbed across the epithelium of the small intestine and subsequently enter the circulation. The large intestine plays a key role in reabsorbing excess water. Finally, undigested material and secreted waste products are excreted from the body via defecation (passing of faeces).

ANATOMY OF THE GASTROINTESTINAL TRACT

The salivary glands

The salivary glands make saliva and empty it into the mouth through openings called ducts. Saliva helps with swallowing and chewing. It can also help prevent

infections from developing in your mouth or throat. There are two types of salivary glands: the major salivary glands and the minor salivary glands.

The major salivary glands are the largest and most important salivary glands. They produce most of the saliva. There are three pairs of major salivary glands: the parotid glands, the submandibular glands, and the sublingual glands.

The parotid glands are the largest salivary glands. They are located just in front of the ears. The saliva produced in these glands is secreted into the mouth from a duct near your upper second molar. About the size of a walnut, the submandibular glands are located below the jaw. The saliva produced in these glands is secreted into the mouth from under the tongue. The sublingual glands are the smallest of the major salivary glands. These almond-shaped structures are located under the floor of the mouth and below either side of the tongue.

There are hundreds of minor salivary glands throughout the mouth and the aerodigestive tract. Unlike the major salivary glands, these glands are too small to be seen without a microscope. Most are found in the lining of the lips, the tongue, and the roof of the mouth, as well as inside the cheeks, nose, sinuses, and larynx.

The oesophagus

The oesophagus acts as a conduit for the transport of food from the oral cavity to the stomach. To carry out this task safely and effectively, the oesophagus is constructed as an 18 to 26 cm long hollow muscular tube with an inner „skin-like“ lining of stratified squamous epithelium. Structurally, the oesophageal wall is composed of 4 layers: innermost mucosa, submucosa, muscularis propria, and outermost adventitia; unlike the remainder of the GI tract, the oesophagus has no serosa [1,2]. The muscularis propria is responsible for the organ's motor function. The upper 5% to 33% is composed exclusively of skeletal muscle, while the distal 50% is composed of smooth muscle [3]. In between is a mixture of both types. The oesophageal wall is innervated by parasympathetic and sympathetic nerves; the parasympathetic nerves regulate peristalsis via the vagus nerve.

The stomach

The stomach, as a J-shaped dilation of the alimentary canal, is continuous with the oesophagus proximally and the duodenum distally. It functions primarily as a reservoir to store large quantities of recently ingested food, thus allowing intermittent feedings, initiating the digestive process, and releasing its contents in a controlled fashion downstream to accommodate the much smaller capacity of the duodenum. The stomach is divided into 4 regions that can be defined by anatomical or

histological landmarks [2]. In anatomical terms, the cardia is a small ill-defined area of the stomach immediately adjacent to its junction with the oesophagus. This region of the stomach has been the focus of intense investigation. Controversy exists as to the nature, location, extent, and indeed existence of cardiac mucosa. The fundus projects upward, above the cardia and the oesophagogastric junction. This dome-shaped area of the stomach is its most superior portion and is in contact above with the left hemidiaphragm and to the left with the spleen. The body, or corpus, the largest portion of the stomach, is located immediately below and continuous with the fundus. The incisura angularis, a fixed, sharp indentation two-thirds of the distance down the lesser curvature, marks the caudal aspect of the gastric body. The gastric antrum extends from its indistinct border with the body to the junction of the pylorus with the duodenum. The pylorus (pyloric channel) is a tubular structure joining the duodenum to the stomach and contains the palpable circular muscle, the pyloric sphincter. The luminal surface of the gastric wall forms thick, longitudinally oriented folds, or rugae, that flatten with distention. Four layers make up the gastric wall: mucosa, submucosa, muscularis propria, and serosa. The autonomic innervation of the stomach stems from the sympathetic and parasympathetic nervous systems, delivered via a complex tangle of nerves running along the visceral arteries.

The pancreas

The pancreas is a soft, elongated, flattened gland that is 12 to 20 cm in length [4]. The adult gland weighs between 70 and 110 g. The head lies behind the peritoneum of the posterior abdominal wall and has a lobular structure. The pancreas is covered with fine connective tissue, but it does not form a true capsule. The head of the pancreas is on the right side and lies within the curvature of the duodenum. The neck, body, and tail of the pancreas lie obliquely in the posterior abdomen, with the tail extending as far as the gastric surface of the spleen. The main pancreatic duct (of Wirsung) begins near the tail of the pancreas. It is formed from anastomosing ductules draining the lobules of the gland. It extends from left to right and is enlarged by additional ducts. The main duct turns caudal and posterior on reaching the head of the pancreas. At the level of the major papilla, the duct turns horizontally to join in most cases with the bile duct. This short common segment is the ampulla of the bile duct, which terminates at the duodenal papilla.

The liver

Traditionally, 4 lobes are distinguished in the liver based on its external appearance: right, left, caudate, and quadrate. On the anterior surface, the falciform ligament divides the liver into the right and left anatomical lobes. The true right and left lobes of the liver are of roughly equal size and

are divided not by the falciform ligament, but by a plane passing through the bed of the gallbladder and the notch of the inferior vena cava. This plane, which has no external indications, is called the Cantlie line [5,7]. Several systems of subdivision have been proposed, but the most widely used systems are those of Couinaud, which follows the distribution of the portal and hepatic veins [8], and Healey and Schroy, which is based on the distribution of bile ducts [10]. In these systems, the subsegments are assigned numbers from 1 to 8, with the caudate lobe being subsegment 1 and the others following in a clockwise pattern [7]. The liver receives approximately 70% of its blood supply and 40% of its oxygen from the portal vein and 30% of its blood supply and 60% of its oxygen from the hepatic artery. The portal vein is formed from the confluence of the superior mesenteric vein and the splenic vein. At the hilum, the portal vein divides into right and left branches, on which the right and left lobes of the liver are based [6,10]. The extrahepatic biliary tract is composed of the common hepatic duct, cystic duct, gallbladder, and right and left hepatic ducts. The right and left hepatic ducts drain the right and left lobes of the liver, respectively. The fusion of the right and left hepatic ducts gives rise to the common hepatic duct. The caudate lobe usually drains into the origin of the left hepatic duct or into the right hepatic duct. The cystic duct usually drains into the lateral aspect of the common hepatic duct below its origin to form the bile duct [10].

The small bowel

The small intestine is a specialised tubular structure within the abdominal cavity, continuous with the stomach proximally and the colon distally. The small bowel increases in length from about 250 cm in the term newborn to about 600 to 800 cm in the adult. The diameter of the small intestine gradually diminishes from proximal to distal, and there is a 4-fold reduction in surface area from the distal duodenum to the terminal ileum. The duodenum is the most proximal portion of the small intestine. It begins with the duodenal bulb, travels through the retroperitoneal space around the head of the pancreas, and ends on its return to the peritoneal cavity at the ligament of Treitz. The biliary and pancreatic ducts join together 1 to 2 cm from the outer margin of the duodenal wall and drain into the second portion of the duodenum through the ampulla of Vater. In 5% to 10% of individuals, an accessory pancreatic duct, also known as the duct of Santorini, enters 1 to 2 cm proximal to the ampulla of Vater. The luminal surface of the small intestine has visible mucosal folds called the plicae circularis or folds of Kerkring. They are more numerous in the proximal jejunum, decrease in number distally, and are absent in the terminal ileum. The jejunum and ileum are freely mobile in the abdominal cavity and are attached to the posterior abdominal wall by the intestinal mesentery. The entire length of jejunum

and ileum is suspended in this mesentery, except for the distal terminal ileum at the cecum, which is retroperitoneal.

The colon and rectum

The colon is a tubular structure about 30 to 40 cm in length at birth and measuring some 150 cm in the adult, or about one quarter the length of the small intestine. The colon begins at the IC valve and ends distally at the anal verge. It consists of 4 segments: cecum and vermiform appendix, colon (ascending, transverse, and descending portions), rectum, and anal canal. The diameter of the colon is greatest in the cecum (7.5 cm) and narrowest in the sigmoid (2.5 cm) until it balloons in the rectum just proximal to the anal canal. The colon is distinguished from the small intestine by several features. It is larger in diameter, mostly fixed in position, and has outer longitudinal muscle fibres that coalesce into 3 discrete bands called taeniae: the taenia libera, taenia omentalis, and taenia mesocolica.

PHYSIOLOGY OF THE GASTROINTESTINAL TRACT

The physiology of the gastrointestinal (GI) tract is complex, owing to the heterogeneity and large number of organs involved. Its functions range from upper food transit, digestion and absorption to stool formation and delivery, as well as maintaining systemic metabolism homeostasis through both endocrine and exocrine activity.

In addition, well-founded evidence nowadays highlights the role of GI microbiota and the gut-brain axis in human pathophysiology, reinforcing a more recent conception of a unique and integrated system.

Here, we mainly focus on topics relating to nuclear medicine studies. Our overview of GI physiology has been subdivided as follows:

- » GI motility and transit
- » Exocrine and endocrine function
- » Nutrient digestion and absorption

GI MOTILITY AND TRANSIT

Oesophageal motility

Swallowing starts voluntarily but is subsequently an automatic reflex involving the brain stem (vagal swallowing centre) which controls both the striated pharynx muscle and upper third of the oesophageal muscle (via somatic nerves) and the smooth lower two-thirds of the oesophageal muscle (via parasympathetic autonomic nerves).

The progression of the bolus along the oesophagus is aided by gravity, but predominantly guaranteed by a specific propulsive pattern of muscle contractions and relaxations known as peristalsis.

So-called „primary peristalsis“ is triggered by swallowing and consists of a coordinated pressure wave, eventually followed by the lower oesophageal sphincter (LES) opening. „Secondary peristalsis“ may follow the primary pressure wave as a result of activation of enteric nervous system reflexes,

triggered by acid or distension of the smooth muscle portion of the oesophagus. Similarly to the primary wave, it is coordinated with LES relaxation, allowing the clearance of residual bolus.

By contrast, „tertiary peristaltic waves“ are neither propulsive nor coordinated with LES opening, and are consequently pathological.

A proper integration of peristalsis and LES relaxation is therefore mandatory to guarantee motility, the impairment of which leads to motility disorders such as achalasia and esophagogastric junction outflow obstruction (EGJO).

Gastric motility and emptying

From a motility point of view, the stomach can be divided into two functional regions: the first, including the cardia, fundus and proximal part of the organ, mainly acts as a distensible reservoir (receptive relaxation) producing tonic contractions that push the gastric content into the second region, which includes the distal portion of the organ and the antrum, where digestion begins with food trituration. Finally, the pylorus is a sphincter which controls gastric outlet.

Receptive relaxation allows gastric wall relaxation as long as gastric emptying is not concluded, and is triggered by swallowing, stretching of gastric mechanoreceptors, feedback signals from vago-vagal reflexes and chemical mediators such as Ach, NO, VIP, CCK (the latter produced by duodenal

cells), and protein or fat concentration in the duodenum.

Distal phasic contractions are regulated by both parasympathetic and sympathetic systems in response to a meal and external triggers, but strictly depend on gastric intrinsic innervation (enteric nervous system) which communicates with the pacemaker interstitial cells of Cajal. Pacemaker cells are responsible for the basal electrical rhythm (BER), which determines the maximum frequency of contractions, their propagation speed and direction; the cells are located within the circular muscle layer in the stomach, along the greater curvature as well as in the proximal small bowel. The BER differs according to the respective gut segments (3 cycles/minute in the stomach, 12 cycles/minute in the duodenum). It is important to point out that the pacemaker cell activity alone is not sufficient to generate action potential in smooth cells, unless an additional potential is superimposed by the enteric nervous system network.

This peristaltic pattern produces circumferential contractions towards the pylorus, allowing food mixing and grinding together with retrograde propulsion of bigger particles and transit of the smallest ones (up to 1 mm) through the pylorus during its partial and transient openings.

During the fed phase pylorus relaxation is never complete: it is regulated by several factors, such as enteric nervous system and vagal reflexes, chemical signals (NO,

CCK, 5-HT₃ receptors), and the nature and caloric density of food contents. CCK and fatty meals are known to decrease gastric emptying, for instance, while serotonin agonists enhance it.

Besides, emptying of solid food only begins after a lag of 1 h, with a half time of 1–2 h.

Impairment or delay in gastric emptying plays an important role in daily clinical practice, since gastroparesis still represents a huge diagnostic and therapeutic challenge.

During the fasting phase the motility pattern changes, and the migrating motor complex (MMC), which starts in the stomach, gradually propels digested food through the entire length of the GI tract.

Gastric motility is therefore the result of a single integrated response involving different organs and feedback responses, regulated by means of reflexes, receptors, and hormones.

Intestinal motility

Small bowel motility is strictly affected by the eating phase and caloric load, and is regulated by intestinal pacemaker, vagal and enteric reflexes and chemical molecules. During the fed phase, motility patterns are not thought to propel the contents aborally, but rather to retain and mix them in order to enhance exposure to absorptive epithelium and, consequently, ensure proper extraction of nutrients.

These contractions (isolated contractions and segmentation followed by peristaltic

waves) are generally faster in the duodenum and jejunum, ensuring better mixing and propulsion in both directions, then gradually decelerate along the ileum, allowing absorption of less permeable particles, especially lipids.

By contrast, during fasting, once the meal is digested and absorbed, the motility pattern is switched to MMC, a relatively quiescent but still propulsive phase allowing contents to progress to the colon.

Transit through the small bowel takes, on average, 2 hours in adults, and is slowed depending on the caloric load in order to provide for a constant level of absorption.

Colonic motility primarily ensures water absorption, stool processing and elimination; it is independent of MMC and far less associated with meal ingestion. While the proximal segments regulate retention and mixing of the contents by shuttling faecal content back and forth between the haustra, hence allowing water absorption, periodical large propulsive contractions of the distal segments push stools towards the rectum, prompting the urge to defecate and, eventually, stool expulsion. This is coordinated by both the internal and external anal sphincters and is therefore subject to voluntary control.

Transit from the ileocaecal valve and rectum usually takes up to 1–2 days, but differs widely from patient to patient.

EXOCRINE AND ENDOCRINE FUNCTION

General principles

The GI tract accounts for a good part of both endocrine and exocrine function in the human organism.

Exocrine function is mainly performed by hepatocytes, the pancreatic acinar epithelium, the parietal and chief gastric cells and the salivary glands, whereas endocrine function is performed by hepatocytes, the insular pancreatic cells, and gastric and duodenal G and enterochromaffin-like cells (ECL).

As stated above, the liver is responsible for both exocrine (bile synthesis) and endocrine function, as well as playing a predominant role in regulating carbohydrate, lipid and protein homeostasis, ammonia and drug metabolism, and synthesis of coagulation proteins.

The pancreas likewise regulates both functions, with acinar and insular cells, respectively, playing a pivotal role in both nutrient digestion and homeostasis.

Liver and pancreas function and gastric secretions will not be examined further in this chapter. Instead, the main focus will be on the physiology of the salivary glands.

Physiology of the salivary glands

Salivary secretion plays a number of different roles in the GI tract. Not only does it ensure food lubrication (water and mucin) and subsequent formation of a bolus suitable for swallowing; it also represents the first step in food digestion (by means

of enzymes such as amylases), enhances sensibilisation of the taste buds on the tongue, performs a defensive function in the oral cavity (antibacterial substances such as lysozyme, lactoferrin and IgA), and prevents oesophageal injury from acid owing to its slightly alkaline pH and consequent buffer activity on the bolus.

Salivary amylase is not necessary in digestive processes in adults, but it may assume a greater role in neonates, where pancreatic function is immature.

Moreover, the salivary glands are thought to produce several growth factors which might contribute to epithelial damage recovery further along the GI tract.

Finally, saliva contains plenty of inorganic solutes which support tooth formation and maintenance.

At the maximum rate of secretion, the major salivary glands (parotid, sublingual and submandibular) can produce up to 1 ml/min/g of gland tissue, and up to 500 ml/day, requiring a high blood supply.

Salivary gland secretion is regulated by both the parasympathetic (crucial to initiate secretion) and the sympathetic systems, though some hormones can also affect its function, cf. the well-established role of aldosterone in enhancing sodium absorption of the salivary ducts.

Parasympathetic nerves are sited in the salivary nucleus of the medulla, providing input from several higher centres as well as conditioned and pressure reflexes from the oral cavity.

For instance, smell, taste or feelings of nausea enhance salivary secretion, while fatigue, sleep, fear and dehydration usually trigger an inhibiting signal.

Parasympathetic signals are mediated by acetylcholine (ACh)-binding type 3 muscarinic receptors, both stimulating acinar and duct cell activity and enhancing blood supply to the glands by vasodilation.

Sympathetic nerves reach the salivary glands from the superior cervical ganglion and (not being capable of starting and maintaining secretion independently) perform a support role to muscarinic activity through beta-adrenergic receptors on the acinar cells and a biphasic effect on blood flow.

Acinar cells release their proteins and mucus via exocytosis, along with chloride, potassium and sodium ions followed by water (aquaporin 5), so that the primary salivary secretion is isotonic to the plasma. Duct cells modify saliva composition as it passes along their length by reabsorbing sodium and chloride via the CFTR chloride channel. At low rates of secretion, therefore, saliva eventually becomes hypotonic to plasma, as well as slightly alkaline due to bicarbonate secretion.

At high rates of secretion, by contrast, saliva flow is too quick to allow proper ion reabsorption and the saliva remains isotonic.

NUTRIENT DIGESTION AND ABSORPTION

Digestion starts with salivary secretion and continues in the stomach and duodenum, where it is co-adjuvated by specific contraction patterns, as described above, and several molecular signals regulated by a feedback mechanism.

The chief gastric cells of the body release pepsinogen in the gastric lumen. The acid pH of the stomach, controlled by gastrin produced by the endocrine cells, then activates the latter into pepsin, which hydrolyses proteins into smaller molecules.

After being exposed to pepsin, gastric lipase and gastric mixing, the bolus converts into chyme and reaches the duodenum, where it merges with intestinal secretions, pancreatic secretions (lipases, amylases and proteases), and bile. Protein remnants are hydrolysed into amino acids and carbohydrates into mono- and disaccharides, while lipids undergo emulsification, allowing their progressive absorption along the small bowel through both the gut wall and the lymphatic system (chyle).

Through the latter, the so-called chylomicrons reach the liver, where lipoprotein metabolism is completed.

Absorption therefore takes place primarily in the small bowel, and partially in the colon.

The average fluid load in the adult gut is approximately 9 litres, with the majority absorbed in the small bowel in association with ions and nutrients. The colon is more

efficient, however, since it can absorb up to 90% of the presented load.

Transport pathways across gut membranes can be both passive (channels) and active, with the latter requiring energy to overcome an unfavourable concentration gradient (usually supported by an ATPase pump or a different ion gradient with cotransporters). Typical examples of active transport are the SGLT1 Na⁺/glucose transporter and the NH₃ sodium-hydrogen exchanger. The latter is inhibited by cAMP, whose concentration increases during cholera infection, causing massive secretive diarrhoea.

All these processes are regulated by both the enteric nervous system and circulating hormones.

Finally, it is mandatory to mention iron, whose absorption takes place in the duodenum provided that gastric acid reduces Fe³⁺ into Fe²⁺, and vitamin B12, which is absorbed in the distal ileum after binding to intrinsic factor produced by the parietal gastric cells. Absorption of other vitamins varies, depending on whether they are lipophilic (A, D, E, K) or hydrophilic (B and C complex).

PATHOLOGY OF THE GASTROINTESTINAL TRACT

Oesophageal transit

Physiological swallowing causes a peristaltic wave, which propagates in a craniocaudal direction with an intensity that depends on the size and consistency of the swallowed substance. Using radioisotopic techniques, it is possible to quantify oesophageal transit. In the case of pathological processes, such as scleroderma and oesophageal achalasia, a considerable reduction (20–40%) is observed in the amount of tracer that reaches the stomach; moreover, due to the absence of oesophageal peristalsis and the slow relaxation of the lower oesophageal sphincter, a slow arrival in the gastric fundus and a stagnation in the lower middle portions of the oesophagus are noted [19].

Gastro-oesophageal reflux

In subjects with heartburn, regurgitation, bilious vomiting and dysphagia, scintigraphic studies make it easy to determine the presence of gastro-oesophageal reflux caused by the decreased resistance of the lower oesophageal sphincter, and quantify its extent.

Gastric emptying

In the presence of food, the stomach is physiologically traversed by peristaltic waves, which allow the progression of food from the gastric fundus towards the body and the

pylorus. From here, by means of slow and regular contractions, the transfer of the gastric contents takes place in the duodenum, after opening of the pyloric sphincter. The speed of emptying is influenced by numerous factors, including the volume, density, pH and chemical composition of the food ingested. Gastroparesis and vegetative neuropathy are conditions capable of delaying the transit of food from the stomach to the intestine [20].

Gastrointestinal bleeding

If, in subjects presenting with melaena, it is not possible to localise the site of the bleeding in the upper tract of the digestive system (stomach, duodenum) with endoscopy, there is a possibility that the blood loss originates from the small intestine and colon. This eventuality must be assessed by means of a series of instrumental investigations aimed at finding the location and the cause of the leak. The most common causes of intestinal bleeding are diverticula, angiodysplasias, neoplasms, inflammatory diseases and blood loss as a postsurgical complication [21]. The presence of gastric mucosa located extragastrically due to congenital malformation (a remnant of the omphalomesenteric duct, called Meckel's diverticulum) remains silent in the majority of cases; only in about 20% of subjects, and chiefly in adulthood, do symptoms such as abdominal pain and melaena appear. The ectopic gastric mucosa is usually located in the terminal tract of the ileum, approximately 50–60 cm from the ileocaecal valve [4].

Malabsorption

Organic and functional disorders such as so-called irritable bowel syndrome (IBS-D) can cause chronic diarrhoea, which can also be caused by bile acid malabsorption (BAM).

To diagnose this type of malabsorption (BAM), the 75-selenium homocholic acid taurine (SeHCAT) scan can be performed. This is the gold standard in nuclear medicine because it can provide a quantitative assessment. Many studies demonstrate that it can be effective in the clinical workout of chronic diarrhoea caused by different conditions.

The SeHCAT test provides a quantitative assessment to estimate the severity of BAM and the possible response to therapy with bile acid sequestrants (BAS).

However, there is no general agreement regarding its cut-off value and the test is not widely available.

BAM can cause another disease called bile acid diarrhoea (BAD), which is commonly characterised by watery diarrhoea, bloating, and faecal incontinence at times. We can recognise BAM in a lot of different pathological conditions that sometimes overlap. 1% of the general population is affected by BAD.

BAM can be caused by surgical resection or structural impairment of the ileum (i.e., Crohn's disease (CD)). It mostly occurs in patients with predominant irritable bowel syndrome diarrhoea (IBS-D) or with functional diarrhoea (FD).

Clinically, BAM is classified as follows [22]: type 1: ileal dysfunction/resection (Crohn's disease); type 2: primary or idiopathic, characterised by watery diarrhoea with (IBS) or without (FD) pain responding to bile acid sequestrant drugs (BAS); type 3: associated with other gastrointestinal disorders such as coeliac disease, small intestinal bacterial overgrowth (SIBO), and chronic pancreatitis; and type 4: due to an impaired FGF-19 feedback inhibition that causes excessive BA synthesis [23]. Currently available therapies are BAS such as cholestyramine, colestipol, and colesevelam. Obeticholic acid might be a promising drug for BAM: it is an agonist of the farnesoid X receptor (FXR) which increases fibroblastic growth factor 19 (FGF-19) synthesis and decreases bile acid (BA) synthesis by hepatocytes [22,24]. Many studies classify BAD into mild, moderate, and severe on the basis of retention values on the seventh day of $\leq 15\%$, $\leq 10\%$, and $\leq 5\%$, respectively. A recent review [25] shows the following percentages in response to BAS therapy: mild BAM—73%, moderate BAM—76%, and severe BAM—88%. BAM severity can allow the clinician to predict the response to therapy and is a starting point for evaluating clinical improvement. To enhance BAS therapy, a better diagnosis is recommended.

Patients with a confirmed diagnosis are more motivated to start and continue a treatment with BAS, which are not palatable and can potentially induce some adverse events [26]. This is especially true of patients

with FD or IBS-D, who have often undergone many different diagnostic tests. The diagnosis of BAM in patients with chronic diarrhoea is of great clinical relevance: since a positive SeHCAT test does not exclude other organic causes of diarrhoea, patients should also undergo other tests as clinically indicated. Prolonged BAS treatment may lead to malabsorption of fats and liposoluble vitamins (A, D, and K), increasing the risk of osteoporosis and possible coagulation abnormalities. For this reason, patients with coagulation defects or those taking oral anticoagulant therapy should undergo a SeHCAT test to obtain a precise diagnosis and evaluate the benefit-risk ratio of BAS administration, as should patients taking life-saving drugs whose absorption could be potentially modified by BAS.

Inflammatory bowel disease (IBD)

In CD with ileal involvement [20], BAM was diagnosed in 116/276 (42%) patients; as expected, the most severe BAM was observed in CD patients with more severe ileal involvement or after resection of the distal ileum. It is common to find CD patients with persistent diarrhoea despite having normal inflammatory and disease activity indexes. BAM should be suspected as a co-factor of diarrhoea, as IBS may co-exist in IBD patients [27]. A Dutch study highlighted that the majority of IBD patients with IBS-type symptoms fulfilled the criteria for IBS or mixed-type IBS [28]. Patients with CD and unexplained persistent diarrhoea

without disease activity should be screened for BAM [20] because therapeutic response to BAS is related to BAM severity [29].

Cholecystectomy

BAM occurs in more than 90% of patients with post-cholecystectomy diarrhoea (PCD) [30]. The pathophysiological mechanism is linked to the lack of BA reservoir and the consequent inability of the gut to absorb the excessive output. Some studies have shown that BAS can improve diarrhoea in many different pathological conditions, including in patients without BAM. In particular, cholestyramine, which is a strong anion-exchange resin that can bind with bacterial toxins and mycotoxins in the colon [29], was effective in improving diarrhoea, including in patients with microscopic colitis without associated BAM [31]. This pharmacological effect may work in the cholecystectomised patient with multifactorial diarrhoea. This suggests the existence of other factors associated with BAM and, above all, a healing role rather than a symptomatic one for this drug.

Habba syndrome

This syndrome is defined by the presence of abnormal gallbladder function and chronic postprandial diarrhoea responding to BAS [32]. Hepatobiliary nuclear scintigraphy using ^{99m}Tc -DISIDA with cholecystokinin (DISIDA with CCK injection) has to be performed to estimate the gallbladder ejection fraction, in accordance

with the standard calculation of gallbladder contraction 30 minutes after CCK injection, to establish the possible relationship between gallbladder dysfunction and chronic diarrhoea. An ejection fraction < 35% is considered grossly abnormal, 35–50% borderline abnormal, and >50% normal. The response of the diarrhoea to BAS is probably due to a mechanism similar to that observed in PCD [30]. However, the poor function of the gallbladder seems to be the common primary factor in this syndrome.

Small- and large-bowel motility

Indications for small-bowel and colon transit scintigraphy include, but are not limited to, evaluation of gastrointestinal and colon transit abnormalities as a cause of symptoms in patients with known or suspected gastroparesis, dyspepsia, irritable bowel syndrome, chronic constipation, chronic diarrhoea, chronic idiopathic intestinal pseudo-obstruction, scleroderma, coeliac disease, and malabsorption syndromes. In the evaluation of patients with constipation, transit measurements may demonstrate a motility disorder or slow colon transit, or may provide evidence to support a diagnosis of defecation disorder or functional rectosigmoid obstruction [33].

During the clinical evaluation of gastrointestinal symptoms suspected of being caused by a motility disorder, it may be difficult for clinicians to determine whether the symptoms are caused by upper or lower gastrointestinal tract dysfunction.

In clinical practice, it is therefore helpful to evaluate motility throughout the entire gastrointestinal tract. At present, whole-gut transit scintigraphy (combined gastric emptying, small-bowel transit, and colon transit) is a relatively easy study to perform and in some centres is a frequently used and validated method to assess motility throughout the gut. Treatment selection may be guided by the finding of upper, lower, or combined gastrointestinal transit abnormalities. In addition, in patients with chronic constipation who are being considered for surgical colectomy, an assessment of upper gastrointestinal motility is important since upper gastrointestinal dysmotility may reduce the clinical response to surgical treatment.

The digestive neoplasms

Gastrointestinal (GI) malignancies encompass a wide range of disease sites, each with its own unique challenges. The GI system is divided into the following **disease site categories: oesophagogastric, colon, hepatobiliary, pancreas, and rectal–anal.**

Oesophageal cancer: Divided into oesophageal squamous cell carcinoma and oesophageal adenocarcinoma, this is the sixth leading cause of cancer mortality worldwide, accounting for about 5% (407,000 deaths) of all cancer deaths annually. It is the eighth most common cancer worldwide.

Gastric cancer: Gastric cancer remains the second leading cause of cancer mortality

in the world, although the overall incidence is declining. In Western countries, the incidence of gastric cancer has decreased dramatically over the past century.

Liver tumours: Hepatocellular carcinoma (HCC) is the most common primary malignant tumour of the liver. In children, hepatoblastoma is the third most common malignant tumour and the most common malignant hepatic tumour. It occurs almost exclusively in the first 3 years of life. Although rare, angiosarcoma is the most common malignant mesenchymal tumour of the liver.

Biliary tumours: Biliary malignancies comprise the vast majority of biliary neoplasms and are divided into 3 categories: (1) carcinomas of the intra- and extrahepatic bile ducts, (2) carcinoma of the gallbladder, and (3) carcinoma of the ampulla of Vater.

Pancreatic cancer: Pancreatic adenocarcinoma, despite its relatively low incidence compared with other malignancies, represents the fourth leading cause of cancer death in men and women. Cystic tumours of the pancreas are relatively uncommon, accounting for less than 10% of pancreatic neoplasms [112]. However, recognition of the prevalence of cystic lesions of the pancreas has increased dramatically.

Colon and rectal cancer: Colon and rectal cancer is a major cause of cancer-associated morbidity and mortality in North America, Europe, and other regions with similar lifestyles and dietary habits.

Small bowel neoplasms

Small bowel neoplasms are rare and usually diagnosed late because of non-specific clinical presentation. They can present as an annular constricting lesion, mass, or nodule. Neoplasms are characterised by asymmetric focal wall thickening and irregular transition from normal to the involved segment. Usually there is proximal luminal dilatation [34,35]. Adenocarcinoma is the most common small bowel neoplasm, with carcinoid tumour, lymphoma, and GI stromal tumour being the other primary bowel tumours [36].

Adenocarcinoma: Adenocarcinoma is the most common primary tumour of the small bowel, seen most commonly in the duodenum and proximal jejunum. Tumours may be polypoid, infiltrating or stenosing [36]. Cross-sectional imaging reveals a well-defined polypoid mass in the duodenum, with central ulceration seen in 10% of cases. Jejunal and ileal lesions are seen as asymmetric wall thickening, causing luminal narrowing and bowel obstruction. There is usually annular constriction with proximal shouldering [37]. Heterogeneous enhancement is seen after contrast administration. There may be infiltration of the surrounding fat, seen as fat stranding on CT and hyperintensity on T2-weighted fat-suppressed MR sequences [37].

Carcinoid: Carcinoid is a neuroendocrine tumour seen most commonly in the ileum.

Non-Hodgkin lymphoma: Non-Hodgkin lymphoma is the third most

common malignancy involving the small bowel. There are 4 main patterns of bowel involvement: diffuse infiltrative form, multiple nodules, mass-forming lesion, and exophytic masses [37]. Wall thickening associated with lymphoma is usually homogeneous and marked. The thickening is in the range of 15 to 20 mm, and the degree of enhancement is lower [118]. This thickening is frequently associated with enlarged lymph nodes. The pattern of involvement of mesenteric lymph nodes can also help in diagnosing lymphoma. These nodes are homogeneous, bulky nodes more commonly involving the margin of the small bowel mesentery. The sandwich sign which is produced by the enlarged lymph nodes in the mesentery encasing the small bowel mesenteric vessels is also commonly seen with lymphoma [38].

Gastrointestinal stromal tumours: Gastrointestinal stromal tumours (GIST) arise from the interstitial cells of Cajal within the Auerbach plexus and can present as submucosal, subserosal/exocentric, or intraluminal masses [39]. Usually these are large masses and can grow exophytically or intraluminally. Histologically, GIST may be **benign, potentially malignant, or malignant**. The imaging features favouring malignancy include a diameter greater than 5 cm, irregular shape, internal necrotic component, and heterogeneous contrast enhancement. Distant metastases and locoregional spread are also common with malignant lesions [40].

Metastases: Metastases to the small bowel are infrequent, with melanoma, lung, breast, thyroid, and bowel being the common primary malignancies [36]. They are usually submucosal or subserosal and appear as smooth, round, or polypoid masses with a target appearance. Surface deposits or extramural nodules occur from primary mucinous tumours. These deposits are seen as bowel wall thickening with mesenteric fat stranding [41].

Neuroendocrine tumours (NET)

NET are a rare and heterogeneous group of tumours, both in terms of primary tumour site and clinical behaviour over time. In fact, their clinical presentation varies from relatively indolent tumours to more aggressive forms showing rapid progression. The most common primary site is the gastroentero-pancreatic (GEP) tract, in particular the pancreas and ileum, and the lungs [42]. Most NET are well differentiated and express somatostatin receptors (SSTR), which are the cellular target for currently approved radiopharmaceuticals used for both diagnosis and therapy. NET are further subdivided into **three pathological grades:** G1 (Ki-67 <2%), G2 (Ki67 3-20%) and G3 (Ki-67 >20%), showing a more favourable behaviour as compared to poorly differentiated neuroendocrine carcinomas (NECs, small and large cells) [43]. Lung tumours are still classified as typical and atypical forms [44].

REFERENCES

- Skandalakis JE, Ellis H. Embryologic and anatomic basis of esophageal surgery. *Surg Clin North Am* 2000; 80:85-155.
- The normal anatomy of the esophagus. In: Fenoglio-Preiser CM, editor. *Gastrointestinal pathology*. An atlas and text. 2nd ed. Philadelphia: Lippincott-Raven; 1999. pp 15-29.
- Achildi O, Grewal H. Congenital anomalies of the esophagus. *Otolaryngol Clin N Am* 2007; 40:219-44.
- Rottenberg N. Macroscopic and microscopic vasculature of the duodenal-biliary-pancreatic complex. *Morphol Embryol (Bucur)* 1989; 35:15-9.
- Skandalakis J, Skandalakis L, Skandalakis P, et al. Hepatic surgical anatomy. *Surg Clin North Am* 2004; 84:413-35.
- Abdel-Misih SR, Bloomston M. Liver anatomy. *Surg Clin North Am* 2010; 90:643-53.
- Rutkauskas S, Gedrimas V, Pundzius J, et al. Clinical and anatomical basis for the classification of the structural parts of liver. *Medicina (Kaunas, Lithuania)* 2006; 42:98-106.
- Couinaud C. Le foie. *Etudes anatomiques et chirurgicales*. Paris: Masson & Cie; 1957.
- Healey J, Schroy P. Anatomy of the biliary ducts within the human liver: Analysis of the prevailing pattern of branching and the major variations of the biliary ducts. *Arch Surg* 1953; 66:599-616.
- Malarkey D, Johnson K, Ryan L, et al. New insights into functional aspects of liver morphology. *Toxicol Pathol* 2005; 33:27-34.
- Kahrilas, P, Pandolfino, JE. (2009) Esophageal motor function. *Textbook of Gastroenterology*. 187-206.
- Mittal, R. (2011). Motor function of the pharynx, esophagus, and its sphincters. *Colloquium Series on Integrated Systems Physiology: From Molecule to Function*, 3(3), 1-84.
- Hasler, WL. (2009). The physiology of gastric motility and gastric emptying. *Textbook of Gastroenterology*. 207-230.
- Bharucha, AE, Brookes, SJH. (2012). Neurophysiologic mechanisms of human large intestinal motility. *Physiology of the Gastrointestinal Tract*. 977-1022.
- Hasler, WL. (2009). Motility of the small intestine and colon. *Textbook of Gastroenterology*. 231-263.
- Catalan, MA., Ambatipudi, KS., Melvin, JE. (2012). Salivary gland secretion. *Physiology of the Gastrointestinal Tract*. 1229-1249.
- Keely, SJ., Barret, KE. (2022). Electrolyte secretion and absorption: small intestine and colon. *Textbook of gastroenterology*. 330-367.
- Barret, KE. (2014). *Gastrointestinal Physiology*. Second edition.
- Sarma A, Grant FD, Kwatra NS. Esophageal transit Scintigraphy in children: a user's guide and pictorial review. *Pediatr Radiol*. 2019 May;49(5):663-677.
- Farrell MB. Gastric emptying Scintigraphy *J Nucl Med Technol*. 2019 Jun;47(2):111-119.
- Grady E. Gastrointestinal Bleeding Scintigraphy in the Early 21st Century. *J Nucl Med*. 2016 Feb;57(2):252-9
- Camilleri M. Bile acid diarrhea: prevalence, pathogenesis, and therapy. *Gut and Liver*. 2015;9(3):332-339.
- Walters J. R. F., Tasleem A. M., Omer O. S., Brydon W. G., Dew T., le Roux C. W. A new mechanism for bile acid diarrhea: defective feedback inhibition of bile acid biosynthesis. *Clinical Gastroenterology and Hepatology*. 2009;7(11):1189-1194.
- Walters J. R. F., Johnston I. M., Nolan J. D., Vassie C., Pruzanski M. E., Shapiro D. A. The response of patients with bile acid diarrhoea to the farnesoid X receptor agonist obeticholic acid. *Alimentary Pharmacology & Therapeutics*. 2015;41(1):54-64
- Riemsma R., Al M., Corro Ramos I., et al. SeHCAT [tauroselcholic (selenium-75) acid] for the investigation of bile acid malabsorption and measurement of bile acid pool loss: a systematic review and cost-effectiveness analysis. *Health Technology Assessment*. 2013;17(61):1-236.
- Jin J., Sklar G. E., Min Sen Oh V., Chuen Li S. Factors affecting therapeutic compliance: a review from the patient's perspective. *Therapeutics and Clinical Risk Management*. 2008;4(1):269-286.
- Berrill J. W., Green J. T., Hood K., Campbell A. K. Symptoms of irritable bowel syndrome in patients with inflammatory bowel disease: examining the role of sub-clinical inflammation and the impact on clinical assessment of disease activity. *Alimentary Pharmacology & Therapeutics*. 2013;38(1):44-51.

28. Hoekman D. R., Zeevenhooven J., D'Haens G. R., Benninga M. A. The prevalence of irritable bowel syndrome-type symptoms in inflammatory bowel disease patients in remission. *European Journal of Gastroenterology & Hepatology*. 2017;29(9):1086–1090.
29. Fernandez-Banares F., Rosinach M., Piqueras M., et al. Randomised clinical trial: colestyramine vs. hydroxypropyl cellulose in patients with functional chronic watery diarrhoea. *Alimentary Pharmacology & Therapeutics*. 2015;41(11):1132–1140.
30. Sciarretta G., Furno A., Mazzoni M., Malaguti P. Post-cholecystectomy diarrhea: evidence of bile acid malabsorption assessed by SeHCAT test. *The American Journal of Gastroenterology*. 1992;87(12):1852–1854.
31. Fernandez-Banares F., Casalots J., Salas A., et al. Paucicellular lymphocytic colitis: is it a minor form of lymphocytic colitis? A clinical pathological and immunological study. *The American Journal of Gastroenterology*. 2009;104(5):1189–1198.
32. Habba S. F. Chronic diarrhea: identifying a new syndrome. *The American Journal of Gastroenterology*. 2000;95(8):2140–2141.
33. Lin HC, Prather C, Fisher R, et al. Measurement of gastrointestinal transit: AMS task force committee on gastrointestinal transit. *Dig Dis Sci*. 2005;50:989–1004.
34. Algin O, Evrimler S, Arslan H. Advances in radiologic evaluation of small bowel diseases. *J Comput Assist Tomogr* 2013;37(6):862–71.
35. Thulkar S, Gupta AK. Malignant lesions of stomach and small intestine. In: Gupta AK, Chowdhury V, Khandelwal N, editors. *Diagnostic radiology: gastrointestinal and hepatobiliary imaging*. 3rd edition. New Delhi (India): Jaypee Brothers; 2009. p. 91–111
36. Amzallag-Bellenger E, Oudjit A, Ruiz A, et al. Effectiveness of MR enterography for the assessment of small-bowel diseases beyond Crohn disease. *Radiographics* 2012;32:1423–44
37. Anzidei M, Napoli A, Zini C, et al. Malignant tumours of the small intestine: a review of histopathology, multidetector CT and MRI aspects. *Br J Radiol* 2011;84(1004):677–90. 118. Zhu QQ, Zhu WR, Wu JT, et al. Comparative study of intestinal tuberculosis and primary small intestinal lymphoma. *World J Gastroenterol* 2014;20(15): 4446–52
38. Dong P, Wang B, Sun QY, et al. Tuberculosis versus non-Hodgkin's lymphomas involving small bowel mesentery: evaluation with contrast-enhanced computed tomography. *World J Gastroenterol* 2008;14(24):3914–8
39. Koh JS, Trent J, Chen L. Gastrointestinal stromal tumors: overview of pathologic features, molecular biology, and therapy with imatinib mesylate. *Histol Histopathol* 2004;19:565–74.
40. Horton KM, Juluru K, Montgomery E, et al. Computed tomography imaging of gastrointestinal stromal tumors with pathology correlation. *J Comput Assist Tomogr* 2003;28:811–7.
41. Sheth S, Horton KM, Garland MR, et al. Mesenteric neoplasms: CT appearances of primary and secondary tumors and differential diagnosis. *Radiographics* 2003;23:457–73.
42. Pavel M, Öberg K, Falconi M, et al. Gastroenteropancreatic neuroendocrine neoplasms: ESMO clinical practice guidelines for diagnosis, treatment and followup. *Ann Oncol*. 2020;31(7):844–60
43. Nagtegaal ID, Odze RD, Klimstra D, et al. The 2019 WHO classification of tumours of the digestive system. *Histopathology*. 2020;76(2):182–8.
44. Travis WD, Brambilla E, Nicholson AG, Yatabe Y, Austin JHM, Beasley MB, Chirieac LR, Dacic S, Duhig E, Flieder DB, Geisinger K, Hirsch FR, Ishikawa Y, Kerr KM, Noguchi M, Pelosi G, Powell CA, Tsao MS, Wistuba I. The 2015 World Health Organization classification of lung tumors: impact of genetic, clinical and radiologic advances since the 2004 classification. *J Thorac Oncol*. 2015;10(9):1243–60.

RADIOPHARMACEUTICALS FOR GASTROINTESTINAL IMAGING

*by Lurdes Gano
Célia Fernandes
António Paulo*

C²TN/DECN, IST, Universidade de Lisboa

INTRODUCTION

Radiopharmaceuticals for gastrointestinal imaging (GI) have been used in nuclear medicine for many decades. Studies depend on physiology and function of organs, and thus provide gastroenterologists with information not provided by anatomical imaging techniques. The liver was one of the first organs to be studied with radiopharmaceuticals, namely radioactive colloids and hepatobiliary derivatives of iminodiacetic acid (IDA), allowing morphological and functional assessment of the liver and hepatobiliary tract, respectively. ^{99m}Tc -sulphur colloid (^{99m}Tc -SC) and ^{99m}Tc -IDAs have long been in use for routine gastrointestinal nuclear medicine studies. Several radiopharmaceuticals have also been used to evaluate the GI tract. Useful procedures include evaluation of gastro-oesophageal reflux and gastric emptying, and detection of GI bleeding and Meckel's diverticulum. In the management of oncological GI patients, 2-deoxy-2- ^{18}F fluoro-d-glucose (2- ^{18}F)FDG for positron emission tomography (PET) imaging is playing an increasingly important role in diagnosis, primary staging, restaging, and therapy monitoring of many gastrointestinal cancers. However, the recent rapid growth of new target-specific radiotracers for PET and single-photon emission computed tomography (SPECT) is expected to further enhance the usefulness of radiopharmaceuticals for GI imaging.

OVERVIEW OF THE MOST RELEVANT RADIOPHARMACEUTICALS IN GI

The most commonly used radiopharmaceuticals for GI in nuclear medicine departments are briefly described below. More detailed information regarding the formulations, preparation and quality control of conventional nuclear medicine radiopharmaceuticals can be found in a previously published EANM Technologists' Guide [1].

Radiopharmaceuticals for liver and hepatobiliary system imaging

Several radioactive colloidal preparations have been used to study the liver. In 1963, ^{99m}Tc -SC was developed and since then has remained the agent of choice for reticuloendothelial system (RES) imaging. Other radioactive colloids have been developed for diagnostic studies but none have displaced the clinical utility of ^{99m}Tc -SC.

^{99m}Tc -sulphur colloid

^{99m}Tc -SC is a colloidal dispersion of sulphur particles labelled with ^{99m}Tc . In this radiopharmaceutical, the radionuclide ^{99m}Tc is in the non-reduced Tc(VII) oxidation state due to the formation of insoluble and quite stable technetium heptasulphide, Tc_2S_7 .

^{99m}Tc -SC is formed from a reaction between [^{99m}Tc]-pertechnetate and a lyophilised mixture of anhydrous sodium thiosulphate, gelatine and a sodium salt of ethylenediaminetetraacetic acid (EDTA).

Upon boiling the kit in acidic conditions there is hydrolysis of thiosulphate with release of elemental sulphur, which aggregates forming particles ranging in size from 0.1 to 1.0 μm . The $^{99m}\text{Tc}_2\text{S}_7$ is formed during the reaction and becomes incorporated into the sulphur particle. Gelatine controls particle size and aggregation by forming a negatively charged protein coat on the sulphur particles, causing them to repel each other. EDTA chelates any Al^{3+} ion that may be present in the sodium pertechnetate solution and prevents its flocculation, which would lead to excessively large particles.

The clinical applications of ^{99m}Tc -SC include imaging of RES in liver, spleen and bone marrow and gastro-oesophageal reflux. When ^{99m}Tc -SC is administered orally, it enters the gastro-oesophageal tract, allowing gastric scintigraphy since it is insoluble in gastric juices. And, when administered intravenously, the uptake of the ^{99m}Tc -SC in the RES of the liver and spleen is dependent on the blood flow and the number and function of the phagocytic cells.

^{99m}Tc -mebrofenin

In addition to its metabolic functions, the liver is also an exocrine gland, secreting bile that is excreted by the hepatobiliary system. It is well established that ^{99m}Tc -complexes with aromatic derivatives of IDA are useful as hepatobiliary agents for imaging the biliary system and evaluating its function. A normal study shows an initial cardiac blood pool, rapid uptake and uniform distribution

in the liver and biliary appearance after a few minutes.

Among the developed ^{99m}Tc -IDA complexes, the ^{99m}Tc -complex with the IDA derivative mebrofenin (2,2'-[[2-[(3-bromo-2,4,6-trimethylphenyl)-amino]-2-oxoethyl]imino] bisacetic acid) is the most commonly used in nuclear medicine. Most probably, it corresponds to a monoanionic and lipophilic ^{99m}Tc (III)-complex that contains two tridentate IDA ligands coordinated to the metal, as typically found in most ^{99m}Tc -IDA complexes.

Like other IDA derivatives, ^{99m}Tc -mebrofenin is rapidly extracted from blood into bile by active transport via the anionic site on the hepatocyte membrane, which is the same site as for transport of bilirubin. It is therefore useful for assessing hepatobiliary function in several liver diseases. ^{99m}Tc -mebrofenin is cleared through the hepatobiliary system, but elevated serum bilirubin levels increase its renal excretion.

Radiopharmaceuticals for gastrointestinal tract imaging

Radiopharmaceuticals to assess GI tract dysfunction include agents to image gastro-oesophageal reflux, gastric emptying, GI motility and Meckel's diverticulum, as summarised below.

- » Radiopharmaceuticals for gastro-oesophageal reflux
Typically, ^{99m}Tc -SC is the most often used, as already mentioned.

» Radiopharmaceuticals for gastric emptying
Provide a non-invasive method of evaluating gastric physiology. These studies require the use of radionuclide markers that should not be absorbed through nor bound to the gastric mucosa, should have no effect on gastric emptying and should mix with ingested food. They can be soluble radiopharmaceuticals that are miscible with aqueous liquids to image the movement of liquids from the stomach. The most commonly used radiopharmaceuticals include ^{99m}Tc -DTPA, ^{111}In -DTPA and ^{99m}Tc -SC. [^{99m}Tc]-pertechnetate cannot be used as it localises in the gastric mucosa. Solid markers are radionuclides incorporated into food by different techniques. A widely used method is to mix ^{99m}Tc -SC with an egg, then cook and scramble the mixture to incorporate the radiopharmaceutical. The scrambled radioactive egg is then eaten. In some instances, a standard mixed solid-liquid gastric emptying meal (^{99m}Tc -SC scrambled eggs and ^{111}In -DTPA solution) may be given.

^{99m}Tc -DTPA and ^{111}In -DTPA

^{99m}Tc -DTPA (diethylenetriaminepentaacetate) is a hydrophilic ^{99m}Tc -complex approved as a radiopharmaceutical for renal scintigraphy. ^{99m}Tc -DTPA undergoes fast blood clearance by glomerular filtration and is excreted unchanged into the urine. It is mainly used to assess kidney function in a variety of

conditions and to measure the glomerular filtration rate. When taken orally, it has suitable features for GI transit imaging.

DTPA is a polycarboxylic acid that also forms stable complexes with indium. Various derivatives of this ligand have been widely used in radiopharmacy as bifunctional chelators for ^{111}In -labelling of biomolecules. It can also be formulated to prepare ^{111}In -DTPA. The final composition of ^{111}In -DTPA contains calcium, sodium chloride and buffer.

» Radiopharmaceuticals for GI motility studies

Evaluation of motility throughout the entire gastrointestinal tract may be helpful to determine whether GI symptoms of motility disorder are caused by upper or lower GI. Whole-gut transit scintigraphy (combined gastric emptying, small-bowel transit, and colon transit) is a relatively easy study to perform. The most physiological measurement of GI tract transit has been shown to be through imaging normal foods labelled with a small amount of radiotracer. This study is usually performed using the same dual-isotope solid-phase (^{99m}Tc) and liquid-phase (^{111}In) approach used in the gastric emptying study, followed by small-bowel and colon follow-through using the ^{111}In energy peak [2].

Although scintigraphic methods for measuring small-bowel and colon transit have been in use for many years, they have not gained widespread use because of the lack of standardised methods for the studies.

» Radiopharmaceuticals for detection of Meckel's diverticulum

[^{99m}Tc]-pertechnetate

The radiopharmaceutical [^{99m}Tc]-pertechnetate is obtained in the chemical form of [^{99m}Tc]- NaTcO_4 by elution of different commercially available ^{99}Mo - ^{99m}Tc generators with saline solution. [^{99m}Tc] TcO_4^- is used primarily as a radioactive precursor to prepare other ^{99m}Tc -radiopharmaceuticals through radiolabelling of the appropriate freeze-dried kits. As a radiopharmaceutical, it is used for thyroid imaging and is the agent of choice to evaluate patients with GI bleeding due to Meckel's diverticulum (MDS).

The clinical applications of [^{99m}Tc]-pertechnetate reflect its in vivo distribution, which is similar to that of the iodide ion due to their similar size and charge. Like iodide, [^{99m}Tc] TcO_4^- is taken up by functional thyroid tissue through the Na^+/I^- symporter. It is also concentrated by the gastric mucosa, which justifies its use in MDS since bleeding Meckel's diverticulum contains ectopic gastric mucosa.

Approximately 2% of the population has Meckel's diverticulum, the most common congenital malformation of the GI tract in humans. MDS has a sensitivity of 85% and a specificity of 95% in surgically proven cases of Meckel's diverticulum with ectopic mucosa.

Salivary activity and secretion may also be monitored after intravenous injection of [^{99m}Tc] TcO_4^- .

Radiopharmaceuticals for GI bleeding scintigraphy

^{99m}Tc -red blood cells

Two main radiopharmaceuticals have been used for gastrointestinal bleeding scintigraphy (GIBS): ^{99m}Tc -red blood cells (RBCs) and ^{99m}Tc -SC. However, ^{99m}Tc -RBCs are the radiopharmaceutical of choice to accurately localise the bleeding site because their prolonged circulation time allows continuous imaging of the GI tract over many hours, ideal for intermittent bleeding detection. Highly efficient RBC labelling with minimal unbound ^{99m}Tc is crucial for acquisition of optimal images. Labelling of RBCs can be achieved by three different methods: in vitro, modified in vivo, and in vivo. The in vitro method using a commercially available pyrophosphate kit to label the RBCs yields the highest labelling efficiency (>95%) and is the method of choice. Using this method, the radiolabelling efficiency can be evaluated prior to administration. If radiolabelling efficiency is lower than expected due to a drug interaction, low haematocrit level, or any other factor it is possible to centrifuge the ^{99m}Tc -RBC sample at 400g for 5 min, remove the supernatant and re-suspend in 0.9% sodium chloride before injection. This method produces good results, but it is time-consuming. In some nuclear medicine departments, the modified in vivo method (90% labelling efficiency) is used as an alternative when the in vitro method is not

available. Briefly, stannous pyrophosphate is first injected to pre-tin the red cells. 30 minutes later a sample of blood is removed, mixed with [^{99m}Tc]-pertechnetate and the cells re-injected. A disadvantage of this technique is the variable labelling efficiency. The in vivo method is not recommended because of suboptimal labelling and a higher likelihood of free ^{99m}Tc-pertechnetate presence. However, the in vivo method may be needed in some nuclear medicine departments or for patients who cannot be injected with blood [3].

Radiopharmaceuticals for pre-treatment assessment of liver cancer

^{99m}Tc-MAA

Although ^{99m}Tc-MAA is not widely available nowadays and its use is primarily indicated for lung perfusion scintigraphy, pre-treatment intra-arterial ^{99m}Tc-MAA scintigraphy is recommended in treatment planning for the radioembolisation of liver tumours with ⁹⁰Y-microspheres [4]. ^{99m}Tc-MAA corresponds to macroaggregated albumin labelled with ^{99m}Tc. The size of these macroaggregates is in the 10–90 μm range, and they are formed by denaturation of the protein when stannous chloride and human serum albumin are heated under controlled conditions.

^{99m}Tc-MAA is a surrogate to estimate the therapeutic activity of ⁹⁰Y- or ¹⁶⁶Ho-microspheres. The radiopharmaceutical is indicated to quantify the amount of liver-

lung shunting and to exclude the presence of extrahepatic activity, especially reflux to bowel, stomach or pancreas, to determine the patient's suitability for transarterial radioembolisation.

Radiopharmaceuticals for molecular imaging of GI cancers

2-deoxy-2-[¹⁸F]fluoro-d-glucose (2-[¹⁸F]FDG)

The radiopharmaceutical 2-[¹⁸F]FDG was initially developed for brain imaging, and originally approved by the Food and Drug Administration (FDA) „for the measurement of regional glucose metabolism in human brain to assist in the diagnosis of seizures“. However, already in the early 1980s, several preclinical and clinical studies pinpointed the usefulness of this radiotracer for PET imaging of myocardial and tumour metabolism. Nowadays, 2-[¹⁸F]FDG still remains the workhorse of PET imaging in the fields of oncology, neurology, and cardiology. The clinical success of 2-[¹⁸F]FDG is justified by its biological performance as a glucose analogue and the possibility of preparing multi-dose batches, on a daily basis and in an automated fashion, at numerous PET facilities worldwide. Currently, 2-[¹⁸F]FDG can be produced in high radiochemical yield in less than 30 min, by nucleophilic [¹⁸F]-labelling of the precursor 1,3,4,6-tetra-O-acetyl-2-O-trifluoromethanesulfonyl-β-D-mannopyranose (“mannose triflate”)

using different commercially available automated synthesis modules.

2-[¹⁸F]FDG enters the cells using the same transporters (GLUT1 to GLUT5) as glucose, also acting as a substrate for the enzyme hexokinase with formation of the radiometabolite 2-deoxy-2-[¹⁸F]fluoro-d-glucose-6-phosphate. This radiometabolite is not a substrate for further enzymes of the oxidative phosphorylation process, and thus remains trapped within the cells in proportion to the metabolism of glucose. In particular, 2-[¹⁸F]FDG-PET has emerged as a relevant imaging procedure for the staging and treatment follow-up of many types of cancers. The use of 2-[¹⁸F]FDG-PET in oncology is based on the differential rates of glucose metabolism in benign and malignant tissues. Thus, hotspots on a PET scan are usually associated with a high number of viable tumour cells, high expression of GLUT1 and GLUT3, and enhanced Warburg effect.

2-[¹⁸F]FDG-PET has been used for imaging of inflammation, fibrosis, and cancer in the GI tract [5,6]. However, the advantages of 2-[¹⁸F]FDG-PET over other modalities to image non-neoplastic conditions of the bowel, such as inflammatory bowel disease (IBD), are not evident and consensual. On the other hand, 2-[¹⁸F]FDG-PET offers the advantage of whole-body imaging, allowing the identification of locoregional and distant metastatic disease. This is useful for initial staging and treatment response assessment of gastrointestinal

tumours, namely colorectal and gastric cancers. The imaging of colorectal cancer might involve the delineation of primary tumour extent (T staging), identification of regional lymphadenopathy (N staging), and detection of metastatic disease (M staging). 2-[¹⁸F]FDG-PET seems more appropriate for nodal staging (N staging), having an overall accuracy of 79%; this is higher than that of MRI, which shows an overall accuracy of only 34% [7]. By contrast, 2-[¹⁸F]FDG-PET has a more limited usefulness for the staging of local gastric cancers, which often are not FDG-avid. 2-[¹⁸F]FDG-PET is also not very useful for the early diagnosis, staging and management of other cancers of the digestive system. For example, 2-[¹⁸F]FDG is not the best choice to detect hepatocellular carcinoma (HCC) or localise liver metastases, due to the relatively high uptake of the radiopharmaceutical by normal liver parenchyma. Also, the diagnosis and staging of pancreatic adenocarcinoma by 2-[¹⁸F]FDG-PET is not clinically relevant due to the high accuracy of CT and MRI for this purpose. 2-[¹⁸F]FDG-PET does have a diagnostic performance superior to CT and MRI in the identification of peritoneal dissemination and distant metastatic dissemination of pancreatic adenocarcinoma, but at the expense of a loss of specificity due to FDG uptake in inflammatory/infectious lesions.

Target-specific radiolabelled peptides for GI of neuroendocrine tumours

Somatostatin (sst) receptor imaging in neuroendocrine tumours (NET) is useful for the primary diagnosis and staging of the disease, as well as for selection of patients for targeted therapy and monitoring of its efficacy.

^{111}In -pentetreotide, as $^{99\text{m}}\text{Tc}$ -Tektrotyd, is used for scintigraphic localisation of primary and metastatic neuroendocrine tumours that bear sst receptors. In the past few years, however, it has started to be replaced by ^{68}Ga -radiolabelled somatostatin analogues, which provide higher sensitivity and resolution using PET imaging.

^{111}In -pentetreotide

^{111}In -pentetreotide (^{111}In]-DTPA-octreotide) is a ^{111}In -labelled somatostatin analogue in clinical use since the 1990s. It was the first radiopharmaceutical approved for peptide receptor imaging and is the ^{111}In -radiopharmaceutical with the greatest clinical impact. ^{111}In -pentetreotide specifically binds to sst receptors, with particular affinity to subtypes 2 and 5. The radiopharmaceutical contains the biologically active ring of octreotide and a DTPA unit that is covalently bound to the D-phenylalanine group and allows fast and stable labelling with ^{111}In . ^{111}In -pentetreotide is prepared by adding $^{111}\text{InCl}_3$ in HCl solution to a freeze-dried kit containing pentetreotide and a few other ingredients.

$^{99\text{m}}\text{Tc}$ -Tektrotyd

This target-specific radiopharmaceutical corresponds to the mixed-ligand complex $^{99\text{m}}\text{Tc}$ -EDDA/HYNIC-Tyr³-octreotide carrying a cyclic bioactive octreotide derivative that recognises some of the sst receptors, particularly subtype 2 and, to a lesser extent, subtypes 3 and 5. It has been introduced as an alternative to ^{111}In -pentetreotide. $^{99\text{m}}\text{Tc}$ -Tektrotyd was developed with the aim of introducing a well-performing $^{99\text{m}}\text{Tc}$ -labelled somatostatin analogue based on the better physical characteristics of the $^{99\text{m}}\text{Tc}$ radionuclide.

$^{99\text{m}}\text{Tc}$ -Tektrotyd is prepared from a freeze-dried kit that contains a Sn(II) salt, EDDA (ethylenediamino-N,N'-diacetic acid), tricine (N-[tris(hydroxymethyl)methyl]glycine) and HYNIC-[D-Phe¹, Tyr³-octreotide]. This mixed-ligand complex contains [D-Phe¹, Tyr³]-octreotide (TOC) as the sst-binding peptide and hydrazinonicotinic acid (HYNIC) as a $^{99\text{m}}\text{Tc}$ -coordinating moiety. Furthermore, it is stabilised by EDDA that acts as a co-ligand and coordinates to $^{99\text{m}}\text{Tc}$ following a tricine/EDDA exchange reaction. Although not fully assessed, it is generally accepted that the molecular structure of the $^{99\text{m}}\text{Tc}$ -mixed-ligand complex contains $^{99\text{m}}\text{Tc}$ (V) coordinated by one HYNIC moiety and two EDDA ligands.

$^{99\text{m}}\text{Tc}$ -Tektrotyd is indicated for detection of pathological lesions in which sst are overexpressed, namely in the case of NET.

^{68}Ga -DOTATATE and ^{68}Ga -DOTATOC

The PET tracers ^{68}Ga -DOTATATE and ^{68}Ga -DOTATOC are radiolabelled derivatives of the somatostatin analogue octreotide (DOTA-(Tyr³-Thr⁶)-octreotide and DOTA-(Tyr³)-octreotide, respectively). The use of these radiotracers in PET is recognised as the most sensitive molecular imaging modality for diagnosis of well-differentiated NETs [8]. Profiting from the availability of the $^{68}\text{Ge}/^{68}\text{Ga}$ generator, efforts were therefore invested in the development of kit-based products to obtain the radiopharmaceuticals by expedite radiolabelling with ^{68}Ga . In 2016, the FDA approved ^{68}Ga -DOTATATE, which is marketed in the United States under the name NETSPOT (kit for the preparation of ^{68}Ga -DOTATATE injection). The European Medical Agency (EMA), on the other hand, approved ^{68}Ga -DOTATOC, which is marketed under the name SomaKit TOC (kit for the preparation of ^{68}Ga -DOTATOC injection). Their availability in kit form is expected to allow widespread use, even in nuclear medicine centres without experience in the production of PET radiopharmaceuticals. NETSPOT and SomaKit TOC are supplied as 2-vial kits containing the formulation of the freeze-dried peptide and a buffer, respectively. Both ^{68}Ga -tracers are prepared by addition of $^{68}\text{GaCl}_3$ to the respective freeze-dried kits (NETSPOT or Somakit TOC) at controlled pH, reaction time and temperature (7 minutes at 95°C). ^{68}Ga -DOTATATE has a higher selectivity for sstr₂, while ^{68}Ga -DOTATOC binds to sstr₂ and

also to subtype 5 (sstr₅). Imaging of sstr can be used for disease staging and to influence treatment decisions, especially in selecting patients for sstr peptide therapy, or more recently for PRRT. In fact, very promising results were obtained for peptides radiolabelled with beta minus emitters, which led to the recent approval of ^{177}Lu -DOTATATE (Lutathera) by the FDA for the treatment of NETs. However, before treatment with Lutathera, tumours should be evaluated by PET imaging with the ^{68}Ga -labelled congeners to confirm sstr expression and select patients for therapy.

^{68}Ga]-fibroblast activation protein inhibitors

^{68}Ga]-FAP (FAP) (^{68}Ga -fibroblast activation protein inhibitor) has emerged in recent years to evaluate digestive system tumours by PET imaging.

Fibroblast activation protein (FAP) is a type II transmembrane glycoprotein overexpressed in cancer-associated fibroblasts of several tumour entities, including colon and pancreatic cancer. By contrast, normal fibroblasts present no or only very low FAP expression. Additionally, FAP is associated with risk of disease progression and poor prognosis in cancer patients. FAP is thus an attractive target with a relatively high tumour-specific expression for the delivery of diagnostic and therapeutic agents. FAP inhibitors have been developed as cancer drugs, and quinoline-based FAP-specific inhibitors have

been designed, radiolabelled and evaluated as theranostic agents for malignant tumours with high expression of activated fibroblasts. Preclinical evaluation of a ^{68}Ga -FAPi suggested promising potential as a molecular target imaging agent.

The design of the quinoline-based radiopharmaceutical comprised the linking of the FAP-targeting moiety to the DOTA chelator, which allows incorporation of the ^{68}Ga as well as different radionuclides suitable both for imaging and therapeutic purposes. For chelation with ^{68}Ga the pH of the reaction mixture is adjusted with sodium acetate and heated to 95°C for 10 min. Before administration, the ^{68}Ga -FAPi is purified by solid-phase extraction [9].

Recent clinical studies of ^{68}Ga -FAPi in patients with various cancers demonstrated that it is a promising new imaging agent for pancreatic, head and neck, lung, breast, and colon cancers, with tumour-to-background contrast ratios equal to or even better than those of 2- ^{18}F -FDG-PET. In contrast to 2- ^{18}F -FDG, no diet or fasting is necessary in preparation for the examination, and image acquisition can potentially be started a few minutes after tracer injection. Favourable characteristics include fast tracer kinetics, low background uptake in liver and oral mucosa, and independence from blood sugar. A systematic review of ^{68}Ga -FAPi for the diagnostic assessment of primary tumours, lymph node metastases and distant metastases in digestive tumours showed that it has a high accuracy and

sensitivity for the diagnosis of these tumours in patients [10].

Future prospects

Gastrointestinal disease comprises a variety of pathologies, such as inflammation, infection, fibrosis, haemorrhage or cancer. A great challenge in the development of radiopharmaceuticals for GI imaging, therefore, is the need for more specific probes to differentiate between these different disease processes (e.g. inflammation vs infection vs cancer) while allowing early diagnosis and treatment follow-up using theranostic approaches. In working towards this goal, significant progress has been obtained with radiolabelled somatostatin analogues and radiolabelled FAPi derivatives for the detection and treatment follow-up of specific cancers related to the digestive system. Further positive developments can be expected thanks to recent improvements in the design of targeting vectors (e.g. antagonist vs agonist peptides), the availability of innovative medical radionuclides (e.g. true theranostic pairs like ^{155}Tb and ^{161}Tb), and the advent of immunotherapy and cellular therapies, which have not yet had a strong impact on the management of GI disease with nuclear medicine procedures [11].

REFERENCES

- Gano L, Paulo A. Conventional nuclear medicine radiopharmaceuticals. In Radiopharmacy: An update. Attard MC ed. Vienna, EANM Publisher, 2019.
- Maurer AH, Camilleri M, Donohoe K, Knight LC, Madsen JL, Mariani G, Parkman HP, Dolsen JV. The SNMI and EANM practice guideline for small-bowel and colon transit 1.0. *J Nucl Med* 2013;54:2004-2013.
- Dam HQ, Brandon DC, Grantham VV, Hilson AJ, Howarth DM, Maurer AH, Stabin MG, Tulchinsky M, Ziessman HA, Zuckier LS. The SNMI procedure standard/EANM practice guideline for gastrointestinal bleeding scintigraphy 2.0. *J Nucl Med Tech* 2014;42:308-317.
- Weber M, Lam M, Chiesa C, Konijnenberg M, Cremonesi M, Flamen P, Gnesin S, Bodei L, Kracmerova T, Luster M, Garin E, Herrmann K. EANM procedure guideline for the treatment of liver cancer and liver metastases with intra-arterial radioactive compounds. *EJNMMI* 2022;49:1682-1699.
- Tyler J Fraum, Daniel R. Ludwig DR, Hope TA, Fowler KJ. PET/MRI for Gastrointestinal Imaging: Current Clinical Status and Future Prospects, *Gastroenterology Clinics of North America* 2018; 47 (3): 691-714.
- Harold KM, MacCuaig WM, Holter-Charkabarty J, Williams K, Hill K, Arreola AX, Sekhri M, Carter S, Gomez-Gutierrez J, Salem G, Mishra G, McNally LR, Advances in Imaging of Inflammation, Fibrosis, and Cancer in the Gastrointestinal Tract, *Int. J. Mol. Sci.* 2022;23, 16109.
- Mainenti PP, Iodice D, Segreto S, et al. Colorectal cancer and 18FDG-PET/CT: what about adding the T to the N parameter in loco-regional staging? *World J Gastroenterol* 2011;17(11):1427-33.
- Pauwels E, Cleeren F, Bormans G, Deroose CM. Somatostatin receptor PET ligands - the next generation for clinical practice. *Am J Nucl Med Mol Imaging.* 2018 Oct 20;8(5):311-331. PMID: 30510849; PMCID: PMC6261874.
- Lindner T, Loktev A, Altmann A, Giesel F, Kratochwil C, Debus J, Jager D, Mier W, Haberkorn U. Development of quinoline-based theranostic ligands for the targeting of fibroblast activation protein. *J Nucl Med* 2018;59:1415-1422.
- Huang D, Wu J, Zhong H, Li Y, Han Y, He Y, Chen Y, Lin S, Pang H. [^{68}Ga]-FAPiPET for the evaluation of digestive system tumors: systematic review and meta-analysis. *EJNMMI* 2023;50:908-920.
- Halama N, Uwe Haberkorn U. The Unmet Needs of the Diagnosis, Staging, and Treatment of Gastrointestinal Tumors, *Semin Nucl Med* 2020;50:389-398.

SALIVARY GLAND STUDIES

by *Carolina Sousa*¹
*Ana Geão*²
*Pedro Quaresma*³

¹*Nuclear Medicine Technologist at Hospital CUF Descobertas, Lisbon, Portugal*

²*Head Nuclear Medicine Technologist at Hospital CUF Descobertas, Lisbon and Invited Adjunct Professor at Lisbon School of Health Technology (ESTeSL), Portugal*

³*Head of the Nuclear Medicine Department at Al Zahra Hospital, Dubai, UAE*

INTRODUCTION

The **major salivary glands** are the parotid (the largest ones, overlaying the masseter muscle), submandibular and sublingual glands. These structures play a fundamental role in the homeostasis of the oral cavity. They are responsible for the secretion of saliva, a multipurpose fluid responsible for mucosa lubrication and containing important electrolytes, enzymes and antibacterial compounds to ensure the protection of the teeth and the surface of oral mucosa.

SALIVARY GLAND SCINTIGRAPHY

Salivary gland functional compromise will thus essentially result in a reduction in saliva secretion. **Salivary gland scintigraphy with [^{99m}Tc]pertechnetate** is a minimally invasive functional imaging modality by means of which perfusion, tracer uptake and excretion of the major salivary glands can be evaluated.

The **main clinical applications** of salivary gland scintigraphy are:

- » Evaluation of complaints of xerostomia
- » Functional assessment of the salivary glands in the setting of Sjogren's syndrome, acute and chronic sialadenitis and sialolithiasis
- » Evaluating the effects of radioiodine and theranostic therapies on salivary gland function
- » Assessing the response following surgical intervention to remove an obstruction or other procedures

- » Monitoring the response to treatment in patients with salivary dysfunction secondary to other treatable diseases
- » Evaluating fistulas and traumatic abnormalities

RADIOPHARMACEUTICAL AND ITS MECHANISM OF UPTAKE BY THE SALIVARY GLANDS

Sodium technetium-99m pertechnetate ($[^{99m}\text{Tc}]\text{NaTcO}_4$) is the radiopharmaceutical used in salivary gland scintigraphy. Salivary gland epithelial cells have sodium/iodine symporters (NIS), which are responsible for taking univalent anions like chloride (Cl⁻) and iodine (I⁻) and concentrating them for subsequent secretion into saliva. Due to the corresponding physico-chemical characteristics, namely the single negative charge and the similar diameter, intravenously administered $[^{99m}\text{Tc}]\text{TcO}_4^-$ is actively taken up by the epithelial cells of the salivary glands through NIS in a manner similar to the Cl⁻ concentration. The uptake of $[^{99m}\text{Tc}]\text{TcO}_4^-$ is mainly in the parotid and submandibular glands, the largest salivary glands, and reflects the function of the **salivary gland parenchyma**. After accumulation of the $[^{99m}\text{Tc}]\text{TcO}_4^-$ loading of a sialogogue stimulates the secretion of the radiopharmaceutical into the glandular ducts and mouth along with saliva. This reflects the **glandular excretory function** and any obstruction of the salivary ducts [1, 2].

PATIENT PREPARATION

Before the scan day, a full verbal as well as written **explanation of the procedure** should be given so that patients have the opportunity to discuss any doubts and concerns (including risks, pausing medication, possible side effects of the radiopharmaceutical, time required for the scan, etc.). The technologist must underline the importance of **fasting for at least 2 hours** before the scan to ensure that no food or drink influences the radiopharmaceutical uptake, allowing for accurate imaging and result interpretation [3, 4]. Patients can be requested to send in a list of medications they are taking and to bring along the results of any previous relevant diagnostic examinations (such as ultrasonography, sialography, computed tomography, magnetic resonance imaging and/or previous scintigraphy of the salivary glands).

Although, to the best of our knowledge, there is no information available regarding the influence of concomitant medication on the outcome of salivary gland scintigraphy, if necessary, and under guidance from the referring clinician, the patient should be off:

- » **thyroid-blocking agents**, such as iodine or perchlorate, for a period of 48 hours before the scan [5]
- » **anticholinergic medication**, such as selective serotonin reuptake inhibitors (SSRIs) or opioids at least 5 times the biological half-life of the drug prior to the study [4, 6].

On the day of the scan, **positive identification** of the patient is a critical step in ensuring the correct patient receives the correct examination. It is an essential process for maintaining patient safety, protecting patient privacy, and ensuring accurate medical records. Positive identification can be done in different ways. Each department has their own method or safety policy, the most common being:

- » **Verbal confirmation:** The patient is asked to provide at least two personal elements such as his/her name, date of birth or other identifying information.
- » **Photo identification:** The patient is asked to show government-issued ID such as a driver's licence or passport.
- » **Patient wristband:** Patient wristbands with the patient's name, identification number, and other relevant information are given to patients to wear during their stay in the hospital.

It is important to note that a positive identification process should be followed at multiple time points throughout the examination, to ensure that the correct patient is addressed all times. This also helps to minimise the risk of error and to ensure accurate medical records are kept.

The technologist is responsible for reviewing the patient's preparation instructions and ensuring that the patient has followed them correctly. It is especially important to make sure the patient has fasted for at least 2 hours. Additionally, the technologist is responsible for explaining

the procedure to the patient and answering any questions he/she may have, as well as preparing them for the injection of the radiopharmaceutical and ensuring safety protocols are followed.

IMPORTANT ASPECT OF PATIENT HISTORY

Information on patient **clinical history**, as well as his/her **symptoms** and **signs** and the results of relevant **imaging examinations** and **chemical diagnostic tests** have to be collected during anamnesis [3, 7, 8, 9]:

- » complaints of swelling or discomfort in the face or neck;
- » sicca symptoms (xerostomia, xerophthalmia);
- » known salivary gland disorders;
- » results of ultrasonography, sialography, computed tomography, magnetic resonance imaging and/or previous scintigraphy of the salivary glands;
- » serological tests results including anti-Sjögren's-syndrome-related autoantibodies: anti-SSA/Ro, anti-SSB/La, antinuclear antibody (ANA) and rheumatoid factor;
- » salivary gland biopsy results;
- » known thyroid disorders;
- » history of iodine-131 treatment for thyroid cancer, theranostic cancer treatment or alpha-particle therapy;
- » history of radiotherapy for head and neck tumours.

It is important to ensure that women of reproductive age have their pregnancy and breastfeeding status checked before undergoing any examination that involves the use of radiopharmaceuticals. **Pregnancy** is considered a contraindication for this examination since the radiation dose received by the foetus can be significant. Pregnant women should therefore not be exposed to this kind of examination and, whenever possible, it should be postponed until after childbirth. It is also important to note that **breastfeeding** should be interrupted for 12 hours after the examination and the milk must be pumped and disposed of during this period in accordance with ICRP 128 [10]. Extra hydration and frequent bladder emptying can further decrease the exposure of the newborn to radioactivity.

Since a substance for salivary gland stimulation will be used, it is important to ensure before the examination that the patient is **not allergic or intolerant to the sialogogue** to be used. Some sialogogues can cause allergic reactions or other adverse effects in some individuals. Therefore, it is important to ask the patient about any known allergies or sensitivities they may have, and to inform the patient of the sialogogue that will be used before starting the scan. If the patient reports any history of an allergic reaction or intolerance to the sialogogue, the examination should not proceed, or an alternative sialogogue should be used. It's also important to consider any medical condition that the patient may have, such as gastroesophageal

reflux disease (GERD), that may contraindicate the use of certain sialogogues. (For more information regarding the sialogogues used, see Sialogogue stimulation during the study).

ACQUISITION PROCEDURE

Patient positioning for the scan

The patient should void before being brought to the camera room to promote patient comfort and minimise the probability of patient movement. The technologist should prepare the sialogogue to be administered so that it is ready to be used when necessary and also prepare the room before starting the scan. An underpad or other similar material can be used to **cover the collimator surface** and protect it from any debris or contaminants (biological and radioactive). This is important given that any radioactive contamination on the collimator's surface can interfere with image quality.

After removing any relevant attenuating objects, such as glasses, earrings and necklaces, the patient should be positioned on the camera table in a **supine position** with his/her neck slightly extended. This positioning technique ensures good separation of both salivary glands and thyroid in the image. The camera is positioned anteriorly because of the anatomical location of the salivary glands. It is important to prevent displacement of the head to the periphery of the field of view and to avoid any rotation or lateral tilt of the head as this will result in asymmetry. This positioning technique is ideal to ensure the best possible image quality for scintigraphy of the salivary glands. The head should preferably be fixed with a head holder or other light head restraint to help reduce patient motion. Additionally, adjusting the gamma-camera table to bring the detector as close as possible to the patient's face will increase the resolution of the image (Figure 1).



Figure 1 – Examples of patient supine positioning
Courtesy of Nuclear Medicine Department – CUF Descobertas, Lisbon, Portugal

At this point, the technologist must be aware of any issues the patient may have regarding position and claustrophobia, as the exam will take quite a long time with the detector very close to the patient's face.

The major salivary glands and the thyroid need to be in the centre of the field of view (having as a **reference point** the eyes at the superior limit and the wishbone at the inferior limit). The anatomical limits should be verified with a radioactive marker prior to injection to ensure all structures to be visualised are included (especially if zoom factor is applied) and to ensure correct study orientation.

It is important to confirm that the patient is comfortable and relaxed during the imaging process, and to ensure this is the case **positioning aids** may be used to maximise patient comfort and aid immobilisation: head support, knee rolls/supports, foam wedges, strap for the arm, blankets, etc. Place the patient's arm for the

injection onto an armrest and the other arm alongside the body. Finally, before starting dynamic acquisition, ensure the patient understands the importance of remaining still during the imaging procedure, especially during sialogogue administration.

In the **lateral projections** two important factors need to be taken into account. The detector has to be as close as possible to the face, and the camera head has to be aligned with the medial line of the head, with the face as parallel as possible to the detector. This helps to ensure that the images are acquired with the correct orientation, reducing the risk of image distortion. Achieving good alignment between the face and the detectors is important for accurate interpretation of the images and accurate diagnosis of any underlying conditions. Left and right lateral views should be acquired in sequential mode (if single-head camera) or simultaneously (if dual-head camera) [9, 11, 12].



Figure 2 – Examples of patient seated positioning
Courtesy of Nuclear Medicine Department – CUF Descobertas, Lisbon, Portugal

Although the supine position is preferable so that patient movement is avoided, **alternative positioning techniques** may be considered depending on the patient's comfort, ability to maintain the position during the imaging procedure or specific patient conditions such as claustrophobia, anxiety, back pain or others. The patient may instead, for instance, remain in an upright or seated position (Figure. 2). This positioning may be more conducive to movement and so the technologist should remind the patient to remain still throughout the entire procedure.

Radiopharmaceutical administration and radiation burden

The radiopharmaceutical used is $^{99m}\text{Tc}[\text{NaTcO}_4]$. It is administered via a bolus intravenous injection and the **administered activity** varies widely from 40 MBq up to 740 MBq, depending on the preferred acquisition parameters and on the equipment performance. The most common range of activities administered to an adult patient is 100 to 200 MBq [1, 2].

According to ICRP 128, the **effective dose** to an adult patient after ^{99m}Tc pertechnetate injection and with no blocking agents given is 1.3×10^{-2} mSv/MBq, which means an effective dose to the patient of 1.95 mSv after 150 MBq of ^{99m}Tc pertechnetate injected [10]. If SPECT/CT acquisition is medically justified, the **CT dose** must be factored into the total effective dose to the patient; CT dose to

the patient is dependent on the acquisition parameters and on the length of the acquisition.

Imaging acquisition

Ensure that the patient is comfortable before starting the study. Instruct the patient to remain motionless and breathe normally. Ensure good venous access. The dynamic scan starts at the same moment as the administration of the radiopharmaceutical. Monitor the patient throughout the scan to ensure safety and watch for motion. Additionally, static planar anterior, lateral and/or oblique images and/or SPECT/CT or SPECT images can be acquired as needed. **Suggested acquisition parameters** according to the consulted references and to clinical experience are listed in Table 1.

It is important to note that the trade-off between spatial resolution and noise in the image should be carefully considered when selecting the imaging parameters, and the technologist should optimise the acquisition time and imaging parameters to produce the best possible image quality while ensuring the patient's comfort and safety.

Although SPECT is not typically performed as a stand-alone modality for salivary gland imaging, it can be used in combination with CT. These images are particularly useful since they combine functional information with three-dimensional anatomical findings, potentially enhancing the diagnostic accuracy of the study.

	Dynamic Study	Static Planar Images	SPECT
Projections	Anterior	Anterior and/or Right and Left Lateral and/or Right and Left Anterior Oblique	—
Photopeak	140 keV		
Window width	15 – 20% centred		
Collimators	LEHR (or LEGP) parallel-hole		
Matrix	128x128	256x256	128x128
Zoom	Optional		
Time / Nº of Counts	30 seconds – 2 minutes/frame (study of 20 – 40 minutes) Recommendation: 1 minute/frame in 30 minutes	2 – 3 minutes/image or 300 – 500 kcounts/image	10 seconds/ projection (Total of 60 projections)
Rotation	—	—	Total angular range: 360° View angle 6° With body contour

Table 1 – Technical acquisition parameters (recommendations)

Sialogogue stimulation during the study

After the accumulation of [^{99m}Tc] pertechnetate in the salivary glands, the administration of a sialogogue stimulates the secretion of saliva which enables a simultaneous evaluation of the excretory function of major salivary glands and any obstruction of the salivary ducts [13].

Sialogogues can be divided into peripheral sialogogues which stimulate a gustatory response, and central sialogogues, which include parasympathomimetics [14, 15].

Lemon juice is the most frequently used sialogogue, being administered orally using a straw, a pipette or a tube attached to a syringe; Figure 3 shows an example of sialogogue preparation together with the device for administration, and Figure 4 shows administration of the sialogogue during the acquisition. It is recommended that the patient be asked to hold the lemon juice in the mouth for a few seconds before swallowing to achieve maximum stimulus of salivary gland excretion [2, 9].

Lime juice, malt vinegar, grapefruit juice, spicy foods such as chili peppers or ginger, and sweets such as chewing gum or boiled sweets (lollipops) are other examples of sialogogues referred to in the literature [14]. Carbachol has the advantage of resulting in a more standardised secretion of the labelled saliva; it may, however, lead to cholinergic side effects [15].

Table 2 shows some examples of the **most common sialogogues** used in salivary gland scintigraphy and the administered quantities in the stimulation phase.

Regardless of the sialogogue stimulation used, the sialogogue should be administered in the middle of the dynamic study in order to evaluate both the baseline and stimulated states of the salivary glands. It is important to note that the timing of sialogogue administration should be standardised to



Figure 3 – Example of freshly squeezed lemon juice used as a sialogogue, together with the administration device

ensure consistency between studies, and the technologist should be aware of the side effects of the sialogogue and take precautions if necessary. The technologist should remind the patient to remain motionless during the administration and for the remainder of the acquisition. Any movement during the imaging process can cause blurring of the images, which can make it difficult to interpret the results.

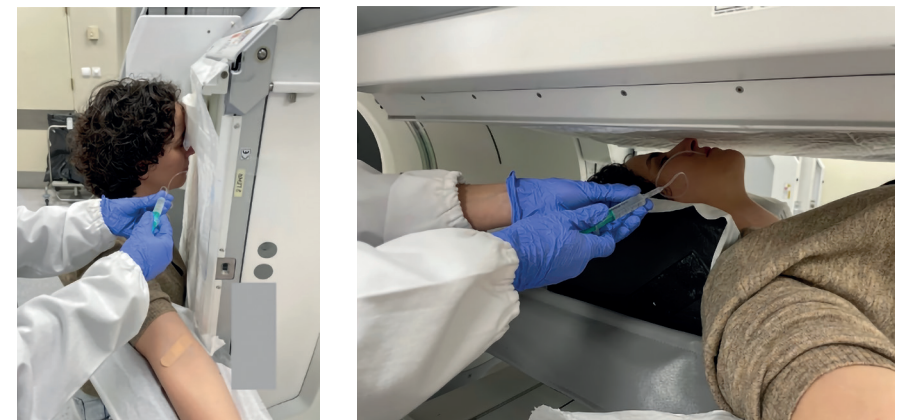


Figure 4 – Administration of the sialogogue during the study
Courtesy of Nuclear Medicine Department – CUF Descobertas, Lisbon, Portugal

Type of Stimulation	Sialogogue	Route of Administration	Quantity	Observations/References
Gustatory	Lemon Juice	Intraorally	3 – 10 mL	Concentrated or diluted in water. Freshly squeezed or the commercially available form [2, 4, 6, 9, 16, 17, 18]
	Orange Juice		200 mL	[13]
	Lemon Powder	Oral or sublingual	2 g	[19]
	Vitamin C		200 – 300 mg	[7, 8]
Parasympathomimetics	Carbachol	Subcutaneous	0.25 mg	[20]

Table 2 – Examples of sialogogues used in salivary gland scintigraphy (recommendations)

POS-SCAN INSTRUCTIONS

Although the activity administered to the patient is quite low, according to the **Basic Safety Standards (BSS)**, technologists should instruct the patient to minimise contact with pregnant women and children, to drink plenty of liquids and void frequently in the 24 hours after radiopharmaceutical injection. **Breastfeeding** recommendations should be repeated and confirmed by the end of the procedure, as detailed in the section Important aspects of patient history.

DATA PROCESSING

The protocol used for data processing may vary depending on the workstation used and from centre to centre. However, the same basic steps need to be followed.

Visual inspection

After acquisition, the images need to be visually inspected in order to identify

technical or patient-related artefacts that might require a repeat examination. It is especially important to check for motion artefacts.

In the case of movement, motion correction algorithms may be used. If motion correction is not successfully accomplished, the curves and the analysis results are less accurate. The study may be classified as invalid and a repeat examination may be needed on another day.

Drawing regions of interest (ROIs)

ROIs should be drawn over the salivary glands to produce time-activity curves (TACs). Each curve represents the function of a particular salivary gland.

ROIs should be defined on the frame immediately before administration of the stimulus, or on the composite image from the pre-stimulus phase, so that a better signal-to-noise ratio is obtained. Different sets of

ROIs are available. Manually drawn elliptical or irregular ROIs are the most commonly used for salivary gland delineation (bilateral parotid and submandibular glands). If the background subtraction is done, a background ROI should be defined in a location with poor vascularisation (cerebral region, supraclavicular region, midline neck region). A mouth ROI may also be drawn so that activity in the mouth can be graphically visualised over time [7, 12, 17, 18]. Figure 5 shows a possible representation of the ROIs on the composite image, as discussed above.

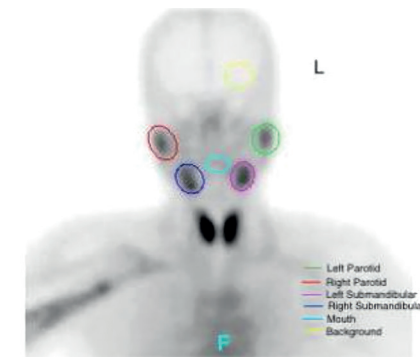


Figure 5 – ROIs on a composite image of dynamic frames
Courtesy of Nuclear Medicine Department – CUF Descobertas, Lisbon, Portugal

Generating time-activity curves (TACs)

The TACs are generated on the basis of the previously defined ROIs. TACs demonstrate the pattern of the radiopharmaceutical accumulation and clearance over time in each specific salivary gland (Figure 6 and 7). TACs should be decay-corrected, size-normalised and background-corrected. The sialogogue administration time should be indicated on the displayed curves. Be aware of motion artefacts; a sudden decrease in all curves may be due to movement of the salivary glands out of the ROIs, if not associated with the time of sialogogue administration [16, 21].

Visual presentation

Along with the TACs, the frames acquired in the dynamic study (reframed or otherwise) as well as any additional planar static images acquired should be

displayed for visual presentation; Fig. 6 and 7 show examples of visual presentation of the data.

When displayed, certain parameters may be changed to facilitate image interpretation: adjust scaling and colour maps, apply zoom factor, label images with relevant information, etc. [9].

Quantitative or semi-quantitative analysis can be performed, although no consensual parameters have been defined [3, 8, 12, 21].

MAJOR SCINTIGRAPHIC FINDINGS

After intravenous injection of the radiotracer, the trapping of ^{99m}Tc pertechnetate usually begins within the first minute of acquisition, increasing over time.

The parotid and submandibular glands are evaluated, while the sublingual glands are typically not visible.

Usually, tracer uptake by the parotid glands will be equal to or greater than that of the submandibular glands.

Mild activity will appear over time in the nasal and oral cavity (due to unstimulated salivary secretion); the thyroid gland uptake typically presents as equal to or greater than the uptake in the salivary gland complex.

The TACs generated demonstrate an initial fast uptake phase lasting for about 6 minutes and a slower increase afterwards, reaching a plateau at approximately the 10-minute mark.

Sialogogue administration will cause a sudden and symmetrical decrease of activity in all the glands, more pronounced in the parotid glands, as well as a marked increase of tracer activity in the oral cavity (see Fig. 6).

Acute sialadenitis, owing to the hyperaemia and oedema which may cause compression of the intralobular ducts, usually presents with a scintigraphic pattern of increased tracer uptake and retention.

In the setting of **chronic sialadenitis**, variable glandular uptake may be registered

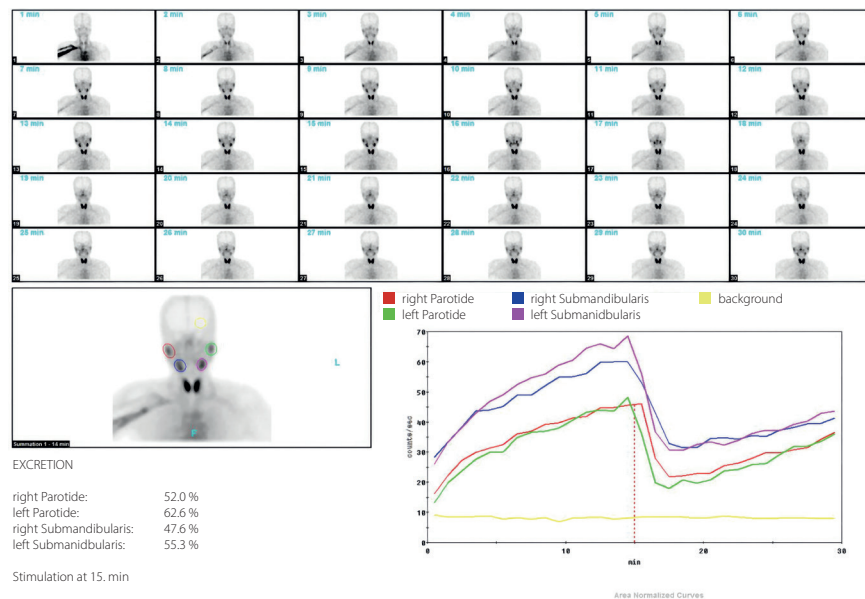


Figure 6 – Normal findings in salivary gland scintigraphy. Patient under evaluation for complaints of xerostomia. There is prompt and symmetrical uptake in the salivary glands from the first minute of the study. After administration of a sialogogue at the 15-minute mark, there is symmetrical emptying of the tracer from all four glands. Functioning and symmetrical submandibular and parotid glands. No evidence of obstructive pathology.

Courtesy of Nuclear Medicine Department – CUF Descobertas, Lisbon, Portugal

depending on the disease stage, with severely compromised uptake in its latter stages.

Sialolithiasis typically demonstrates a pattern of poor or absent tracer excretion after sialogogue administration and possibly dilated ducts. The overwhelming majority of salivary calculi (80 to 90%) occurs in the submandibular gland.

The technique is also useful for evaluation of the extent of the salivary involvement in **Sjögren's syndrome**. Semi-quantitative results appear to correlate with histological grading of glandular involvement [22].

Salivary gland scintigraphy, having historically been included in the diagnosis of Sjögren's syndrome and defined as positive if demonstrating reduced uptake or excretion of the radiotracer [23], was later omitted from the ACR-EULAR Diagnostic Criteria [24].

Some articles suggest that salivary gland scintigraphy's major use should be that of objectively quantifying the glandular dysfunction in Sjögren's syndrome, as opposed to the diagnosis of the disease itself [25, 26]. Scintigraphic findings, by themselves, show a correlation with the disease's severity, with the most severe patterns (see Fig. 7) being a risk factor for the development of extraglandular manifestations [27].

Despite some studies suggesting a preponderance of excretion-based indicators in this setting [6], other studies have supported the claim of tracer uptake parameters being more reliable for the

evaluation of Sjögren's syndrome [28]. Some studies have explored the possibility of obtaining more robust and reproducible quantitative data by resorting to the use of SPECT/CT imaging [19, 29].

Compromised salivary gland function is frequently seen after **radiotherapy in head and neck cancer patients**, as well as in patients following **radioiodine therapy for differentiated thyroid cancer**. In the latter, radioiodine is incorporated into the salivary glands due to the NIS receptor expression, with possible development of the phenomena of acute or chronic sialadenitis.

The possibility of acute sialadenitis post radioiodine therapy should be prevented by the use of sialogogues, like lemon sweets, as well as salivary gland massage. The parotid glands are frequently more affected; treatment should begin promptly to address progression.

Salivary gland excretion is typically the first one to be affected in the chronic phase. The maximum secretion and uptake ratio seems to provide a sufficient assessment of the extent of salivary gland damage [30].

Regarding **salivary gland mass lesions**, the majority of neoplastic lesions will appear as an area of increased perfusion and reduced tracer uptake, with the notable exception of benign functional salivary gland neoplasms like Warthin's tumour.

Ideally, the initial approach for salivary gland space-occupying lesions should consist of computed tomography or magnetic resonance imaging [7].

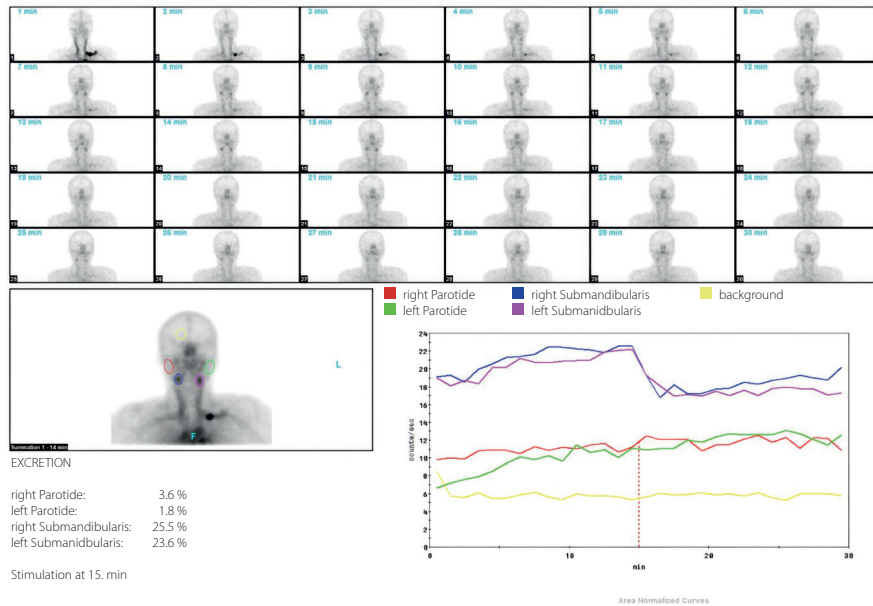


Figure 7 – Primary Sjogren's syndrome findings in salivary gland scintigraphy. There is severely reduced tracer uptake in both submandibular glands, and virtually no identifiable activity in the area corresponding to the parotid glands. Excretion profile evaluation is compromised due to severely impaired parenchymal uptake. TACs appear flattened, with severely decreased amplitude.

Courtesy of Nuclear Medicine Department – CUF Descobertas, Lisbon, Portugal

OTHER NUCLEAR MEDICINE IMAGING TECHNIQUES

Gallium-67 scintigraphy

[⁶⁷Ga]gallium has a pattern of non-specific uptake in both inflammatory and tumoural conditions.

The absence of gallium uptake will be supportive of a benign lesion or a low-grade tumour; focal uptake, on the other hand, can, in the appropriate clinical and imaging setting, support the diagnosis of Warthin's tumour.

Some studies have suggested the usefulness of [⁶⁷Ga]gallium scintigraphy as a supplement to [^{99m}Tc]pertechnetate scintigraphy in the evaluation of patients with Sjögren's syndrome [31].

[¹⁸F]FDG PET/CT

[¹⁸F]FDG uptake in the salivary gland is highly variable.

In the setting of Sjögren's syndrome, aside from assessing the salivary gland uptake/inflammation, it is suggested that the particular use of [¹⁸F]FDG positron emission tomography (PET) scan resides in evaluating systemic disease activity. Pathological uptake may be observed in up to 75 – 85% of patients, particularly in the salivary glands, lungs and lymph nodes [32].

The technique's spatial resolution may hinder the detection of some of the organic involvement, namely neuropathy and cutaneous vasculitis.

If used in the evaluation of MALT lymphoma associated with Sjogren's syndrome, the variable [¹⁸F]FDG activity and the possibility of false positive uptake in non-neoplastic lymph nodes should be taken into account [33].

REFERENCES

- Nakayama M, Okizaki A, Nakajima K, Takahashi K. Approach to Diagnosis of Salivary Gland Disease from Nuclear Medicine Images. *Salivary Glands - New Approaches in Diagnostics and Treatment* [Internet]. 2019 Jan 30; Available from: <http://dx.doi.org/10.5772/intechopen.70622>
- Klutmann S, Bohuslavizki KH, Kröger S, et al. Quantitative salivary gland scintigraphy. *J Nucl Med Technol.* 1999;27(1):20-26
- ChenYC, ChenHY, HsuCH. Recent Advances in Salivary Scintigraphic Evaluation of Salivary Gland Function. *Diagnostics (Basel).* 2021;11(7):1173. Published 2021 Jun 28. doi:10.3390/diagnostics11071173
- European Nuclear Medicine Guide. 2020. EANM and UEMS/EBNM. Chapter 6.1. Salivary Gland Scintigraphy. Available from: <https://www.nucmed-guide.app/#!/chapter/301>
- MacDonald A, Burrell S. Infrequently performed studies in nuclear medicine: part 2. *J Nucl Med Technol.* 2009;37(1):1-13. doi:10.2967/jnmt.108.057851
- Kaldewey HP, Ter Borg EJ, van de Garde EMW, Habraken JBA, van Buul MMC. Validation of quantitative salivary gland scintigraphy in relation to the American-European consensus criteria for Sjögren's syndrome. *Nucl Med Commun.* 2019;40(4):343-348. doi:10.1097/MNM.0000000000000983
- Wu CB, Xi H, Zhou Q, Zhang LM. The diagnostic value of technetium 99m pertechnetate salivary gland scintigraphy in patients with certain salivary gland diseases. *J Oral Maxillofac Surg.* 2015;73(3):443-450. doi:10.1016/j.joms.2014.09.013
- Chen J, Zhao X, Liu H, et al. A Point-Scoring System for the Clinical Diagnosis of Sjögren's Syndrome Based on Quantified SPECT Imaging of Salivary Gland. *PLoS One.* 2016;11(5):e0155666. Published 2016 May 19. doi:10.1371/journal.pone.0155666
- Farrell M, Mantel E, Basso D, Thomas K, Kerr B. Quick-Reference Protocol Manual for Nuclear Medicine Technologists. 1st Edition. USA: Society of Nuclear Medicine and Molecular Imaging Inc; 2014. *The Gastrointestinal System*; p. 181 - 183.
- Mattsson S, Johansson L, Leide Svegborn S, et al. Radiation Dose to Patients from Radiopharmaceuticals: a Compendium of Current Information Related to Frequently Used Substances [published correction appears in *Ann ICRP.* 2019 Sep;48(1):96] [published correction appears in *Ann ICRP.* 2019 Sep;48(1):97]. *Ann ICRP.* 2015;44(2 Suppl):7-321. doi:10.1177/0146645314558019
- American College of Radiology. ACR-ACNM-SNMMI-SPR Practice Parameter for the Performance of Gastrointestinal Tract, Hepatic, and Splenic Scintigraphy. Practice Parameter. Revised 2020; Available from: <https://www.acr.org/-/media/ACR/Files/Practice-Parameters/GI-Scint.pdf>
- Anjos DA, Etchebehere EC, Santos AO, et al. Normal values of [^{99m}Tc]pertechnetate uptake and excretion fraction by major salivary glands. *Nucl Med Commun.* 2006;27(4):395-403. doi:10.1097/01.mnm.0000202864.52046.b1
- Hwang JH, Han YH, Rahman MDT, Lee CS. Quantitative assessment of dry mouth in scrub typhus using salivary scintigraphy. *Sci Rep.* 2021;11(1):23633. Published 2021 Dec 8. doi:10.1038/s41598-021-03185-z
- Morris S, Ahmed J, Browning S. Sweet Shop Sialogogues: A Sour Solution to Sialolithiasis. *Cureus.* 2022;14(12):e32097. Published 2022 Dec 1. doi:10.7759/cureus.32097
- Akker H. Aspects of Salivary Gland Scintigraphy with ^{99m}Tc-Pertechnetate [dissertation on the internet]. Amsterdam: University of Amsterdam; 1988. [cited 2023 February 1]. Available from: https://inis.iaea.org/collection/NCLCollectionStore/_Public/20/026/20026566.pdf
- Tenhunen M, Collan J, Kouri M, et al. Scintigraphy in prediction of the salivary gland function after gland-sparing intensity modulated radiation therapy for head and neck cancer. *Radiother Oncol.* 2008;87(2):260-267. doi:10.1016/j.radonc.2008.02.017
- Gupta T, Hotwani C, Kannan S, et al. Prospective longitudinal assessment of parotid gland function using dynamic quantitative pertechnetate scintigraphy and estimation of dose-response relationship of parotid-sparing radiotherapy in head-neck cancers. *Radiat Oncol.* 2015;10:67. Published 2015 Mar 15. doi:10.1186/s13014-015-0371-2
- Hughes PM, Carson K, Hill J, Hastings D. Scintigraphic evaluation of sialadenitis. *Br J Radiol.* 1994;67(796):328-331. doi:10.1259/0007-1285-67-796-328
- Park J, Lee JS, Oh D, Ryoo HG, Han JH, Lee WW. Quantitative salivary gland SPECT/CT using deep convolutional neural networks. *Sci Rep.* 2021;11(1):7842. Published 2021 Apr 9. doi:10.1038/s41598-021-87497-0
- van Acker F, Flamen P, Lambin P, et al. The utility of SPECT in determining the relationship between radiation dose and salivary gland dysfunction after radiotherapy. *Nucl Med Commun.* 2001;22(2):225-231. doi:10.1097/00006231-200102000-00015
- Afzelius P, Fuglsang S. A kinetic compartment model for evaluating salivary gland scintigraphies. *Clin Physiol Funct Imaging.* 2014;34(2):143-150. doi:10.1111/cpf.12078
- Aksoy T, Kiratli PO, Erbas B. Correlations between histopathologic and scintigraphic parameters of salivary glands in patients with Sjögren's syndrome. *Clin Rheumatol.* 2012;31(9):1365-1370. doi:10.1007/s10067-012-2024-2
- Vitali C, Bombardieri S, Jonsson R, et al. Classification criteria for Sjögren's syndrome: a revised version of the European criteria proposed by the American-European Consensus Group. *Ann Rheum Dis.* 2002;61(6):554-558. doi:10.1136/ard.61.6.554
- Shiboski CH, Shiboski SC, Seror R, et al. 2016 American College of Rheumatology/European League Against Rheumatism Classification Criteria for Primary Sjögren's Syndrome: A Consensus and Data-Driven Methodology Involving Three International Patient Cohorts. *Arthritis Rheumatol.* 2017;69(1):35-45. doi:10.1002/art.39859
- Świecka M, Maślińska M, Paluch Ł, Zakrzewski J, Kwiatkowska B. Imaging methods in primary Sjögren's syndrome as potential tools of disease diagnostics and monitoring. *Reumatologia.* 2019;57(6):336-342. doi:10.5114/reum.2019.91273
- Ramos-Casals M, Brito-Zerón P, Perez-DE-Lis M, et al. Clinical and prognostic significance of parotid scintigraphy in 405 patients with primary Sjögren's syndrome. *J Rheumatol.* 2010;37(3):585-590. doi:10.3899/jrheum.090835
- Brito-Zerón P, Ramos-Casals M, Bove A, Sentis J, Font J. Predicting adverse outcomes in primary Sjögren's syndrome: identification of prognostic factors. *Rheumatology (Oxford).* 2007;46(8):1359-1362. doi:10.1093/rheumatology/kem079
- Nishiyama S, Miyawaki S, Yoshinaga Y. A study to standardize quantitative evaluation of parotid gland scintigraphy in patients with Sjögren's syndrome. *J Rheumatol.* 2006;33(12):2470-2474.
- Kim J, Lee H, Lee H, et al. Quantitative Single-Photon Emission Computed Tomography/Computed Tomography for Evaluation of Salivary Gland Dysfunction in Sjögren's Syndrome Patients. *Nucl Med Mol Imaging.* 2018;52(5):368-376. doi:10.1007/s13139-018-0547-4
- Raza H, Khan AU, Hameed A, Khan A. Quantitative evaluation of salivary gland dysfunction after radioiodine therapy using salivary gland scintigraphy. *Nucl Med Commun.* 2006;27(6):495-499. doi:10.1097/00006231-200606000-00004
- Luk WH, Yeung JTH, Fung EPY, Lok CM, Ng YM. Salivary Gland Scintigraphy in Patients with Sjögren's Syndrome: A Local Experience with Dual-tracer. *Asia Ocean J Nucl Med Biol.* 2017 Winter;5(1):56-65. doi: 10.22038/aojnmb.2016.8029. PMID: 28840140; PMCID: PMC5221687.
- Cohen C, Mekinian A, Uzunhan Y, et al. 18F-fluorodeoxyglucose positron emission tomography/computer tomography as an objective tool for assessing disease activity in Sjögren's syndrome. *Autoimmun Rev.* 2013;12(11):1109-1114. doi:10.1016/j.autrev.2013.06.012
- Keraen J, Blanc E, Besson FL, et al. Usefulness of 18 F-Labeled Fluorodeoxyglucose-Positron Emission Tomography for the Diagnosis of Lymphoma in Primary Sjögren's Syndrome. *Arthritis Rheumatol.* 2019;71(7):1147-1157. doi:10.1002/art.40829



GASTROINTESTINAL MOTILITY STUDIES

by Maryam Jessop

Nuclear Medicine Department, University Hospitals Sussex NHSFT

INTRODUCTION

Gastric emptying studies are physiological studies of gastric motor function and are used to assess gastric motility in a wide patient demographic, ranging from the very young to the elderly. Patients may be referred for these studies when presenting with post-prandial symptoms such as nausea or early satiety, vomiting, gastro-oesophageal reflux, aspiration, suspected rapid gastric emptying and upper abdominal discomfort. Clinical gastroparesis (delayed gastric emptying or gastric stasis), particularly in diabetic patients, can also be investigated, in addition to disease response to therapeutic procedures (1,2).

It is important to be aware of related conditions such as hiatus hernia and previous surgery, and whether the patients are taking prokinetic drugs which may need to be discontinued. The role of the nuclear medicine technologist is multifactorial, from ensuring proper patient preparation and looking at the clinical history and understanding why the test is being performed, to carrying out the imaging procedure (which can sometimes present certain challenges) and image processing. This chapter will look at these processes and perhaps give a few ideas on how to address some of the challenges that may arise.

PATIENT PREPARATION

To ensure standardisation of this process and subsequent validity of the results, it is important for the patient to understand the importance of following the instructions given to them. If the patient is particularly anxious (such as some with eating disorders), extra reassurance will go a long way to prevent vomiting at the time of the procedure. Facilitating special dietary requirements is useful at this juncture. Ideally, diabetic patients should have their study carried out in the morning, following their regular morning insulin dose 20–30 minutes prior to the study (3).

Fasting

The patient should fast for a minimum of 4 hours (2,3), with only a light meal prior to this. Anecdotal evidence suggests that this time can be reduced to 2 hours for young children having liquid gastric emptying studies.

Medication

Gastric emptying is altered by a number of medications, therefore these should be stopped for a period of time prior to the procedure, depending on their half-life. Prokinetic drugs, e.g. cisapride, metoclopramide, and domperidone, should be stopped 48 hours prior to the study (1), and erythromycin should be discontinued for 72 hours prior. Anticholinergic antispasmodic agents and antacids (1) should be stopped 1-2 days prior.

Laxatives should not be taken from the day prior. Opiates should not be taken on the day of the test, and, if possible, should be avoided from the day before. Pre-assessment of the patient (e.g. through a phone call) may prove valuable, as may the provision of a complete, easy-to-follow leaflet. Medication such as lansoprazole can be taken on the morning of the day before, but if taken on the morning of the test this can alter the transit of the meal through the stomach. Smoking also delays gastric emptying time, so this should be avoided on the day of the study until study completion (3).

MEAL PREPARATION

Perkins et al. (4) comment on the permutations of meal composition and their nature, saying that these are wide-ranging and scientifically diverse. The type of food and its calorific content affect the rate of gastric emptying (2). Gastric emptying has been shown to be faster after a fatty meal compared with a protein-based meal, highlighting the significance of food type in standardisation of gastric emptying studies (5). Volume may have an effect (2), however Bonner et al. (5) showed no significant correlation of volume with measured gastric emptying.

The use of a specific type and consistency of meal, e.g. solid, semi-solid, or liquid, may depend on the clinical question to be addressed, the age of the patient, their ability to swallow, and any surgery that has taken place. It is also important to ensure that any

feeding tubes are correctly placed in the stomach before proceeding with the study.

Liquid

Liquid studies are most often performed on children under the age of 8 years, in the experience of the author. Unavailability of normal ranges for solid and semi-solid studies in this age group is a contributing factor to this practice. Liquid studies are also performed in older children and adults, for reasons mentioned in the previous paragraph. Liquid gastric emptying studies may also prove useful in patients who are unable to tolerate a solid or semi-solid meal without vomiting, or those allergic to eggs.

[^{99m}Tc]Tc-DTPA can be used as the radiopharmaceutical for a liquid meal. 12 MBq is added to a glass of milk, which is then drunk through a straw to minimise radioactivity remaining in the mouth. An additional half a cup of non-radioactive milk is then swallowed to clear the activity remaining in the oesophagus into the stomach. Some departments use water or orange juice as a feed, with normal ranges adjusted accordingly. Flavoured milk can also be used.

[¹¹¹In]In-DTPA (5 MBq) can be used if transit of the whole gut is being assessed following the gastric emptying procedure (4). [¹¹¹In]In-DTPA can also be used in dual isotope simultaneous liquid and solid studies (1,3), which are performed less frequently. It is important to use scatter correction in these dual isotope acquisitions.

Alternative types of milk, such as soy, coconut, or almond milk, can be used for those with dairy intolerances. For patients with specific feeds that may be of a thicker consistency, these can be watered down to approximate the consistency of milk in an attempt to standardise the test as much as possible.

For feeds being administered through tubing, correct placement of the tubing can be verified by other imaging, or by withdrawing some fluid up through the tubing and testing the acidity with pH paper. Staff involved with the administration of radioactive feeds through feeding tubes should be suitably trained. It is important to ensure the use of the correct attachments for the enteral syringes which are to be connected to the feeding tube, and to place absorbent pads under the place where dose administration is occurring. Following administration of the radiopharmaceutical, a previously prepared syringe of non-radioactive feed should be used to flush the tubing, ensuring complete delivery to the stomach, and the tubing then closed or clamped. It is prudent to introduce the feed slowly so as not to cause regurgitation, but preferably the feed should still be completed within 5 minutes. When removing the enteral syringes and any attachments, wipe the end of the tubing to reduce the risk of surface contamination. Flushing with the non-radioactive feed is usually effective in removing most of the radioactivity from the feeding tube. There is no need to replace the feeding tube, and

the enteral syringes and any attachments are disposed of as normal radioactive waste.

Solid

Radiolabelled egg albumin is commonly used as a solid gastric emptying meal. It is labelled with Tc-99m sulphur colloid, as this binds to the egg white (not the yolks) (2,3). The egg whites are scrambled with 37 MBq Tc-99m sulphur colloid and microwaved, stirring a couple of times to reach the consistency of an omelette. The radiolabelled egg white is then administered orally, with toast or bread or as an egg sandwich. This has a labelling efficiency of approximately 85% (3). The meal should be eaten within 5–10 minutes.

Semi-solid

Radiolabelled mashed potato (7) or porridge (8) are meals commonly used in this category. They are generally better tolerated than the radiolabelled solid meal over a wide patient demographic, and are useful for those with an egg allergy. The porridge meal can also be adapted for those who require a gluten-free alternative or who are dairy-intolerant. The meal should be eaten within 5 minutes. Below are examples of recipes for semi-solid meals.

Radiolabelled mashed potato:

- » Swell 0.5 g Dowex anion exchange resin (2 X 8) (mesh 20–50), with 5–10 mL water for injection for 5 minutes, then withdraw excess fluid.

- » Dilute 37 MBq [^{99m}Tc]Tc-pertechnetate with enough water for injection, e.g. 5 mL, to immerse the swollen Dowex resin for 5 minutes, then withdraw excess fluid.
- » Reconstitute 200 g of potato mash.
- » Evenly mix the radiolabelled Dowex particles through the potato mash.

Porridge:

- » 5 mg 'All-Bran' (or another high-fibre wheat bran cereal) reconstituted and shaken with 20 ml of water for injection (Figure 1).



Figure 1 – 'All Bran' (5mg) reconstituted with 20mls water for injection.

- » 1 g Dowex anion exchange resin (1 x 4) (mesh 20–50) in a Sterilin universal container, swelled for 5 minutes with 5

mL water for injection. Withdraw excess water (Figure 2) and radiolabel Dowex resin with 15 MBq [^{99m}Tc]Tc-pertechnetate diluted to 5 mL with water for injection for 5 minutes. Then withdraw excess water, add reconstituted 'All Bran' to this container and shake vigorously to disperse the beads.

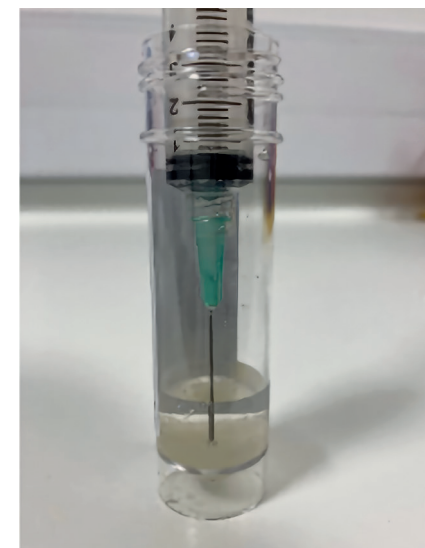


Figure 2 – Withdraw excess water from anion exchange resin (1mg) swelled with 5ml water for injection.

- » 50 g 'Ready Brek' (or another oat-based breakfast cereal that reconstitutes easily) reconstituted with 250 mL milk and then briefly microwaved.
- » Take the cooked porridge and add the radiolabelled Dowex and 'All Bran' mixture. Measure the residual activity in the 'All Bran' / Dowex container by placing

it in a glove so as not to contaminate the dose calibrator. Then shake porridge vigorously, or mix well if in a bowl. Mark the level of the porridge mixture on the container. This is now ready for the patient to eat, and once started should be ingested within 5 minutes (Figure 3).

- » A little sugar at the time of ingestion can be used to make the meal more palatable for those patients who strongly dislike the taste.



Figure 3 – Porridge (semi-solid meal) ready for ingestion.

Alternatives for patients with gluten-free requirements could include gluten-free porridge with gluten-free bran or 'Nutribex'. As already mentioned, soy, coconut, and almond milk can be chosen for those with dairy-free requirements.

Prior to meal ingestion

Before the patient ingests the meal, the equipment should be prepared (e.g. correct collimators and positioning of detectors) and the acquisition software initiated. General-purpose collimators are used to maximise the count statistics with the low radioactive dose. The usual ID checks and pregnancy status checks should be carried out and an explanation of the procedure given; check any medications that needed to be stopped, the patient's fasting status, and clarify any questions about the patient's history. This will avoid any delay in starting the imaging process. An apron or gown should be worn to prevent spillage onto the patient, hair should be secured, and the patient should be given gloves to wear to avoid contamination of clothing and the acquisition area.

PROCEDURE

Using pre- and post-meal images of the container with the radiolabelled meal is one way of accurately assessing how much the patient has eaten and the dose they have actually received. Alternatively, the practitioner can note the level on the container to estimate the proportion of the meal that is ingested. The meal should be ingested in 5–10 minutes, as described in the previous sections for the different types of meals.

Positioning

Procedures can be performed upright (Figure 4) or supine (Figure 5) depending on patient requirements and the clinical question(s) that have been asked by the referrer. The ability of the patient to stand for a short period makes performing the study in an upright position more convenient, as the patient can sit comfortably between images during this lengthy procedure. Lying down during liquid gastric emptying studies may be useful for the assessment of gastro-oesophageal reflux. Both types of positioning enable geometric means to be obtained, thus providing more accurate assessment of the radiolabelled meal in the stomach throughout the study. It is, of course, necessary for the patient to be positioned in such a way as to avoid movement during image acquisition. It is also helpful for the positioning to be reproducible to facilitate image processing (Figures 4 and 5).

For patients who are wheelchair bound, and especially those requiring neck support (e.g. those with a severe form of cerebral palsy), a camera head can be turned to an outward position and then angled downwards slightly. This will accommodate the imaging of the patient from an anterior aspect only, while the patient remains in their wheelchair.

Acquisition

General-purpose collimators and a 128x128 matrix are used to maximise count statistics. Imaging begins immediately



Figure 4 – Upright positioning



Figure 5 – Supine positioning

Solid and Semi-solid	T ₀ 30 second static image. 10-minute intervals up to 90 mins (30 second static images). 4-hour imaging, if delayed emptying (30 second static).
Liquid	T ₀ 30 second static image. 10 minute dynamic (30s / frame). Sequential 30 second images at 10-minute intervals, up to 60 minutes. Continue sequential imaging up to 90 minutes if delayed emptying.

Table 1 – Examples of acquisition sequences for solid, semi-solid, and liquid studies.

following ingestion of the meal. Sequential images of 30 seconds each or dynamic imaging are used, depending on the requirements of the study (Table 1). Imaging at four hours is increasing in use as it

increases the sensitivity of the study with added information, where less than or equal to 10% meal retention is considered normal (Figure 6) (9,1).

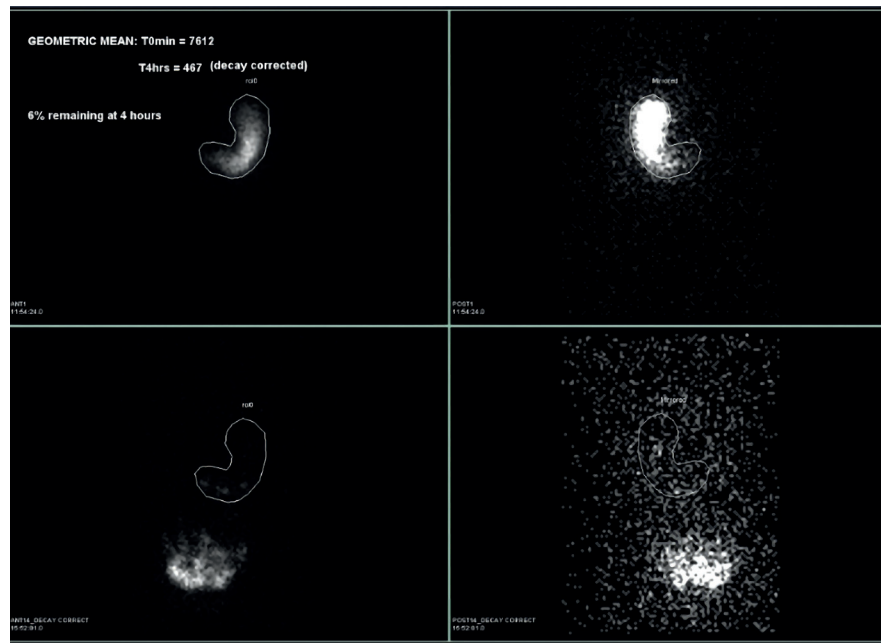


Figure 6 – Delayed imaging at four hours.

IMAGE ANALYSIS AND DISPLAY

Anterior and posterior images are used to obtain geometric mean data points. When drawing regions of interest (ROI) around the stomach ensure all the initial activity is included, particularly any still left in the oesophagus. Additionally, it is important to keep the ROI curved quite tight at the lower end of the stomach to avoid counts from the gut interfering with gastric emptying analysis (Figure 7). In addition, it is expedient to keep the ROIs

the same shape throughout the analysis unless there is interference from gut activity. Additional ROIs can be drawn to assess reflux, should any occur, and time-activity curves created.

There are various software packages in use for analysing gastric emptying, but whichever one is used, the images should be decay corrected. Applying power exponential modelling is useful in obtaining good curve fits from the resulting data to determine the gastric emptying half time

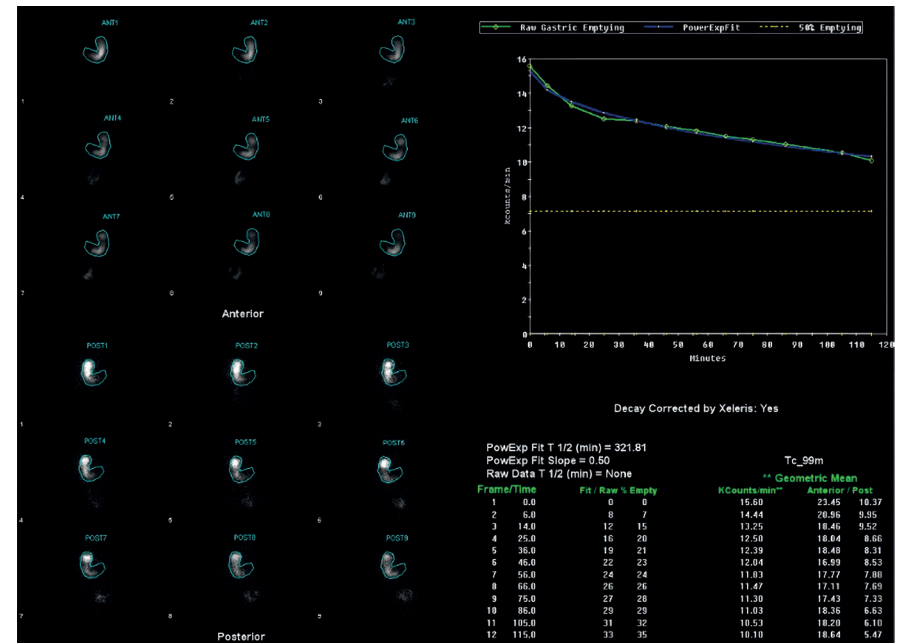


Figure 7 – Semi-solid gastric emptying with delayed emptying, demonstrating ROIs which are kept tight around the inferior aspect of the stomach.

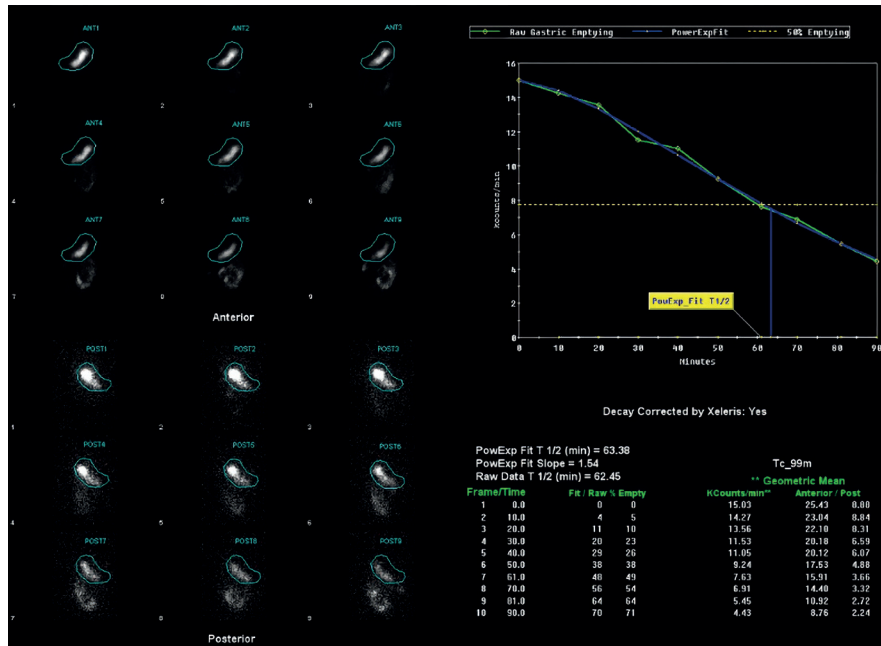


Figure 8 – Normal semi-solid gastric emptying study with power exponential fit applied.

(Figures 8 and 9) and examining lag times (10). As meal particle size reduces in the antrum, for solid meals there is an initial lag time of sometimes 20–30 minutes (2).

Suggested normal ranges for half-emptying time (HET): 18–73 minutes for the porridge meal (10) and 44–116 minutes for the scrambled egg meal (10). The HET for a normal liquid gastric emptying study has been suggested as approximately 23 minutes (2).

To manually process the 4-hour images (T_4), they first have to be decay corrected back to time zero (T_0). A ROI is drawn around

the stomach on the anterior T_0 , copied onto the decay-corrected (T_4) anterior image, and mirrored onto the posterior images at T_0 and T_4 . Geometric means are obtained, after which the percentage remaining is calculated (Figure 6).

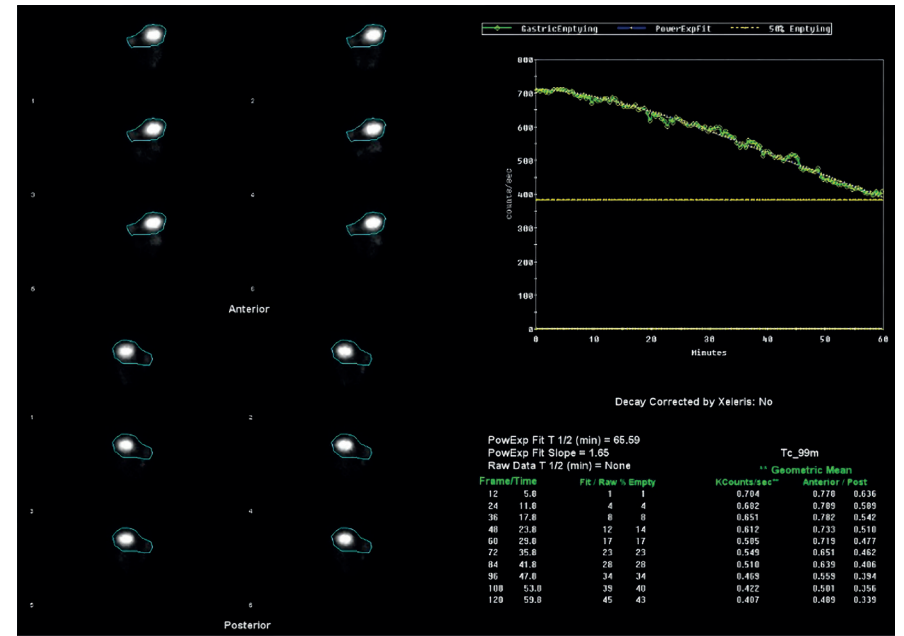


Figure 9 – Delayed liquid gastric emptying study with power exponential fit applied.

FINAL REMARKS

While a gastric emptying study is a seemingly simple study to perform, obtaining good results relies on attention to detail and detailed preparation. As always, care when drawing the ROI as the data is being analysed can prevent artefact in the results. Finally, we should acknowledge the anxieties in this particular group of patients and respond accordingly.

REFERENCES

1. Banks KP, Syed K, Parekh M, McWhorter N. Gastric Emptying Scan. [Internet] Treasure Island (FL): StatPearls Publishing; Last update Sept 2022. Available from: <https://www.ncbi.nlm.nih.gov/books/NBK531503>
2. Farrell M. Gastric Emptying Scintigraphy. Originally published in: Abdominal Imaging 2017: Quality, Safety, & Dose Optimization in 2017. JNMT 2019; 47(2):111-119. doi: 10.2967/jnmt.117.227892
3. Seok J. How to interpret Gastric Emptying Scintigraphy. J Neurogastroenterol Motil 2011; 17(2):189-191. doi: 10.5056/jnm.2011.17.2.189
4. Perkins A, Hay P, Corsetti M. Gastric emptying: a dog's dinner. Nucl Med Commun. 2020; 41(6):497-498. doi: 10.1097/MNM.0000000000001195
5. Bonner J, Vajjah P, Abduljalil K, Jamei M, Rostami-Hodjegan A, Tucker G, et al. Does age affect gastric emptying time? A model-based meta-analysis of data from premature neonates through to adults. Biopharm. Drug Dispos. 2015; 36:245-257
6. Donohoe K, Maurer A, Ziessman H, Urbain J, Royal H, Martin-Comin J. Procedure Guideline for Adult Solid-Meal Gastric-Emptying Study 3.0. J Nucl Med Technol. 2009; 37(3):196-200
7. Lipp R, Hammer H, Schnedl W, Dobnig H, Passath A, Leb G, et al. A simple scintigraphic method for continuous monitoring of gastric emptying. Eur J Nucl Med 1993; 20:260-263
8. Rydning A, Berstad A, Berstad T, Hertenberg L. The effect of guar gum and fiber enriched wheat bran on gastric emptying of a semi-solid meal in healthy subjects. Scand J Gastroenterol. 1985 Apr; 20(3):330-4
9. Pathikonda M, Sachdeva P, Malhotra N, Fisher RS, Maurer AH, Parkman HP. Gastric emptying scintigraphy: is four hours necessary? J Clin Gastroenterol 2012 Mar; 46(3):209-15. doi: 10.1097/MCG.0b013e31822f3ad2
10. Hansrod S, Janes G, Notghi A, Croasdale J, O'Brien J, Thomson W. Gastric emptying: methodology and normal ranges for two commonly used meals in the UK. Nucl Med Commun. 2020 July; 41(7):p 636-650. doi: 10.1097/MNM.0000000000001209

ACKNOWLEDGEMENTS

Nuclear Medicine Department, University Hospitals Sussex NHS Foundation Trust (East), Brighton, UK

GASTROINTESTINAL BLEEDING AND ECTOPIC GASTRIC MUCOSA

by *Gracinda Costa*¹
*Raquel Silva*²

¹*Nuclear Medicine Department, Hospital and University Centre of Coimbra,
Coimbra, Portugal*

²*Nuclear Medicine Technologist at Hospital and University Centre of Coimbra, CHUC-HUC,
Visiting Assistant Professor at ESTeSC, Coimbra Health School*

INTRODUCTION

Gastrointestinal bleeding (GIB) is a frequent condition, present in several digestive system disorders with varying degrees of severity. Bleeding can occur anywhere along the 8–10 metres of digestive tract, can be acute or chronic, continuous or intermittent, heavy or light, can range from mild to severe and can even be a life-threatening event.

Signs and symptoms of GIB can be either *overt* (clinically obvious, characterised by visible blood loss, such as haematemesis, haematochezia or melaena) or *occult* (hidden blood loss which, due to its microscopic nature, is only detected on guaiac faecal occult blood testing). When, after a complete initial work-up (including endoscopic and radiological procedures), the origin of persistent/recurrent *overt* or *occult* blood loss is unclear, GIB is classified as *obscure*.

Although it is more common in adults, especially the elderly, GIB can also be found in younger age groups, including children. In a very general approach, the most common primary causes of GIB include angiodysplasia, peptic ulcers, several different inflammatory diseases of the digestive tract, oesophageal varices, neoplasms, diverticula/diverticulosis, polyps, infectious bowel disease and Meckel's diverticulum (MD). MD is the most common cause of lower GIB in previously healthy infants (1).

As the choice of treatment for GIB depends on the correct diagnosis, medical

imaging, including radiological and endoscopic techniques, plays an important role in this context and is often needed to locate and determine the cause of the bleeding. However, whenever some features are combined, the imaging investigation of GIB can include nuclear medicine techniques.

NUCLEAR MEDICINE IMAGING IN PATIENTS WITH GASTROINTESTINAL BLEEDING

Nuclear medicine provides a purely functional approach to GIB by offering two different non-invasive imaging techniques focused on this specific context. One detects the bleeding and the other identifies one of the possible causes of bleeding:

- » Gastrointestinal bleeding scintigraphy – **detects** active bleeding;
- » Meckel's diverticulum scintigraphy – identifies whether Meckel's diverticulum is the **cause** of active bleeding.

GASTROINTESTINAL BLEEDING SCINTIGRAPHY

Gastrointestinal bleeding scintigraphy (GIBS) is an easy, safe and non-invasive nuclear medicine study, focused on detecting digestive tract bleeding. It was first described in the USA by Alavi et al., who in 1977 used ^{99m}Tc-sulphur colloid (2). Also in 1977, in Europe, Miskowiak et al. described the use of ^{99m}Tc-human serum albumin, and in 1979, at the Massachusetts General Hospital, Winzelberg et al. introduced the

^{99m}Tc-labelled autologous red blood cells (RBC) methodology (3,4).

Although GIBS does not provide anatomical and structural details concerning the origin of bleeding, it combines several advantages over first-line imaging examinations (*computed tomography angiography* and *endoscopy*) (5,6):

- » Is positive with a bleeding rate as low as 0.1 mL/min;
- » Allows for continuous monitoring over several hours (up to 24 hours);
- » Does not require bowel preparation;
- » Has no contraindications;
- » Is well tolerated.

Clinical indications

As upper digestive bleeding is easily identified using a nasogastric lavage, and guaiac faecal occult blood testing may detect bleeding at rates well below 0.1 mL/min, GIBS turns out to be more useful in **mid or lower overt GIB**, including bleeding of **obscure origin**. In that context, the main indications, according to *The SNMMI Procedure Standard/EANM Practice Guideline for Gastrointestinal Bleeding Scintigraphy 2.0* (5), include:

- » Determining whether the bleeding is active;
- » Localising the bleeding site;
- » Estimating the rate of blood loss for prognostic purposes.

The information provided by GIBS can assist in clinical decision-making on whether to perform invasive procedures such as *catheter angiography* or *surgery*.

Optimal timing of gastrointestinal bleeding scintigraphy

GIBS has the best detection rates in ***overt*** bleeding. ***Occult*** bleeding, identified by guaiac faecal testing, has a lower sensitivity and, therefore, is not an appropriate indication. Very often, the slow or intermittent microscopic or low-volume blood loss identified in stool is below the scintigraphy detection limit (4, 5).

Contraindications

There are no absolute contraindications for GIBS.

Importance of patient's personal history

It is important to collect all clinical information to help characterise the blood loss. It is also important to have the following information (4):

- » The results of other diagnostic investigations carried out to study the clinical situation;
- » The patient's medication, since the efficacy of RBC radiolabelling can be affected by several drugs;
- » Whether or not the patient has undergone examinations with oral contrast agents like barium, as these can produce artefacts in the images and the findings can be hidden.

Specific patient preparation

GIBS does not require specific patient preparation. However, it is important to consider the following aspects (5):

- » Fasting is not required for GIBS unless other diagnostic procedures or surgery are being considered for the patient;
- » If haemodynamically unstable, a nurse or physician should monitor the patient during the procedure;
- » Patients should empty the bladder before each image acquisition, both for their own comfort and because urine activity may obscure sigmoid or rectal bleeding.

Relevant information for the patient

The patient should be **clearly informed** about all steps of the procedure. It is important to emphasise the need to handle and reinject blood, as religious beliefs may reject this practice. The patient should be alerted to the possible need for imaging for up to 24 hours.

Written informed consent

A written informed consent document may be needed for the procedure, in accordance with the applicable legislation in each country.

Radiopharmaceuticals

Autologous RBC radiolabelled with $[^{99m}\text{Tc}]\text{NaTcO}_4^-$ ($[^{99m}\text{Tc}]\text{Tc-RBC}$) has shown diagnostic superiority over other radiopharmaceuticals such as radiolabelled sulphur colloid (4,7). Additional information regarding radiopharmaceuticals available for GIBS can be found in Chapter 2.

Erythrocyte radiolabelling techniques

There are **three methods** to radiolabel the RBC: *in vivo*, modified *in vivo* and *in vitro*. All methods are based on a redox reaction: $[^{99m}\text{Tc}]\text{NaTcO}_4^-$ diffuses across the red cell membrane and is reduced by the stannous ions previously administered. The reduced $[^{99m}\text{Tc}]\text{NaTcO}_4^-$ binds to the β -chain of haemoglobin (4,8). Table 1 summarises advantages, disadvantages, and the labelling efficiency of each method.

Erythrocyte radiolabelling efficiency

Both high efficiency and **in vivo stability** of RBC labelling are crucial to produce good-quality images. Free $[^{99m}\text{Tc}]\text{NaTcO}_4^-$ negatively impacts the diagnostic accuracy of the procedure, once the tracer leaves the vascular compartment and accumulates in salivary glands, thyroid and gastrointestinal tract. Such a biodistribution pattern results in a lower target-to-background ratio, so imaging interpretation will be compromised.

There are several factors that can decrease RBC labelling efficiency, including technical problems (Table 2) and drug interaction, low haematocrit level and other problems (Table 3).

Activity and dosimetry

According to *The SNMMI Procedure Standard/EANM Practice Guideline for Gastrointestinal Bleeding Scintigraphy 2.0* (5), the recommended $[^{99m}\text{Tc}]\text{NaTcO}_4^-$ activities for RBC labelling are:

- » Adult patients – 555 to 1110 MBq (15 to 30 mCi);
- » Patients < 18 years old – based on the *EANM Paediatric Dosage Card (Version 5.7.2016)* (9), which uses a baseline activity of 56 MBq (1.51 mCi) multiplied by a weight-based multiple [range: 80 MBq (2.16 mCi) to 784 MBq (21.19 mCi)].

Considering the above-mentioned activities of $[^{99m}\text{Tc}]\text{Tc-RBC}$, the radiation dose to the patient is relatively low if ALARA principles are applied.

- In adult patients, the estimated (5):
- » Absorbed dose in the heart = 0.023 mGy/MBq
- » Effective radiation dose = 0.0070 mSv/MBq
- » Whole-body dose = 4 mSv/925 MBq

The critical organs for $[^{99m}\text{Tc}]\text{Tc-RBCs}$ are the spleen and the myocardial wall (10).

Instructions should be given to patients after the exam in order to minimise radiation exposure to family members, children and the public. CT dose reduction protocols should be used whenever SPECT/CT is performed.

In pregnant women, a careful risk-benefit analysis should be performed, balancing the potential benefit of the scan against the potential risks of ionising radiation. In lactating patients, breastfeeding should be interrupted for 12 hours (5,11).

Imaging acquisition protocols

Typically, the GIBS image protocol includes a dynamic early-phase acquisition (flow study) followed by an extended

dynamic equilibrium-phase acquisition of the abdomen and pelvis. Serial intermittent static images are not recommended (5). The dynamic early-phase acquisition starts immediately after administration of the radiolabelled $[^{99m}\text{Tc}]\text{Tc-RBCs}$. Table 4 summarises the main aspects relating to image acquisition (5).

Processing the results

Cinematic display of the dynamic images (initial and delayed) is fundamental in order to improve diagnostic performance and ensure accurate localisation of the bleeding site (4). For SPECT or SPECT/CT, refer to the *SNMMI Guideline for General Imaging*. If the patient moves during the acquisition, motion correction software can be used (5).

	<i>In Vivo</i>	Modified <i>In Vivo</i>
Concept	The entire labelling process is performed inside the patient	The labelling process is performed inside and outside the patient
Technique Description	I.V. administration of stannous pyrophosphate (15µg/kg body weight)	I.V. administration of stannous pyrophosphate (15µg/kg body weight)
	20–30 minute interval	20–30 minute interval
		Preparation of a shielded syringe containing 555–1110 MBq (15–30 mCi) of $^{99m}\text{Tc}[\text{NaTcO}_4^-]$ and an anticoagulant (ACD solution or heparin)
		Withdraw 5–8 mL of blood to the pre-prepared syringe using an I.V. line that remains attached to the patient during incubation
		10-minute incubation period – the contents of the syringe are gently agitated at room temperature
	I.V. administration of 555–1110 MBq (15–30 mCi) of $^{99m}\text{Tc}[\text{NaTcO}_4^-]$	^{99m}Tc -RBC administration to the patient
RBC labelling efficiency	75%–80% (sometimes < 65%)	85%–90%
Advantages	Simple	Improved labelling efficiency
	Rapid	Improved target-to-background ratio
Disadvantages	Free or reduced outside RBC $^{99m}\text{Tc}[\text{NaTcO}_4^-]$ may degrade image quality	Good but suboptimal image quality
Routine use	Not recommended (option for patients that do not accept injection of blood)	Good alternative when the in vitro methods are not available

Table 1 – Methods of labelling red blood cells with $^{99m}\text{Tc}[\text{NaTcO}_4^-]$: comparison between in vivo, modified in vivo and in vitro methods (Brookhaven and commercial kit) (4,8,10)

<i>In Vitro (Commercial Kit)</i>	<i>In Vitro (Brookhaven)</i>
The entire labelling process is performed outside the patient	The entire labelling process is performed outside the patient
Addition of 1–3 mL of heparinised blood to the reagent vial (50–100 µg SnCl_2 + 3.67 mg sodium citrate)	Addition of 4 mL of heparinised blood to the reagent vial (2 mg Sn^{2+} + 3.67 mg sodium citrate + 5.5 mg dextrose + 0.11 mg NaCl)
Incubation for 5 minutes	Room temperature incubation of blood mixture for 5 minutes
Addition of syringe-1 contents (0.6 mg of NaClO and mix by inverting four or five times	Addition of 2 mL of 4.4% EDTA
Addition of syringe-2 contents (8.7 mg citric acid + 32.5 mg sodium citrate + dextrose) and mix	Centrifugation for 5 minutes at 1300 g
Addition of 370–3700 MBq (10–100 mCi) of $^{99m}\text{Tc}[\text{NaTcO}_4^-]$ to the reaction vial	Withdraw 1.25 mL of packed RBC and transfer to sterile vial containing 555–1110 MBq (15–30 mCi) of $^{99m}\text{Tc}[\text{NaTcO}_4^-]$
Incubation for 20 minutes to react, with occasional mixing	Incubation of RBC at room temperature for 10 minutes
^{99m}Tc -RBC administration to the patient	^{99m}Tc -RBC administration to the patient
≥ 95%	≥ 98%
Excellent labelling efficiency	Higher labelling efficiency
Radiolabelling efficiency can be evaluated	Radiolabelling efficiency can be evaluated
A salvage technique may be attempted whenever radiolabelling efficiency is suboptimal	A salvage technique may be attempted whenever radiolabelling efficiency is suboptimal
The best labelling efficiency and target-to-background ratio	The best labelling efficiency
Commercial ready-to-use kit (simplified procedure) No centrifugation needed	The best target-to-background ratio
More costly	Time-consuming
Best option (rapid and high labelling efficiency)	Best option (low cost and high labelling efficiency)

ACD – anticoagulant citrate dextrose; EDTA – ethylenediamine tetraacetic acid; I.V. – intravenous; NaCl – sodium chloride; NaClO – sodium hypochlorite; RBC – red blood cells; SnCl_2 – stannous chloride; Sn^{2+} – stannous ion

Cause	Mechanism of disrupted radiolabelling
Stannous ion (Sn^{2+})	Insufficient Sn^{2+} compromises the Tc^{7+} reduction. Too much Sn^{2+} will result in Tc^{7+} reduction outside the RBC
Interval between Sn^{2+} and $^{99m}\text{TcNaTcO}_4$ administration	< 20 minutes, tinning cannot occur
$^{99m}\text{TcNaTcO}_4$ from an "old elution"	Carrier ^{99}Tc presence
$^{99m}\text{TcNaTcO}_4$ exposure to air	$^{99m}\text{TcNaTcO}_4$ oxidation
Injection of Sn^{2+} and $^{99m}\text{TcNaTcO}_4$ in the same intravenous line	$^{99m}\text{TcNaTcO}_4$ reduction outside the RBC
Improper syringe flushing (e.g. with dextrose instead of saline)	$^{99m}\text{TcNaTcO}_4$ reduction in the line

Table 2 – Low RBC labelling efficiency associated with technical problems.

Adapted from Mariani G. et al. *Radionuclide Evaluation of the Lower Gastrointestinal Tract. Journal of Nuclear Medicine. 2008 May;49(5):776–787. RBC – red blood cells; Sn^{2+} – stannous ion*

Cause	Mechanism or comment
Heparin	Formation of complexes with $^{99m}\text{TcNaTcO}_4$ in the presence of Sn^{2+} , causing renal excretion
Methyl dopa / Hydralazine	Sn^{2+} oxidation; decrease in reduction capacity
Quinidine / Dipyridamole	Possible increase in production of antibodies to RBC / transmembrane transport inhibition
Doxorubicin	Decreased RBC labelling efficiency in proportion to drug concentration
Digoxin, calcium channel blockers, cyclosporin, metronidazole, ranitidine, propranolol	Sn^{2+} uptake interference
Iodinated contrast (less than 24h before GIBS)	Multiple mechanisms: Sn^{2+} distribution alteration, competition for RBC binding sites, decrease in Sn^{2+} reduction capacity, alteration of $^{99m}\text{TcNaTcO}_4$ binding
Recent blood transfusion / transplantation	Unknown / circulating antibodies to RBC / cell membrane alteration
Low haematocrit value	$^{99m}\text{TcNaTcO}_4$ reduction outside RBC
Sickled red blood cells / Thalassemia	Impaired labelling due to abnormal haemoglobin structure
Chocolate	Unknown
Tobacco	Sn^{2+} oxidation, possible damage to RBC plasma membrane or possible chelating action on Sn^{2+} or $^{99m}\text{TcNaTcO}_4$ ions
Renal failure, recent stroke, acute myocardial infarction, diabetes mellitus	Unknown

Table 3 – Low RBC labelling efficiency associated with drugs and related factors (4,5,10)
GIBS – gastrointestinal bleeding scintigraphy; RBC – red blood cells; Sn^{2+} – stannous ion

Patient Position in the Gamma Camera	Gamma Camera Settings	Imaging Acquisition Protocol
Patient must remove any item that can produce image artefacts	A large field of view gamma camera is recommended	An initial 60-second flow study (angiographic phase) can be performed, with 1–3 seconds/frame
Supine position	A dual-head gamma camera is recommended (increases sensitivity and may enhance visualisation of a rectal bleed)	Followed by a minimum of 60 minutes dynamic acquisition with no more than 60 seconds/frame (alternatively, dynamic images can be obtained in 10-to-15-minute sequences, which may facilitate review of the images)
Patient's upper extremities should be kept outside the abdominal and pelvic regions (to prevent image artefacts and obscure findings)	Low-energy high-resolution collimator	If the bleeding site is not identified, the study should be extended with delayed images acquired up to 24h (typically at 2–6 h or 18–24 h). Dynamic acquisitions are recommended, with the same frame rate as described above.
Detector positioned in anterior view with abdomen and pelvis in the field of view	Energy photopeak centred on 140 keV (^{99m}Tc) with a 20% window	Since GIB occurs intermittently, the patient should be imaged continuously for as long as practical to identify the bleeding source as delayed images increase the likelihood of localising the site of bleeding
	Matrix (minimum): 128x128	Lateral views can be helpful in differentiating anterior vascular penile activity (which can move or change in intensity during imaging) from bleeding in the more posteriorly located rectosigmoid colon
	SPECT or SPECT/CT gamma camera can be used for more precise localisation of the bleeding site	For in vivo quality control of RBC labelling, gastric and thyroid images to confirm the presence of free $^{99m}\text{TcNaTcO}_4$ (if gastric activity is visualised)

Table 4 – Image acquisition description for gastrointestinal bleeding scintigraphy (4,5)

RBC – red blood cells; GIB – gastrointestinal bleeding; SPECT – single-photon emission computed tomography; SPECT/CT – single-photon emission computed tomography/computed tomography

Image interpretation

Normal biodistribution of [^{99m}Tc]Tc-RBCs includes the cardiac blood pool, great vessels, liver, spleen, penile circulation and, usually mildly, kidneys and bladder.

Specific standard criteria must be followed (5) to avoid incorrect interpretations of GIBS images (Table 5). All the stated criteria must be satisfied in order to diagnose active bleeding.

GIBS has limitations when it comes to identifying the bleeding site. However, with correct interpretation of the study using the **Standard Diagnostic Criteria**, followed by close observation of the pattern and behaviour of the abnormal focal activity over time (Table 6), it is possible to identify the origin of the bleeding (5) (Figures 1 and 2).

Also, SPECT or SPECT/CT images help with interpretation of the GIBS (4). Yoichi Otomi et al. (6) showed the additional value of SPECT or SPECT/CT in the localisation of the bleeding site. Nevertheless, no data exist on the use of SPECT/CT when planar GIBS shows no evidence of gastrointestinal bleeding (5).

The bleeding site can usually be localised to the proximal or distal small bowel, caecum, ascending colon, hepatic flexure, transverse colon, splenic flexure, descending colon, sigmoid colon, or rectum. This information can serve as a guide when selecting the vessel for contrast injection in angiography (coeliac, superior mesenteric or inferior mesenteric artery) (10).

Standard diagnostic criteria for positive [^{99m}Tc]Tc-RBC scintigraphy

Focal activity appears outside the expected anatomical blood pool structures
Focal extravascular activity appears in an area where none was seen initially
Activity increases over time
Activity moves in a pattern consistent with intestinal anatomy, which might be antegrade or retrograde

Table 5 – Standard criteria for gastrointestinal bleeding diagnosis with [^{99m}Tc]Tc-RBC scintigraphy. RBC – red blood cells.

Bleeding site	Image Pattern and Behaviour
Small bowel	Usually central in the abdomen or pelvis
	Rapidly through the small curvilinear intestinal loops
Large bowel	Usually occurs in the periphery of the abdomen or pelvis
	More linear pattern
Rectosigmoid	Usually central pelvis
	S-shaped pattern

Table 6 – Image patterns for bleeding localisation.

Quality criteria and artefacts

It is very important to be aware of some pitfalls that can interfere with correct image interpretation. These can be due to **physiological, technical or pathological factors** (4,5,10).

- » Free [^{99m}Tc]NaTcO₄: caused by poor radiolabelling or dissociation of the labelled RBCs *in vivo*, would be considered a technical pitfall. The uptake of free [^{99m}Tc]NaTcO₄ can be visualised in the salivary glands, in the upper gastrointestinal tract secondary to swallowed saliva, in the gastric mucosa and in the urinary tract. As free [^{99m}Tc]NaTcO₄ can move from the stomach into the small bowel over time, it can be mistaken for upper gastrointestinal bleeding. In order to avoid misinterpretation, images of the neck to detect thyroid and salivary gland activity should be obtained to confirm the presence of free [^{99m}Tc]NaTcO₄.
- » Increased RBC activity due to other causes: rectal bleeding, uterine activity with menses and normal penile blood pool can be misunderstood as GIB. Lateral or anterior oblique views of the abdomen and pelvis may be helpful to clarify the image interpretation.

- » Vascular causes: include aneurysms of the abdominal aorta and other arterial vessels, vascular grafts, arterial leaks, aortoduodenal fistula rupture, liver or small bowel haemangiomas, and abdominal varices. Varices are most commonly seen as static blood pool structures, but they can also rupture and cause bleeding.
- » Increased uptake can be visualised in accessory spleen, ectopic kidneys and renal transplants, all of which show fixed and non-moving activity. Activity clearing through the hepatobiliary system and gallbladder may be related to a rare haemobilia; however, patients with renal failure may have gallbladder visualisation as a result of radiolabelled fragmented haem breakdown products (porphyrins).

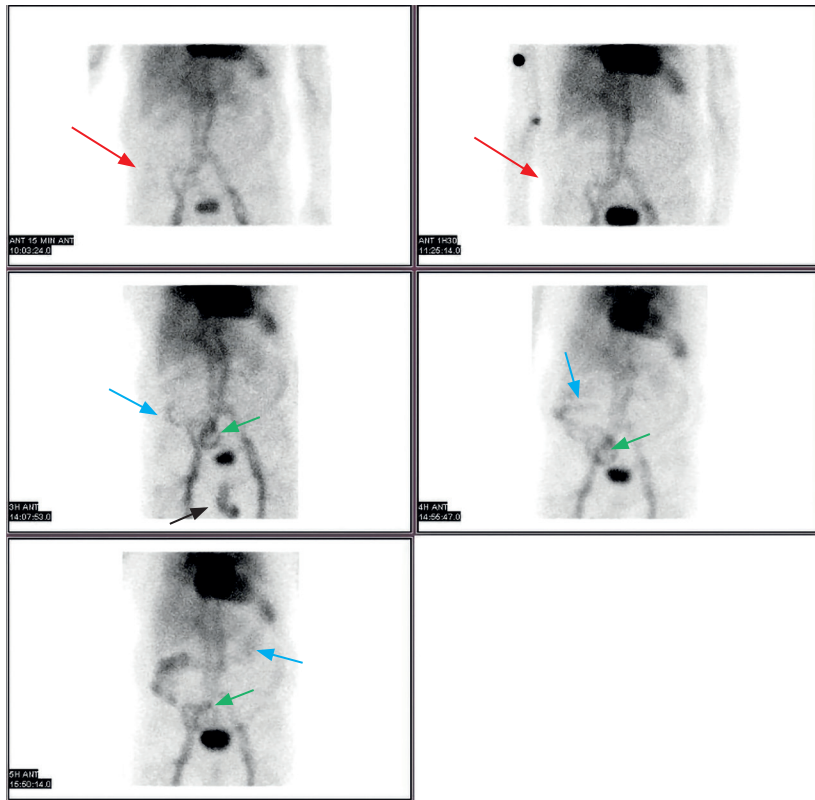


Figure 1 – 86-year-old man with melaena. Patient refuses colonoscopy. Gastrointestinal bleeding scintigraphy was performed: in early images, faint abnormal RBC accumulation was observed in the periphery of right flank (red arrow). Activity increases over time and moves anterograde (blue arrow) and retrograde (green arrow), in a pattern consistent with intestinal anatomy. In the report, this behaviour was related to active bleeding in ascending colon. Physiological penile activity (black arrow). RBC – red blood cells.

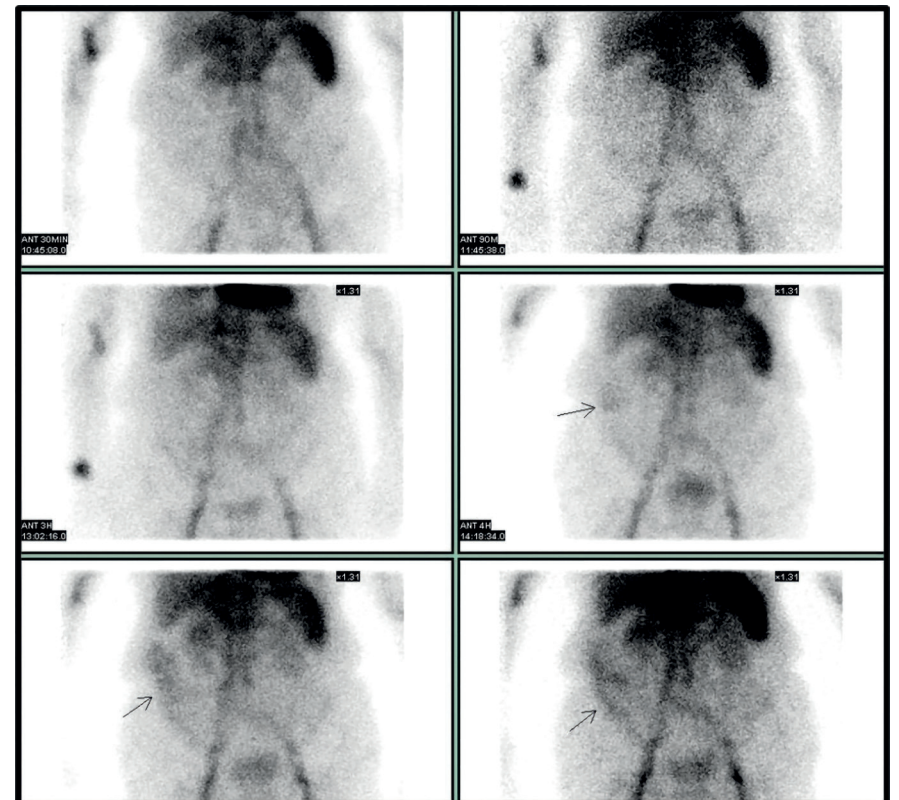


Figure 2 – 74-year-old woman with melaena. Colonoscopy was inconclusive. Gastrointestinal bleeding scintigraphy was performed: abnormal RBC accumulation was observed in the periphery of right flank (arrow) and related to active bleeding in ascending colon. The scan was positive only 4 hours after ^{99m}Tc -RBC injection. RBC – red blood cells.

MECKEL'S DIVERTICULUM SCINTIGRAPHY

In 1967 Harden proposed the use of the radiotracer $[^{99m}\text{Tc}]\text{NaTcO}_4^-$ for the non-invasive diagnosis of **ectopic gastric mucosa** in a Meckel's diverticulum (MD). At present, *Meckel's diverticulum scintigraphy* (MDS) has an accuracy of around 90% in detecting ectopic gastric mucosa (12).

MD corresponds to the vestigial remnant of the omphalomesenteric duct, is the most common structural congenital anomaly of the gastrointestinal tract, and is responsible for more than 50% of unexplained lower gastrointestinal tract bleeding in children (12).

It was first described in 1598 by Wilhelm Fabry von Hilden and intensively studied by Johann Friedrich Meckel in 1809 (13). It is frequently located in the distal ileum, and ectopic gastric mucosa, present in about 50%–60% of cases, secretes the hydrochloric acid responsible for mucosal ulcerations (12).

A feature of MD is the *Rule of Twos*: it affects about 2% of the population, is two times more frequent in males, can have two main types of ectopic tissue (gastric and pancreatic) and 2% become symptomatic, presenting in the first 2 decades of life and often within the first 2 years.

Because most cases are asymptomatic, diagnosis of MD is typically made in one of two clinical situations:

- » Incidental finding during surgery;
- » Occurrence of complications (acute diverticular inflammation, ulceration, haemorrhage, small bowel obstruction,

perforation, retained foreign bodies, enterolith formation, and neoplasm development).

Bleeding from an MD can occur at any age, but is far more common in children; it requires surgical resection.

Clinical indications

As bleeding from an MD usually occurs in young children, *Meckel's diverticulum scintigraphy* (MDS) is mainly performed in paediatric care settings. The main clinical indication is to localise ectopic gastric mucosa in an MD, often the cause of unexplained intermittent lower GIB in children (1,12).

Optimal timing of Meckel's diverticulum scintigraphy

MDS should be performed when the patient is not actively bleeding. Active bleeding is best studied by GIBS, followed by MDS in negative cases and if concern about MD persists (1,12).

The interval between $[^{99m}\text{Tc}]\text{Tc}$ -RBC scintigraphy and MDS depends on the method of RBC labelling used, being shorter (about 24 hours) for in vitro labelling. The larger amount of stannous ions used in the in vivo method, which can persist for up to a week, shifts the $[^{99m}\text{Tc}]\text{NaTcO}_4^-$ from the ectopic gastric mucosa to the RBCs (14).

Contraindications

There are no absolute contraindications for MDS.

Importance of patient's personal history

It is important to collect all clinical information, particularly if there are signs of active bleeding, and to have the results of other diagnostic investigations carried out to study the clinical situation. It is also important to know if:

- » An RBC labelling scan has recently been done, particularly with the *in vivo* technique (stannous pyrophosphate may give an indeterminate result);
- » Whether or not the patient has undergone examinations with oral contrast agents like barium, as these can produce artefacts in the images.

Specific patient preparation

All pertinent clinical information should be reviewed and the correct patient preparation procedure carried out before the examination. Preparation includes (1,12):

- » Fasting for 3–4 h before imaging (the smaller size of the stomach will improve sensitivity). However, fasting may not always be possible and this exam can also be done after food intake.
- » Finding out about previous use of drugs (e.g. enemas) or procedures (endoscopy, colonoscopy) that may irritate the gastrointestinal tract. Any relevant medication should be interrupted 2–3 days before the study, if possible.

- » Ensuring the patient has not undergone barium or in vivo radiolabelled RBC studies in the last 3–4 days, as barium can cause attenuation and circulating stannous ions from the cold pyrophosphate may cause RBCs labelled with $[^{99m}\text{Tc}]\text{NaTcO}_4^-$ to concentrate in the gastric mucosa.
- » Thyroid blockage uptake with potassium perchlorate should not be done before the study as it will also block $[^{99m}\text{Tc}]\text{NaTcO}_4^-$ uptake by the gastric mucosa. It can be administered after the study to improve radiopharmaceutical excretion and reduce radiation exposure.
- » Patients should be instructed to empty the bladder immediately before the procedure.

Written informed consent

Depending on the applicable legislation in each country, written informed consent may be required. The patient should be provided with the relevant documents before the procedure. As most patients undergoing this procedure are children, parents or caregivers must be informed about all the procedures and give their consent.

Pharmacological intervention

Although it is not mandatory, study **sensitivity** can be improved through prior administration of some drugs, as described in Table 7 (1,10,12). Proton pump inhibitors can also be used to control acid secretion in this context.

Pharmacological Pre-treatment and Pharmacological Action		Neonates	Infants / Older children	Adults	
Histamine H2 blockers	Inhibit acid secretion by the parietal cells, which also reduces mucosal cells' release of $[^{99m}\text{Tc}]\text{NaTcO}_4^-$	Cimetidine	Oral 10–20 mg/kg/dose (a minimum of one dose in the evening before and one dose 1 h before imaging)	Oral 20 mg/kg/dose (a minimum of one dose in the evening before and one dose 1 h before imaging)	Oral 300 mg/4 times/day in 2 days
			I.V. 300 mg/100 mL of 5% dextrose over 20 min, 1 h before imaging		
		Ranitidine	Oral 2 mg/kg/dose (a minimum of one oral dose the evening before and one dose 1 h before imaging)	Oral 150 mg/kg	
			I.V. 1 mg/kg (max. 50 mg) over 20 min, 1 h before imaging		
		Famotidine	Oral 0.5 mg/kg/dose (a minimum of one oral dose the evening before and one dose 1 h before imaging)	Oral 20 mg	
			I.V. 0.25–0.5 mg/kg, 1 h before imaging		I.V. 20 mg or 0.25 mg/kg, 1 h before imaging
Glucagon	Relax smooth muscle and reduce peristalsis of the gastrointestinal tract, slowing the transit of the secreted $[^{99m}\text{Tc}]\text{NaTcO}_4^-$	I.V. 50 µg/kg (max. 1 mg), diluted in 10 mL of sterile water (never with saline!) infused slowly over 2 min. immediately before injection of the $[^{99m}\text{Tc}]\text{NaTcO}_4^-$ Flush with sterile water immediately before and after the infusion of glucagon Side effects include nausea and vomiting, so it is given before the radiotracer to avoid vomiting and aspiration during the study Attention must be paid to diabetic patients, who should not be pre-treated with this pharmaceutical			

Table 7 – Recommended pharmacological pre-treatment dosage in Meckel's diverticulum scintigraphy (4,5,10)
I.V. – intravenous

Radiopharmaceuticals

$[^{99m}\text{Tc}]\text{NaTcO}_4^-$ is the radiopharmaceutical of choice. After intravenous injection it avidly accumulates in gastric mucosa, which can reveal ectopic gastric mucosa in an MD. The uptake occurs in the mucosa of the gastric fundus via the mucin-producing cells, and it is then secreted into the gut lumen. The excretion of $[^{99m}\text{Tc}]\text{NaTcO}_4^-$ is not dependent on the presence of parietal (acid-producing) cells.

Activity and dosimetry

The recommended $[^{99m}\text{Tc}]\text{NaTcO}_4^-$ activity for DMS in the **paediatric population** can easily be calculated using the *EANM Paediatric Dosage Card (Version 5.7.2016)* (9) or the *online SNMMI Paediatric Injected Activity Tool* (15). In adults, the recommended activity for this procedure is 185–440 MBq (1).

The radiation dose to the patient is relatively low if ALARA principles are applied. The critical organ for this study is the upper large intestine, which would receive 0.20 mGy/MBq. The effective dose is 0.040 mSv/MBq (1).

Instructions should be given to patients after the exam in order to minimise radiation exposure to family members, children and the public. CT dose reduction protocols should be used whenever SPECT/CT is performed, particularly in children.

In pregnant women, a careful risk-benefit analysis should be performed, balancing the potential benefit of the scan against

the potential risks of ionising radiation. In lactating patients, breastfeeding should be interrupted for 12 hours (1).

Imaging acquisition protocols

The DMS imaging protocol includes a dynamic acquisition immediately after the intravenous injection of the radiopharmaceutical. Table 8 summarises the main aspects relating to image acquisition (1,12).

When the MD is adjacent to the bladder and the patient is unable to void, urinary catheterisation can be helpful. Sometimes changing patient positioning in the gamma camera (upright images, for example) is sufficient to localise MD as it falls away from the bladder. Administration of furosemide (intravenous; 1 mg/kg) may help avoid false positive scans by clearing renal or ureter physiological activity (1).

If the diverticulum is small, or if there is interference from the bladder, a SPECT or SPECT/CT can be performed.

Typically, sedation is not necessary to perform an MDS. However, tomographic imaging acquisition, mainly SPECT/CT, increases the potential need for child sedation.

Processing the results

Cinematic display of the dynamic images, or reformatting to longer time intervals along with additional static images, can improve DM localisation. Scaling of the images is helpful to detect small, abnormal

Patient Position in the Gamma Camera	Gamma Camera Settings	Imaging Acquisition Protocol
Patient must remove any item that can produce image artefacts	A large field of view gamma camera is recommended	An initial 60-second blood flow study with 1–5 seconds/frame
Supine position	Low-energy high-resolution collimator	Followed by a dynamic acquisition for at least 30 minutes with a frame rate of 30–60 seconds/frame
Patient's upper extremities should be kept outside the abdominal and pelvic regions (to prevent image artefacts and obscure findings)	Energy photopeak centred on 140 keV (^{99m} Tc) with a 20% window	Imaging for 60 minutes can be performed when clinical suspicion is high and the initial images are negative. However, imaging for more than 60 minutes is not helpful as activity will begin to move from the stomach to the intestine
Detector placed in anterior view should include stomach and bladder (in infants and small children up to 2 years of age, the thorax should be included in the field of view to assess for possible bronchopulmonary foregut malformation with ectopic mucosa)	Matrix (minimum): 128x128	Additional delayed static 5-minute images can be acquired (anterior, anterior oblique, lateral, posterior or upright) at the end of the dynamic acquisition. Lateral views may be useful to localise renal pelvic activity
	Zoom appropriate for patient size	
SPECT or SPECT/CT	Matrix: 128x128 or 64x64 Zoom appropriate for patient size	360° rotation, 30 seconds/frame, 3° per step

Table 8 – Image acquisition description for Meckel's diverticulum scintigraphy (1,16)
SPECT – single-photon emission computed tomography; SPECT/CT – single-photon emission computed tomography/computed tomography

areas of increased uptake (1). If the patient moves during the acquisition, motion correction *software* can be used.

Image interpretation

The flow study should show the radiotracer in the heart, lungs, major blood vessels, liver, spleen, and kidneys. The normal biodistribution of [^{99m}Tc]NaTcO₄⁻ includes uptake in the thyroid, salivary glands, gastric mucosa, and choroid plexus.

An MD is identified as a hotspot of increased activity, usually in the lower abdomen or upper pelvis, the intensity depending on the amount and secretory activity of mucosa. It is visualised simultaneously with physiological stomach uptake, within 5 or 10 minutes after [^{99m}Tc]NaTcO₄⁻ administration (Figures 3 and 4). The activity increases over time, usually with a rate similar to that of normal gastric mucosa (10,16). The [^{99m}Tc]NaTcO₄⁻ secreted by the gastric mucosa will gradually accumulate in the small bowel, and can be distinguished from an MD by its delayed appearance (1).

Quality criteria and artefacts

When performed correctly, in the appropriate clinical setting, the accuracy of MDS is high. Sensitivity and specificity in children are 85% and 95% respectively, while in adults the accuracy ranges between 20% and 60% (12). Pharmacological intervention can improve the accuracy.

It's important to be aware of **pitfalls** that might mask or mimic an MD and thus interfere with correct image interpretation, leading to false-positive or false-negative results (Table 9).

Conclusion

In an era when *PET/CT molecular imaging and theranostics* monopolise the attention and enthusiasm of the nuclear community, conventional scintigraphic studies of the gastrointestinal tract remain clinically interesting, despite a downward trend in their use in the past few years. However, in a clinical setting where sensitivity and precision in localisation are key elements for the success of a diagnostic tool, the new SPECT/CT systems may herald a new era for these two classic imaging techniques.

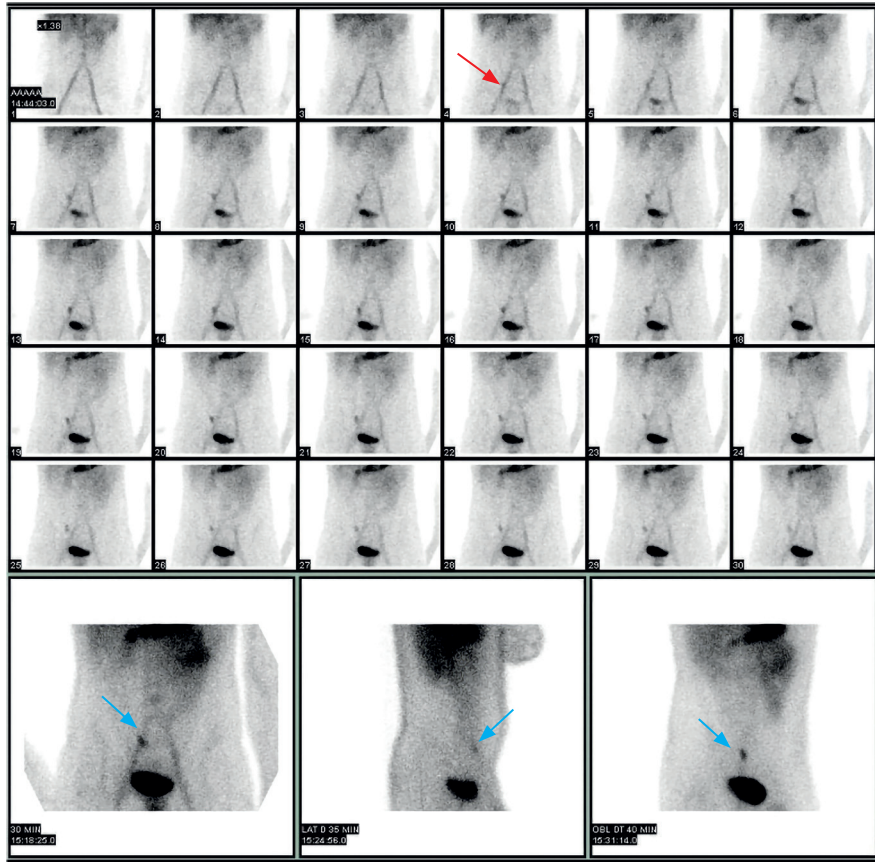


Figure 3 – 16-year-old boy with medical history of recurrent low digestive bleeding and abdominal pain. Meckel's diverticulum scintigraphy was performed: abnormal focal ^{99m}Tc NaTcO₄ uptake was observed 4–5 minutes after injection (red arrow), at same time as stomach activity. The scintigraphy findings were related to the presence of ectopic gastric mucosa in the Meckel's diverticulum. a. Dynamic anterior 1 min/frame images. b. Delayed anterior, right lateral and right anterior oblique planar 5 minutes images. Premedication with oral cimetidine.

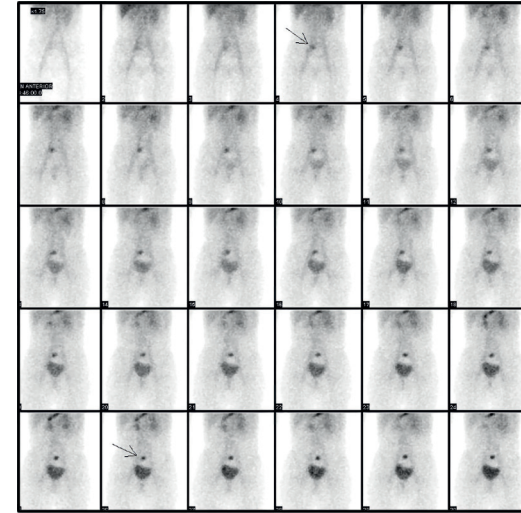


Figure 4 – 12-year-old girl with low digestive bleeding. Meckel's diverticulum scintigraphy was performed: abnormal focal ^{99m}Tc NaTcO₄ uptake was observed 2–3 minutes after injection (arrow) above the bladder. The scintigraphy findings were related to the presence of ectopic gastric mucosa in the Meckel's diverticulum. Dynamic anterior 1 min/frame images. Premedication with oral cimetidine.

False Results	Description of Artefacts and Pitfalls
Causes of false negative results	<ul style="list-style-type: none"> Recent barium study may cause activity attenuation in the diverticulum Previous in vivo radiolabelled RBC study with pyrophosphate Previous sodium perchlorate administration Previous atropine administration Small MD (< 1.8 cm²) Rapid mucosa washout or movement GIB during circulation of the tracer (can obscure the MD uptake) Full urinary bladder or dilated ureter (can obscure the MD uptake) Impaired blood supply (e.g. intussusception or volvulus)
Causes of false positive results	<ul style="list-style-type: none"> Recent colonoscopy, endoscopy, enemas or laxatives as irritation of the bowel can occur Urinary tract activity (extrarenal pelvis, hydronephrosis, vesicoureteral reflux, horseshoe kidney, bladder diverticulum) Vascular (aneurysm of intraabdominal vessel, haemangioma, arteriovenous malformation, angiodysplasia) Gastroenteric duplication cysts Inflammation (Crohn's disease, ulcerative colitis, appendicitis, abscess) Small bowel obstruction (intussusception, volvulus) Neoplasm (carcinoma of sigmoid colon, carcinoid lymphoma leiomyosarcoma) Other areas of ectopic gastric mucosa (gastrogenic cyst, enteric duplication, duplication cyst, Barrett's oesophagus, retained gastric antrum, pancreas, duodenum, colon)

Table 9 – Artefacts and pitfalls in Meckel's diverticulum scintigraphy (1,10,16)
GIB – gastrointestinal bleeding; MD – Meckel's diverticulum; RBC – red blood cells

REFERENCES

1. Spottswood SE, Pfluger T, Bartold SP, Brandon D, Burchell N, Delbeke D, et al. SNMMI and EANM Practice Guideline for Meckel Diverticulum Scintigraphy 2.0. *J Nucl Med Technol*. 2014 Sep; 42(3):163-169.
2. Alavi A, Dann RW, Baum S, Biery DN. Scintigraphic Detection of Acute Gastrointestinal Bleeding. 1977 Sep;124(3):753-6.
3. Winzelberg GG, McKusick KA, Strauss HW, Waltman AC, Greenfield AJ. Evaluation of gastrointestinal bleeding by red blood cells labeled in vivo with technetium-99m. *J Nucl Med*. 1979 Oct;20(10):1080-6.
4. Grady E. Gastrointestinal Bleeding Scintigraphy in the Early 21st Century. *J Nucl Med*. 2016 Feb;57(2):252-9.
5. Dam HQ, Brandon DC, Grantham V v, Hilson AJ, Howarth DM, Maurer AH, et al. The SNMMI Procedure Standard/EANM Practice Guideline for Gastrointestinal Bleeding Scintigraphy 2.0. *J Nucl Med Technol*. 2014 Dec;42(4):308-317.
6. Otomi Y, Otsuka H, Terazawa K, Yamanaka M, Obama Y, Arase M, et al. The diagnostic ability of SPECT/CT fusion imaging for gastrointestinal bleeding: a retrospective study. *BMC Gastroenterol*. 2018 Dec 10;18(1):183.
7. Siddiqui AR, Schauwecker DS, Wellman HN, Mock BH. Comparison of technetium-99m sulfur colloid and in vitro labeled technetium-99m RBCs in the detection of gastrointestinal bleeding. *Clin Nucl Med*. 1985 Aug;10(8):546-9.
8. Mariani G, Pauwels EKJ, AlSharif A, Marchi S, Boni G, Barreca M, et al. Radionuclide Evaluation of the Lower Gastrointestinal Tract. *Journal of Nuclear Medicine*. 2008 May;49(5):776–787.
9. EANM Pediatric Dosage Card. Available from: https://www.eanm.org/docs/EANM_Dosage_Card_040214.pdf
10. Harvey A, Ziessman M, Janis O'Malley M, James Thrall. *NUCLEAR MEDICINE: THE REQUISITES*. 4th Edition. Elsevier Health Sciences, editor. 2013;307–320.
11. Khan AU, Mandiga P. Gastrointestinal Bleeding Scan. 2022 Aug 8. In: StatPearls [Internet]. Treasure Island (FL): StatPearls Publishing; 2022 Jan–.
12. Aboughalia HA, Safa , Cheeney HE, Elojeimy S, Blacklock LC, Parisi MT. Meckel diverticulum scintigraphy: technique, findings and diagnostic pitfalls. *Pediatr Radiol* 53, 493–508 (2023).
13. Edmonson JM. Johann Friedrich Meckel the younger: Meckel's diverticulum. *Gastrointest Endosc*. 2001 Jul;54(1):19A-20A.
14. Yen CK, Lanoie Y. Effect of stannous pyrophosphate red blood cell gastrointestinal bleeding scan on subsequent Meckel's scan. *Clin Nucl Med*. 1992 Jun;17(6):454-6.
15. Nuclear Medicine Radiation Dose Tool – SNMMI. Available from: <http://www.snmmi.org/clinicalpractice/pediatrictool.aspx>
16. Farrell MB, Zimmerman J. Meckel's Diverticulum Imaging. *J Nucl Med Technol*. 2020 Sep;48(3):210-213.

HEPATOBIILIARY AND SPLEEN STUDIES

*by David Gilmore¹
Krystle Glasgow²
Daniel Tempesta³*

¹*Massachusetts College of Pharmacy & Health Sciences Boston, Massachusetts*

²*Clinical Coordinator Master of Science Nuclear Medicine and Molecular Imaging Sciences
Program Clinical and Diagnostic Sciences Department | School of Health Professions UAB |
The University of Alabama at Birmingham*

³*Nuclear Medicine Supervisor Dana-Farber Cancer Institute Boston, MA, Adjunct professor
MCPHS University Boston, MA*

Disclaimer: Medical practice may vary between Europe and North America. The following chapter essentially reflects American practice.

HEPATOBILIARY SCINTIGRAPHY

Indications

Hepatobiliary scintigraphy is most commonly performed for the evaluation of right upper quadrant pain that may be related to gallbladder dyskinesia or inflammation due to cystic duct obstruction (cholecystitis), often due to gallstones. Gallbladder ejection fraction (GBEF) studies can also be performed using an adjunct medication known as sincalide. Radiopharmaceutical flow through the biliary system can be useful in checking for biliary system patency, presence of a bile leak, and diagnosing biliary atresia in neonates. Less common indications for hepatobiliary imaging include assessment of liver transplant, identifying a sphincter of Oddi dysfunction, and detecting enterogastric reflux.¹

Patient preparation and image acquisition

Prior to performing hepatobiliary imaging, a thorough patient history should be taken. Relevant information includes: history of prior gastrointestinal or biliary surgery, time of last meal, recent opioid administrations, bilirubin or liver enzyme levels, and results of other gallbladder imaging such as ultrasound.¹

Patients should have nothing by mouth, also known as NPO or nil per os for four (4) hours prior to hepatobiliary scintigraphy. Ideally, all patients should not be NPO for more than 24 hours because prolonged fasting can cause bile stored in the gallbladder to thicken, preventing radiotracer flow into the gallbladder. Such a situation can cause a false-positive result for cholecystitis. If the patient has been NPO for more than 24 hours, see the adjunct pharmaceutical and physiological intervention section below for details on pre-treatment with sincalide. If the patient has had a cholecystectomy and the study is being performed to assess for a bile leak, the patient does not need to be NPO. For patients that have taken opioids, radiotracer injection and imaging should be delayed for a time equivalent to 4 half-lives of the opiate medication. If performing the exam to differentiate biliary atresia from neonatal hepatitis, the patient should be pre-treated with phenobarbital for 3–5 days prior to the study.³

The patient should be positioned under a large-field-of-view camera fitted with a low-energy all-purpose or high-resolution collimator. Imaging should begin immediately after tracer administration once the liver is visualised. The entire liver should be included and placed in the upper

left corner of the field of view. Dynamic imaging should continue for one hour using a 128 x 128 matrix at a rate of 1 frame per minute. After the one hour dynamic study, a right lateral static for 3–5 minutes should be acquired to differentiate activity in the bowel from activity in the gallbladder. If the gallbladder is not visualised after 1 hour, morphine may be administered or delayed imaging can occur as described in the section below. If the gallbladder is visualised and a gallbladder ejection fraction is desired, sincalide (or a fatty meal substitute) should be administered and imaging continued. For bile leak studies, no pharmaceutical intervention is needed, and if a leak is not visualised during the first hour of imaging, delayed imaging can be performed at the direction of the reporting physician. During biliary atresia studies, if no transit of radiotracer is visualised leaving the liver into the duct system, gallbladder, or small bowel, then delayed static or dynamic imaging should take place at 6 and 24 hours post injection.

Radiopharmaceutical dosage

Today, most of the radiopharmaceuticals used for hepatobiliary imaging are derivatives of [^{99m}Tc]Tc-iminodiacetic acid (Tc-99-IDA). Two of the most commonly used agents are [^{99m}Tc]Tc-disofenin (2,6-diisopropylacetanilido iminodiacetic acid) and [^{99m}Tc]Tc-Tc-mebrofenin (bromo-2,4,6-trimethylacetanilido iminodiacetic acid). The trade name for Tc-99m disofenin

is Hepatolite and the trade name for mebrofenin is Choletec® or BRIDATEC®. Due to the fact that these are Tc-99m agents, the physical half-life is 6 hours. Both agents have a similar mechanism of action or uptake.

The activity for both agents, according to the Society of Nuclear Medicine and Molecular Imaging (SNMMI) Practice Guidelines, is 111–185 MBq (3–5 mCi) and is administered intravenously¹. For paediatric patients, the dosage should be altered with a standard of 1.8 MBq/kg (0.05 mCi/kg).²The European Association of Nuclear Medicine's paediatric dosage card shows a minimum recommended activity of 20.0 MBq (0.54 mCi), whereas the SNMMI practice guideline states a minimum activity of 18.5 MBq (0.5 mCi).^{1,2}

Alteration of the dosage for hepatobiliary scintigraphy scan may also be considered for patients who have hyperbilirubinemia. Elevated bilirubin may cause less radiotracer extraction by the liver; therefore, administering a slightly higher dose may help with increasing imaging counts and quality.^{1,3}

Adjunct pharmaceutical and physiological intervention

Hepatobiliary imaging can require a pharmacological or physiological intervention. It is important to understand who can administer adjunctive pharmacological agents, as this can be different in specific regions and institutions.

Delayed imaging or administration of morphine sulphate

If the gallbladder is not visualised 60 minutes post injection, delayed imaging can be performed at four (4) hours to differentiate acute cholecystitis from chronic cholecystitis. Another alternative to delayed imaging is to administer morphine sulphate to the patient, which increases the tone of the sphincter of Oddi and causes it to contract. After administering morphine, if the cystic duct is patent, flow of the tracer will allow for visualisation of the gallbladder. Morphine sulphate dosage is 0.04 mg/kg or a standard dosage of 2 mg according to the SNMMI Practice Guidelines.¹ Administration of morphine sulphate should occur over 2–3 minutes intravenously.¹ Imaging then continues for another 30 minutes to 60 minutes.^{1,3} A second injection of the radiopharmaceutical may be needed if there is no visible activity in the liver at the start of the delayed imaging or administration of the morphine sulphate dose. If the gallbladder is not visualised after the physical delay in imaging or post morphine sulphate injection, then the study is indicative of acute cholecystitis.³ If the gallbladder is visualised after the delayed imaging or post morphine sulphate, it is an indication of chronic cholecystitis.^{1,3}

Gallbladder ejection fraction calculations

If the gallbladder is seen within the first 60 minutes (normally between 30–60 minutes),

the gallbladder ejection fraction (GBEF), expressed as a percentage of emptying, can be determined. In order to calculate this percentage, sincalide, a synthetic C-terminal octapeptide of cholecystokinin, may be administered. The trade name of sincalide is Kinevac®, and the dosage is 0.02 µg/kg administered intravenously over 30–60 minutes.

An alternative to sincalide is a fatty meal. Neither the EANM nor the SNMMI have a standard guideline on the type of meal, the dosage or amount of the meal, or any validation of the ejection fraction calculations. A fatty meal substitute commonly used in the USA is Ensure®, which can be used as a high-calorie meal replacement with a high fat content.

GBEF can be calculated by first subtracting the net minimum gallbladder counts from the net maximum gallbladder counts and then dividing by the net maximum gallbladder counts. GBEF can be expressed as a percentage by multiplying the answer by 100.

Sincalide pre-treatment

A patient who has been fasting for more than 24 hours should be pre-treated with an administration of sincalide to empty any viscous bile that may have accumulated in the gallbladder, which could cause a false positive. The dosage is 0.02 µg/kg, administered 15–30 minutes prior to the radiopharmaceutical used for hepatobiliary imaging. This will contract the gallbladder

and allow any collection of bile to be removed from the cystic duct and emptied into the common bile duct.

Suspected biliary atresia

In jaundiced neonates, phenobarbital may be used to pre-treat the patient prior to the hepatobiliary study.¹ The suggested dosage is 5 mg/kg/d orally in

2 divided doses at least 3–5 days before the study.¹ This may enhance the biliary excretion of the radiotracer. An alternative to phenobarbital is ursodeoxycholic acid, given as 2 divided doses 2–3 days prior to the study.¹ An imaging decision flow chart can be found in Figure 1 to guide the technologist in choosing the appropriate procedure.

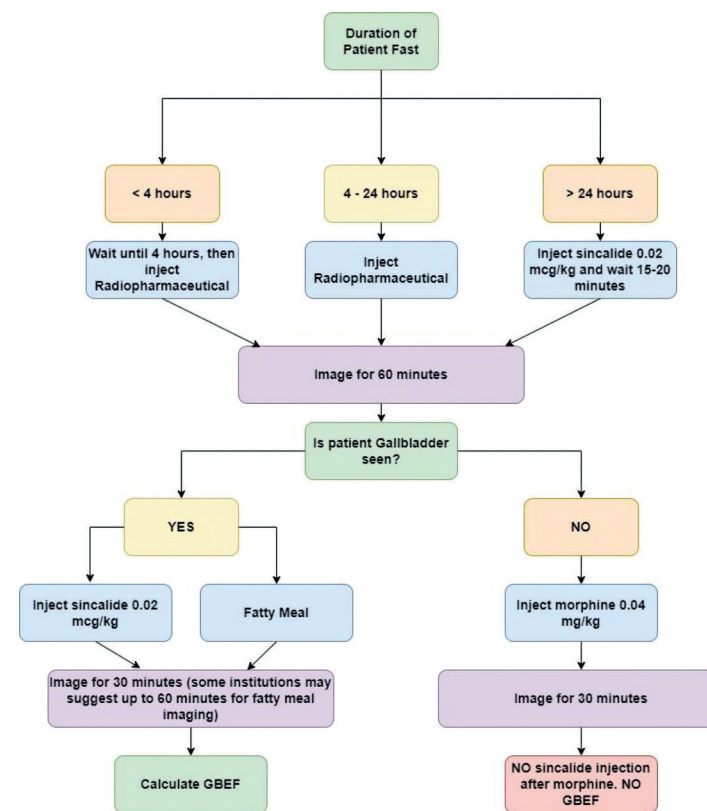


Figure 1 – Hepatobiliary scintigraphy decision flow chart

Image processing and interpretation

All dynamic images should be summed as 5-minute images for ease of display, and care should be taken to ensure that all images are labelled appropriately. Dynamic images should also be reviewed as a cine to show flow of tracer through the biliary system.

Normal hepatobiliary scintigraphy (Figure 2) shows radiotracer flow from the liver into the gallbladder and small intestine during the first 60 minutes of imaging. Non-visualisation of the gallbladder after 60 minutes of imaging indicates cholecystitis, with non-visualisation after morphine or delayed imaging confirming the presence of acute cholecystitis. If the gallbladder is visualised after the administration of morphine or delayed imaging, chronic cholecystitis should be suspected. If the gallbladder is visualised after 60 minutes and sincalide imaging is performed, a gallbladder ejection fraction can be calculated by drawing a region of interest (ROI) around the gallbladder and a second one around the adjacent liver for background. Care should be taken to exclude any duct or bowel loops from both ROIs. An ejection fraction of 38% or more after administration of sincalide and imaging for an additional hour is considered normal. Activity outside of the liver, ducts, gallbladder, and small bowel should arouse suspicion of a bile leak.¹

Delayed transit of radiotracer from the liver to the duct system during the first hour of imaging is indicative of liver dysfunction.

In neonates, absence of the tracer in the duct system, gallbladder, or small bowel, in the presence of pre-treatment with phenobarbitol, is indicative of biliary atresia at the standard 1 hour, 4 hours, and 24 hours (Figure 3). In the figure presented, images were acquired at additional time points that are not required.

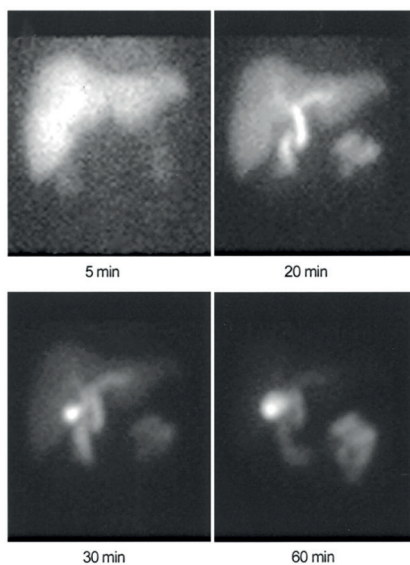


Figure 2 – Normal hepatobiliary scintigraphy showing radiotracer flow into the small bowel at 20 minutes and into the gallbladder at 30 minutes. Images from SNMMI JNMT Journal.5

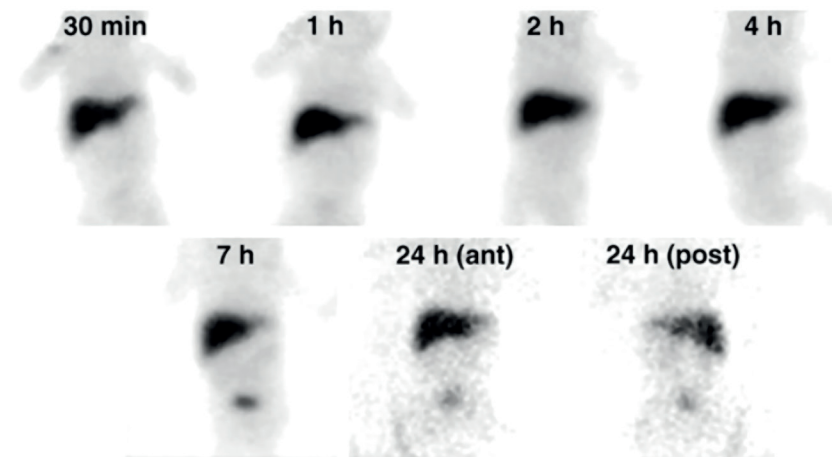


Figure 3 – Non-visualisation of the biliary tree, gallbladder, and bowel at 24 hours in an infant during hepatobiliary imaging. This is consistent with biliary atresia. Images from SNMMI JNMT Journal.5

LIVER/SPLEEN SCINTIGRAPHY

Indications

Radiocolloid accumulation provides opportunities to assess the size and position of the liver and spleen. While other imaging modalities, such as computed tomography (CT), can provide better anatomical detail of the liver and spleen, liver and spleen scintigraphy is still useful in further classifying abnormalities such as cirrhosis, hepatomegaly, functional asplenia, and ectopic or accessory splenic tissue.³ In addition to liver/spleen imaging with radiocolloids, investigating the spleen specifically with heat-damaged (denatured) Tc-99m-labelled red blood cells (RBC) may

also be useful. Specific indications for spleen imaging include identifying functioning splenic tissue, detection of ectopic splenic tissue or splenule, and evaluating suspected functional asplenia.

Patient preparation and image acquisition

There is no specific patient preparation for liver/spleen imaging. However, the study should be performed before any other imaging containing iodinated or barium contrast. These contrast agents can create artefacts, especially if they are retained in the gastrointestinal tract.³ Relevant patient history, including any recent imaging procedures and results, should be presented with images to the interpreting physician. Imaging begins approximately 20 minutes

after radiopharmaceutical injection, allowing sufficient time for uptake in the reticuloendothelial cells of the liver and spleen. Planar imaging is accomplished with the patient in the supine position and the detector, fitted with a low-energy all-purpose or high-resolution collimator, centred over the liver and spleen. The anterior image should be acquired first for approximately 1 million counts. Posterior, right anterior oblique (RAO), left anterior oblique (LAO), right posterior oblique (RPO), left posterior oblique (LPO), right lateral, and left lateral images should be acquired for the same amount of time as the 1 million count anterior image. If using a dual-head gamma camera, the anterior and posterior views can be acquired simultaneously with the images set to stop when the anterior reaches 1 million counts. Subsequently, the RAO/LPO, right lateral/left lateral, and LAO/RPO views

can be acquired in pairs for the same time as it took to acquire the anterior view. The LPO and left lateral views may be omitted if there is no clinical interest in the spleen. Additionally, a lead marker with known length may be placed over the liver and the anterior image repeated. Placing the marker appropriately can help identify the liver's position in relation to the right inferior costal margin and the xyphoid process, as well as assist in estimating the size of the liver.⁴

When available, SPECT or SPECT/CT can be useful for better anatomical localisation of the liver and spleen. SPECT parameters can be found in Table 1. If imaging the spleen with heat-damaged red blood cells, the patient should be imaged 20–30 minutes after injection of the radiopharmaceutical. The same views should be acquired regardless of which radiopharmaceutical is used.

Parameter	Value
Matrix size	128 x 128
Projections	60 per head
Degree of sampling	3 degrees
Time per projection	20–30 seconds

Table 1 – Liver/spleen SPECT parameters for a multi-detector camera.⁴

Radiopharmaceutical dosage

The most common radiopharmaceutical used is [^{99m}Tc]-sulphur colloid. The activity administered intravenously is 111 to 222 MBq (3–6 mCi) for planar imaging and 370 MBq (10 mCi) when single photon emission computed tomography (SPECT) is used⁴. Sulphur colloid is comprised of particles that range in size from 0.1 to 1.0 µm. Once the particles are administered, the reticuloendothelial cells of the liver, spleen and bone marrow phagocytise them, allowing them to be visualised through scintigraphy imaging. The maximum uptake occurs 10–20 minutes post injection, but imaging can be delayed due to the slow clearance from the reticuloendothelial cells.⁴

For paediatric patients, the dosage should be altered, with a standard of 1.8 MBq/kg (0.05 mCi/kg).² The EANM's paediatric dosage card shows a minimum recommended activity of 15.0 MBq (0.40 mCi).

When imaging the spleen with heat-damaged RBC, an adult dose of 37 to 222 MBq (1–6 mCi) for planar imaging and 555 to 1110 MBq (15–20 mCi) for SPECT imaging should be used. After labelling the autologous red blood cells using the in-vitro method, the radiopharmaceutical should be heated in a water bath for 15 minutes at a temperature of 49–50°C.⁴ The mechanism of accumulation of the damaged red blood cells in the spleen is cell sequestration.

^{99m}Tc-labelled RBC may also be used in liver spleen imaging, but are typically reserved to better define lesions such as liver haemangiomas.

Image processing and interpretation

Image processing is fairly basic for liver/spleen imaging. Static images should be arranged in a single display, appropriately windowed based on the anterior image. Sagittal, coronal, and transaxial reconstructions should be available from the SPECT and fused with the CT images if a SPECT/CT was acquired.

Normal length of the right lobe of the liver is approximately 15 cm, measured from the dome using a lead marker with known length. The maximum size of the spleen, measured diagonally, is 14 cm, which can be estimated using the marker placed over the liver. Distribution of the radiocolloid is about 80% in the liver, 15% in the spleen, and 5% in the bone marrow at the time of imaging. The bone marrow is typically not visualised on anterior static images of the abdomen unless there is liver or spleen disease present. Visualisation of the bone marrow, a process called “colloid shift”, can occur in patients with diffuse liver disease or patients who have had a splenectomy.

Focal lesions typically present as photopaenic regions and include cysts, hepatomas, haematomas, adenomas, injuries, and infarcts. Many of these lesions may require additional imaging procedures for better classification. Diffuse lesions seen on liver/spleen scans typically represent cirrhosis and hepatitis.

REFERENCES

1. Tulchinsky M, Ciak, B, Delbeke, D, et. al. SNM Practice Guideline for Hepatobiliary Scintigraphy 4.0. *J Nucl Med Technol* 2010;38(4): 210-218.
2. Lassmann, M., Treves, SD. Paediatric radiopharmaceutical administration: harmonization of the 2007 EANM paediatric dosage card (version 1.5.2008) and the 2010 North American consensus guidelines. *European Journal of Nuclear Medicine and Molecular Imaging*. 2014. DOI 10.1007/s00259-014-2731-9
3. Tempesta, D. Gastrointestinal System. In D. Gilmore & K. Waterstram-Rich (Eds.). *Nuclear Medicine and Molecular Imaging: Technology and Techniques* 9th ed. St. Louis: Elsevier; 2023.
4. ACR–SNM–SPR Practice Guideline for the Performance of Liver and Spleen Scintigraphy. (2010). Available at: <http://www.snmmi.org/ClinicalPractice/content.aspx?ItemNumber=6414#GI>
5. Doonan, M. Hepatobiliary Imaging. *J Nucl Med Technol*, 2020;48(4): 304-310. DOI: 10.2967/jnmt.120.257.436

BILE ACID MALABSORPTION STUDY

*by Daniela Teixeira-Macarico¹
Raquel Martins²*

*¹Department of Nuclear Medicine, Queen Elizabeth University Hospital,
Department of Clinical Physics and Bioengineering, NHS Greater Glasgow and Clyde*

²Department of Nuclear Medicine, West Suffolk Hospital NHS Foundation Trust

INTRODUCTION

Chronic diarrhoea (CD) is defined by alterations in stool frequency and consistency for a period longer than 4 weeks (1). This is a prevalent condition worldwide, estimated to affect 4–5% of the Western population (2), which can increase to 7–14% in those over 65 years old (3). Of all confidently diagnosed cases of diarrhoea-predominant irritable bowel syndrome (IBS-D), 25% to 33% of these patients have underlying primary bile acid diarrhoea (BAD) (4–6).

BAD reduces quality of life, meaning that having the correct diagnosis and treatment is highly important, not only to improve the symptoms (e.g., faecal incontinence (4)), but also to allow patients to be able to make adjustments to their personal and professional lives (7). It is therefore imperative to establish the best tools and tests for early diagnosis of bile acid malabsorption (BAM), as well as to provide easy access to such tests.

BILE ACID ABSORPTION AND MALABSORPTION

Bile acids (BA) are small amphipathic molecules produced in the hepatocytes from cholesterol, secreted into the biliary tree and stored in the gallbladder during fasting (3,8). After meals, they are moved into the duodenum to aid in breaking down long-chain fatty acids, aromatic-aliphatic amino acids, lipo-soluble vitamins, and intact proteins along the small bowel

(3,8,9). Once reaching the terminal ileum, the unbound BA are reabsorbed by the ileal BA transporters, returning to the liver for recycling through the portal circulation (8,9). After reabsorption, the BA increase fibroblast growth factor-19 (FGF-19), an endocrine hormone which is responsible for reducing hepatic synthesis by down-regulating the production rate of 7 α -hydroxy-4-cholesten-3-one (C4), thus controlling the BA synthesis from cholesterol via negative feedback (8), and allowing the recycled acids to undergo subsequent re-secretion from the gallbladder. This process is called enterohepatic circulation, which has a mean recycling time of 3.4h, with a total of 4.6 cycles a day (10). Normally, around 95–97% of BA are recycled (5), with only 5% of BA being lost in the course of the reabsorption process and reaching the colon (9–11).

BAM occurs whenever there is defective absorption of BA in the terminal ileum or increased production in the liver, thus unbalancing their retention equilibrium during enterohepatic circulation (3,8,9). BAM may be present in several pathological conditions (Table 1) (which should be excluded by the technologist as part of taking the patient's history) and is classified into Type 1 to Type 4 (Figure 1) (5,8,10,12).

Diagnosing bile acid malabsorption

Misdiagnosing BAM and/or BAD has various implications for patients' outcomes, including impacting on patients' mental health and their ability to perform daily tasks

BAM in other Conditions	
Inflammatory bowel disease	Co-condition that responds to BAM treatment, improving patients' symptoms and quality of life.
Post-surgery and oncological conditions	High percentage of oncological patients presenting with diarrhoea and referred for treatment showed diagnosis of BAM. Due to the general debilitation of this cohort of patients, correct diagnosis is particularly important to avoid unnecessary exposure to inappropriate treatment options.
Cholecystectomy	Higher risk of BAM due to higher levels of BA because of surgical removal of the reservoir for the acids.
Habba syndrome	Chronic postprandial diarrhoea and abnormal gallbladder function, consequently increasing BA and causing BAM.

Table 1 – BAM in other pathological conditions (12)

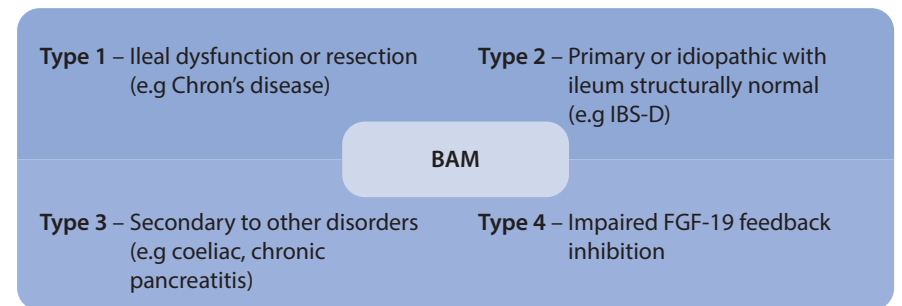


Figure 1 – Classification of BAM (5,8,10,12)

such as leaving the home. It can also lead to additional unnecessary tests and ineffectively prescribed treatments, which are associated with increased costs in healthcare (3). However, due to the small sample of studies available, which are generally only performed on positive patients, the economic model is based on several assumptions and therefore its cost-effectiveness cannot be accurately assessed (7).

Amongst the different diagnostic methods available, the nuclear medicine study with 23-[⁷⁵Se]Se-tauroselcholic acid is the gold standard, despite not being widely available worldwide and using ionising radiation (13,14). Other diagnostic methods have also emerged in the meantime, which are summarised in Table 2 (2–4,8,12–15).

Method	Sensitivity & Specificity	Advantages	Limitations
Empirical trial with BAS	N/A	Easily available	Not enough data available to assess accuracy and validity. False results reported due to placebo effect. Side effects of the treatment affect patient compliance. Success of treatment is dependent on the dose, which is difficult to calculate due to patient compliance and false results.
²³ -[⁷⁵ Se]Se-Tauroselcholic Acid Test	100% & 91%	Well-established and recognised. Well-tolerated. Predictor of therapy response. Better compliance with treatment after diagnosis.	Radiation exposure. Not licensed in some countries. Not widely available. Fairly expensive. Cannot exclude other reasons for CD. Protocol and cut-off values not currently standardised.
Serum Measurement of C4	85.2% & 71.1%	No radiation involved	Technique not widely available. Specialised laboratory equipment required. Assay difficult and time-consuming.
Serum Measurement of FGF-19	63.8% & 72.3%	No radiation involved	24h faecal collection. Variation of values according to circadian cycle. Not widely available. Requires further validation.
Faecal BAS/ Faecal Metabolomics	66.6% & 79.3%	No radiation involved	High-fat diet needed. All stools need to be collected for 48h. Not widely available. Complex technique.

Table 2 – Methods available for the diagnosis of BAM, with their respective sensitivity & specificity, advantages and limitations (2–4,8,12–15)

NUCLEAR MEDICINE IN THE EVALUATION OF BILE ACID MALABSORPTION

The nuclear medicine study to assess BAM is simple and well tolerated, allowing the retention of a radiolabelled synthetic BA to be measured with two scans, one week apart (3,8,10). The radiopharmaceutical used is tauro-H-23(⁷⁵Se) seleno-25-homocholeic acid (23-[⁷⁵Se]Se-tauroselcholic acid), most

commonly known as SeHCATTM. This is a synthetic bile acid manufactured by GE HealthCare® which is used for the diagnosis of BAM, to assess BA pool loss and ileal function in patients with CD and diagnosed with inflammatory bowel disease (13,16).

[⁷⁵Se] has a physical half-life of 119.78 days (17) and it decays by electron capture to [⁷⁵As], emitting gamma radiation with principal energies at 136, 265 and 279 keV

(8,9). Studies report that 97% to 100% of SeHCATTM is excreted, having a biological half-life of 2.6 days in healthy individuals (8). According to the manufacturer, each capsule has an activity of 370 kBq on the reference date, with its expiry occurring 12 weeks (84 days) after its reference date (16,18).

The sensitivity and specificity of this study are high, though it seems to vary according to the cut-off value used (2) (Table 3). Normal studies will have a retention range of over 10–15%, and while some centres report their scans as normal/abnormal, others classify them as normal (>15%) or mild (≤15%), moderate (≤10%) and severe (≤5%) BAM.

There is a correlation between the severity of retention and treatment response. The lower the radiopharmaceutical retention, the higher the likelihood the patient will respond to therapy with bile acid sequestrants (BAS) (12,13). According to Farrugia *et al.* (2021), the clinical response to colestyramine occurred in 96% of patients with a severe BAM diagnosis, in 80% with moderate BAM and in 70% with mild BAM (13).

Historically in nuclear medicine, BAM and BA pool loss studies were firstly performed with a whole-body counter (WBC). However, since WBC are rare nowadays, these studies are usually performed with a gamma camera, the most widely available equipment in departments throughout the world. It is worth noting that some authors mention the possible use of a probe commissioned specifically for SeHCATTM retention studies using a commercially available scintillation detector, a piece of equipment that is as sensitive as a WBC but with the potential for the same accessibility and availability as a gamma camera (19).

SeHCATTM scanning, while extremely useful for diagnosis of BAM, is still not widely available. Some of the reasons for this phenomenon were highlighted by M. Smith *et al.* (2013), and include lack of high demand from clinicians, lack of availability of adequate equipment, and large variability of normal thresholds, as well as patient preparation and scanning protocols (20).

Cut-off	Sensitivity	Specificity
8%	67%	97%
15%	100%	91%
5%	86%	100%

Table 3 – Variation of sensitivity and specificity of SeHCATTM per cut-off value (2)

Patient preparation

For a week before the start of the study and for the duration of it (another week), it is recommended that the following medication be suspended (12):

- » BAS (e.g., colestyramine and colestipol), which directly interfere with BA enterohepatic circulation by inducing higher BA retention;
- » High cholesterol medication (e.g., colesvelam), as cholesterol is used in hepatic BA production;
- » Anti-diarrhoea drugs (e.g., loperamide), since they might prevent a proper BA retention reading.

Patients may be taking other medications which can interfere with enterohepatic circulation, such as drugs affecting gastric motility (e.g., cisapride and metoclopramide) and urinary retention drugs (e.g., bethanecol). If patients are unable to stop taking these medications, then this should be documented on their record; this will assist in assessing BA retention properly, allowing for a more accurate interpretation of the results. This should be communicated to the technologist team ahead of radiopharmaceutical administration.

Some authors advise fasting for 3 to 4h prior to capsule administration to allow even redistribution of the radiopharmaceutical within the enterohepatic circulation system (8,10,12). Moreover, fasting can also facilitate capsule ingestion.

It is also relevant to ask patients if they have had any other tests involving radionuclides in the two weeks prior to the study, to determine if a patient baseline should be acquired (16). Colonoscopy studies should be avoided during the seven-day window of the SeHCAT™ so as not to disrupt the test (8).

Immediately before image acquisition, the patient is instructed to remove any attenuating objects from their pockets and abdomen (e.g., belt, keys, belly button piercings, bra).

Radiopharmaceutical dose, administration and dosimetry

The recommended activity of $^{23}\text{-}[^{75}\text{Se}]$ Se-tauroselcholic acid to administer is 370 kBq¹ (8,13,16). This comes in the form of a capsule, which is administered orally (Figure 2). Patients are advised to ingest the capsule whilst sitting upright or standing. They should drink about 15 mL of water before, during and after swallowing the capsule, totalling 45mL, to assist the passage into the stomach (16).

¹ In the United Kingdom, legislation allows for a 10% dose allowance (± 37 kBq). Given the physical half-life of ^{75}Se to be 119.78 days and a reference day activity of 370 kBq, and the fact that capsule delivery can be up to four weeks before the reference day, the capsule will be within 10% of the required dose from sixteen days before to eighteen days after the reference day. Table 4 shows the activity of a 370 kBq ^{75}Se capsule between those dates.

Female patients of childbearing age must be asked if they are pregnant or breastfeeding at the time of administration (8,16) and the risk/benefit of the study should be assessed accordingly. Breastfeeding will need to be



Figure 2 – SeHCAT™ capsule (courtesy of the Department of Nuclear Medicine, WSH)

interrupted 3–4h post-administration and milk discarded for this time period (16).

The effective dose for a full activity capsule is 0.26mSv, though the nature of the pathology means that most patients will be exposed to a lower dose. However, individuals with severe liver disease (e.g., cholestatic jaundice) can have an organ

exposure 100 times higher, therefore special consideration should be given to the benefit vs. risk of the procedure (16).

GAMMA CAMERA PROTOCOL

As previously mentioned, acquisition can be done using the gamma camera or a WBC.

To maximise gamma camera sensitivity, the study must be performed with the camera on intrinsic mode or uncollimated (8,21). This will, however, expose the scintillation crystals to possible damage, which can be minimised by using the protective covers which are available on some equipment. The uncollimated scanner is the most common approach, performed in 92% of the UK centres (20).

Days from Reference Day	Activity (kBq)	Days from Reference Day	Activity (kBq)	Days from Reference Day	Activity (kBq)
-16	405.8938	-4	378.6643	8	353.2615
-15	403.5518	-3	376.4794	9	351.2232
-14	401.2233	-2	374.3071	10	349.1966
-13	398.9082	-1	372.1473	11	347.1817
-12	396.6064	0	370	12	345.1785
-11	394.318	1	367.8651	13	343.1868
-10	392.0427	2	365.7425	14	341.2065
-9	389.7806	3	363.6321	15	339.2378
-8	387.5316	4	361.5339	16	337.2803
-7	385.2955	5	359.4478	17	335.3342
-6	383.0723	6	357.3738	18	333.3993
-5	380.8619	7	355.3117		

Table 4 – Activities of a 370 kBq capsule of $^{23}\text{-}[^{75}\text{Se}]$ Se-tauroselcholic acid in relation to its reference date within the period it can be used

There are studies, however, that show the relevance of assessing BA retention with collimated detectors for radiopharmaceutical distribution, with the use of collimator pressure sensitive devices (PSD) for patient safety (10,18). Wright *et al.* (2013) proved that the collimated technique is viable but not identical to the standard uncollimated approach, despite its clinical application remaining unclear (9). On the other hand, Bronte *et al.* (2021) managed to prove that images acquired with LEHR collimators at 1h, 2h, 3h and seven days post-administration allow the identification of specific patterns, which can not only be associated with a final diagnosis of BAM or non-BAM, but also correlated with the different types of BAM (10).

The biggest concern with using collimators for imaging remains the low number of counts detected, which directly impacts the overall uncertainty of the radiopharmaceutical retention measurement (18). James *et al.* (2021) determined that the best way to reduce these uncertainties is by means of equations, advising each department to measure their own values for their specific gamma camera system and acquisition protocol before using the technique. The same authors mention that the acquisition time must be increased in order to achieve acceptable counting statistics (18).

Timing and image acquisition

Shielded rooms used for SPECT/CT gamma cameras are ideal for SeHCAT™ imaging, since reducing the background count rates during any of the acquisitions will assist in obtaining more accurate results (18). The room should be monitored for any external sources of radiation, and any radioactive sources (including other patients) or waste should be removed prior to the scan (4).

According to the main literature, anterior and posterior images must be acquired on the day the capsule is ingested (day 0) – 1 to 3h post-administration – and then a week later (day 7) (10,16,21,22). Day 0 images allow measurement of transit times between stomach and gallbladder, as well as the capsule activity, while day 7 images allow measurement of BA retention from how much radioactivity is left within the patient (16).

The optimum time of acquisition for day 0 is 3h post-capsule ingestion, to achieve physiological equilibration of the enterohepatic circulation (16). However, some studies mention that the acquisition can start as early as 30 min post-ingestion, which allows higher patient turnaround in the department (22), while others suggest acquisition at 4 hours post-administration (3). In a different approach, Smout *et al.* (2021) developed a model to predict the 3h counts with a single acquisition on day 7 only. Apart from highlighting the limited value of performing the 3h measurement,

this model explains variables affecting the accuracy of retention values obtained, reducing the error impact in the predictive model for clinically relevant results (23).

The imaging acquisition consists of either a whole-body (WB) scan of the patient's torso, abdomen, pelvis and upper thighs (22) of 100 to 120 cm², or 300 s statics (3,10,23) with the centre of the crystal positioned midway between the patient's umbilicus and the base of their sternum. Regardless of the type of imaging, a standard axial positioning of the patient along the centreline of the detector should be maintained (16). Patients are scanned supine, and images are acquired with the detectors at maximum radius above and below the patient for dual-head cameras (Figures 3A and 3B) (23), which allows maximum sensitivity by minimising the effect of geometric variations (16). For single-head equipment, the detector is still at maximum radius, but patients can start

supine for anterior image acquisition and then be scanned prone for posterior image acquisition (Figures 4A and 4B) (22). Arms can be positioned alongside the patient's body or above the head, but positioning needs to be maintained for both sets of images.

² To ensure replicability of the day 0 scan on day 7, technologists can perform the 100-120cm WB from shoulders down.

The energy window used for imaging should include both the 265keV and the 279 keV [⁷⁵Se] energy peaks, which can be achieved by utilising a window of 265 keV ± 10% (11,23). The 136 keV peak is used by some centres to increase the sensitivity of the study. However, its results can also be affected by external background noise due to its proximity to the [^{99m}Tc] peak, the most-used radioisotope in nuclear medicine (11,20).

Immediately before and after each patient acquisition, a background at anterior and posterior positions must be acquired



Figure 3A, 3B – Patient in supine position with arms alongside the body (A) and above the head (B) for dual-head cameras (courtesy of the Department of Nuclear Medicine, QEUH, Glasgow)

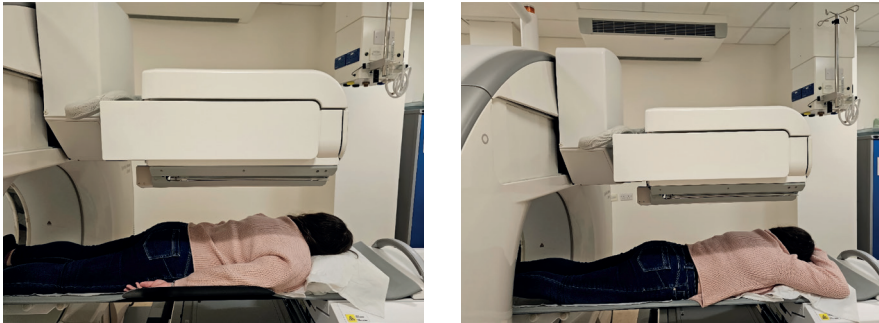


Figure 4 – Patient in prone position with arms alongside body (A) and above the head (B) for single head cameras (courtesy of the Department of Nuclear Medicine, QEUH, Glasgow)

(8,10) with the same duration as the patient image acquisition. If obtaining two sets of background images is not deemed workable by the department, at least one background should always be acquired immediately before patient imaging.

On day 7 the same imaging protocol is used, recreating identical positioning and image acquisition for the same amount of time and length of scan. This is essential to minimise the presence of positioning errors, and each department should have a designated method to record and replicate the conditions (e.g., scanning shoulders down or making a note of camera positioning, among other possibilities). Images are ideally acquired at 171 hours post-capsule ingestion (7 days plus 3h post-capsule ingestion), guaranteeing an exact seven-day interval between the acquired images (23). Due to the efficient nature of the enterohepatic cycle, it is possible to acquire the last scan at other data points than day 7, even though this is the best interval in

terms of logistics (being exactly one week post-administration) and for differentiating between normal and abnormal retention. However, the ability to scan at a different time point is particularly useful if, for example, a patient is unable to attend the appointment or if there are technical issues with the scanner, so the study is not completely lost and still has diagnostic value (11).

WHOLE-BODY COUNTER PROTOCOL

A WBC is a heavily lead-shielded room ensuring low background activity, primarily used to measure low levels of contamination in personnel and members of the public.

It can, however, be used for clinical tests with low levels of activity as it is purely measures radiation within the body, which makes it ideal for SeHCAT™ studies (24).

This equipment utilises sodium iodide ([NaI]) crystal detectors above and below a movable bed powered by a variable speed

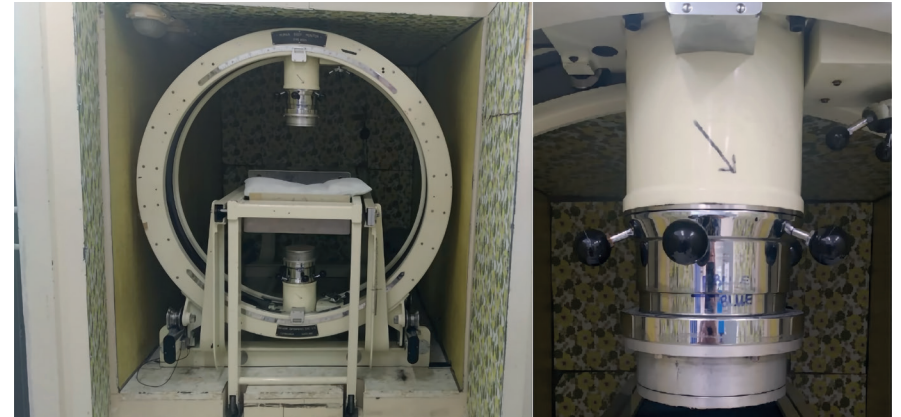


Figure 5 – WBC equipment and room, with a close-up of one of the detectors where the black rods for adjusting the lead shutters are visible (courtesy of the Department of Nuclear Medicine, Addenbrooke's Hospital, CUH)

motor. The positioning of the crystals is such that each one is set transversely to the bed axis with the sensitivity for detection controlled by adjustable lead shutters (Figure 5) (21).

Since the detectors are large and uncollimated, this equipment is more sensitive than a traditional gamma camera. Sensitivity is largely independent of the distribution of radioactivity, thus any errors are minimised when changes in distribution of the radiopharmaceutical occur during the study. The system is designed to detect higher energy ranges, including those of ^{75}Se . The room's low background activity ensures more accurate results, as the likelihood of any radiation interference is practically non-existent (21).

Timing and data acquisition

The acquisition times (day 0 and day 7) as well as the images acquired (whole-body

or statics and backgrounds) are exactly the same as for the gamma camera protocol (16). Here too the positioning conditions should be the same on both days, and to minimise background radiation interference the doors to the WBC room need to be closed before starting the acquisitions.

The main advantages and limitations of each technique are summarised in Table 5.

IMAGE AND DATA PROCESSING FOR GAMMA CAMERA AND WBC SYSTEMS

The retention of the radiopharmaceutical is expressed as a percentage accounting for both counts collected on day 0 and day 7. All count rates are corrected for background (BG) activity³ and for the ^{75}Se radioactive decay (1.04). The counts are taken as the geometric mean of the anterior (Ant) and

Gamma Camera				Whole-Body Counter
Uncollimated		Collimated		
Advantages	Limitations	Advantages	Limitations	
Higher sensitivity Protocol more standardised and more frequently used	Interference from external background activity Crystal exposed Unable to perform intrinsic patient acquisitions with some equipment (safety measures)	Less external background interference Available for all scanners Pressure sensitive devices in place for patient safety Identification of specific patterns for each type of BAM	Reduced sensitivity Longer acquisition time	Extremely reliable results, though not widely available
Image Acquisition Protocol				
Image and background acquisitions 1–3h post-administration and on day 7. Models now available to predict counts on the day of administration without need to perform images at that point Patient supine with camera heads at maximum radius Anterior/posterior whole-body scan (torso, abdomen, pelvis and upper thighs) or statics centred on the abdomen for 300s (longer for collimated camera) Window 265 keV ± 10%. Photopeak of 136keV can be used to increase sensitivity, although it will cause more interference from background radiation			Image and background acquisitions 1–3h post-administration and on day 7 Patient supine Anterior/posterior whole-body scan acquisition of torso, abdomen, pelvis and upper thighs, or static acquisition of patient's abdomen	

Table 5 – Advantages and limitations of the use of gamma camera and WBC for calculation of SeHCAT™ retention values (2,3,8–11,18,21–23)

posterior (Post) views to reduce the effect of anatomical position (8,16). This results in the following equation (8,11):

Usually, these calculations are performed automatically by existing software and may result in a graphic representation. Figures 6 and 7 represent the images acquired with a

gamma camera and the results for normal retention and severe BAM, respectively.

³ If two background readings were acquired (one before and one after patient imaging), please calculate their average and use it to determine the 23-[⁷⁵Se]Se-Tauroselcholic Acid retention.

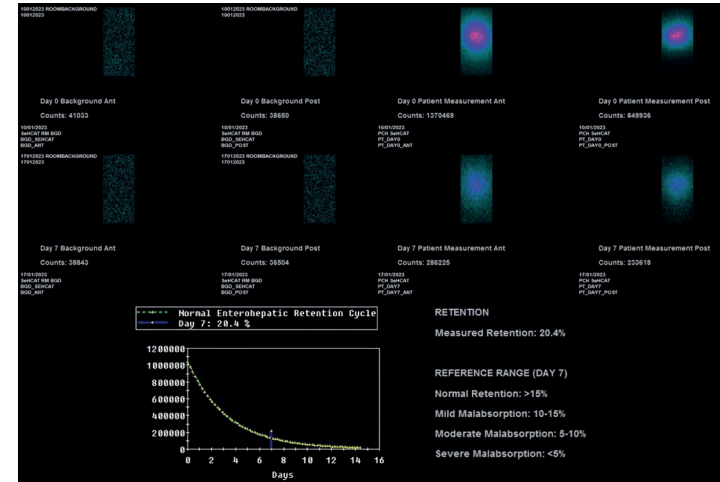


Figure 6 – Background and patient images acquired with an uncollimated gamma camera at day 0 and day 7. Results indicate there is no BAM, as retention of 23-[⁷⁵Se]Se-Tauroselcholic Acid is 20.4% (courtesy of the Department of Nuclear Medicine, Addenbrooke's Hospital, CUH)

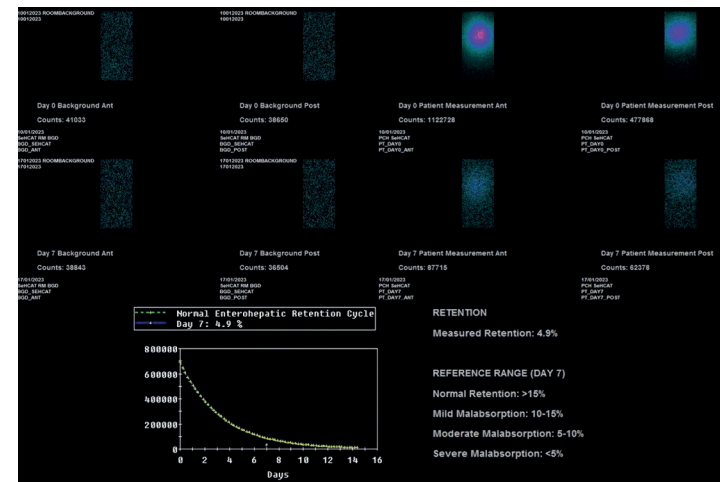


Figure 7 – Background and patient images acquired with a uncollimated gamma camera at day 0 and day 7. Results indicate severe BAM, as retention of 23-[⁷⁵Se]Se-Tauroselcholic Acid is 4.9% (courtesy of the Department of Nuclear Medicine, Addenbrooke's Hospital, CUH)

$$\% \text{ retention at day 7} = \frac{1.04 * \sqrt{\text{Ant Count day 7} - \text{Ant BG Counts day 7}} * \sqrt{\text{Post Counts day 7} - \text{Post BG Counts day 7}}}{\sqrt{\text{Ant Count day 0} - \text{Ant BG Counts day 0}} * \sqrt{\text{Post Counts day 0} - \text{Post BG Counts day 0}}} * 100$$

The same equations are used for the calculations with a WBC, even though the measurement is obtained in counts per second (cps/s). Previously formulated spreadsheets can be used for this purpose. Figures 8 and 9 are examples of data spreadsheets for BA retention calculation using a WBC, with results for normal retention and severe BAM, respectively.

The results are usually expressed as normal/abnormal (11,20) or according to

severity (8,10), as per each department's standard operating procedures.

TREATING BILE ACID MALABSORPTION

BAM is treated using BAS and dietary changes, particularly the avoidance of high-fat foods which trigger symptoms (3).

BAS have several side effects but seem to have a high level of treatment

Date / Time	Upper		Lower		Geo Mean cps	Corrected cps	Uncertainty (%)
	Count time (s)	Counts	Count time (s)	Counts			
20/10/2022							
Background 1 20/10/2022 09:42	240	1286	240	1283	5.35		
Background 2 20/10/2022 11:45	240	1226	240	1278	5.22	5.28	5.62
Patient 1 20/10/2022 11:07	240	3218637	240	882013	7020.41	7015.12	0.12
27/10/2022							
Background 1 27/10/2022 10:14	240	1206	240	1265	5.15		
Background 2 27/10/2022 11:05	240	1183	240	1287	5.14	5.14	5.69
Patient 2 27/10/2022 10:32	240	1187144	240	386867	2823.72	2934.87	0.19

Result Geometric mean **41.8 %**

Figure 8 – Data obtained from a WBC measurement with a retention value for 23-[⁷⁵Se]Se-Tauroselcholic Acid of 41.8%, deemed normal (courtesy of the Department of Nuclear Medicine, Addenbrooke's Hospital, CUH)

Date / Time	Upper		Lower		Geo Mean cps	Corrected cps	Uncertainty (%)
	Count time (s)	Counts	Count time (s)	Counts			
21/10/2022							
Background 1 21/10/2022 11:00	240	1257	240	1385	5.50		
Background 2 21/10/2022 14:32	240	1245	240	1268	5.24	5.37	5.58
Patient 1 21/10/2022 12:35	240	4366462	240	356455	5198.24	5192.87	0.17
28/10/2022							
Background 1 28/10/2022 09:20	240	1257	240	1246	5.21		
Background 2 28/10/2022 13:15	240	1188	240	1288	5.15	5.18	5.67
Patient 2 28/10/2022 12:42	240	18832	240	8204	51.79	48.53	1.32

Result Geometric mean **0.9 %**

Figure 9 – Data obtained from a WBC measurement with a retention value for 23-[⁷⁵Se]Se-Tauroselcholic Acid of 0.9%, classified as severe BAM (courtesy of the Department of Nuclear Medicine, Addenbrooke's Hospital, CUH)

success in terms of retention values <10%. Cholestyramine, one of the primary BAS used, reduces symptoms by lowering the levels of cholesterol. More recent drugs, such as colestipol and colesevelam, are better tolerated by patients but more expensive (5). Some of the side effects of BAS are constipation, gastrointestinal issues, headache, nausea, and vomiting (25). Higher compliance with the treatment has been reported in several studies involving patients diagnosed with BAM, which shows the great importance of this condition's correct diagnosis (1,26,27).

FINAL CONSIDERATIONS


Considering the incidence and prevalence of BAM within the modern population, the demand for BAM studies is increasing yearly. The role of nuclear medicine in diagnosing BAM and assessing BA pool loss is clear, with an accessible, well-established test which can predict response to treatment, providing better results and avoiding unnecessary follow-up examinations. Despite the exposure to ionising radiation, the high sensitivity and specificity of this technique substantiates its position as the ideal study for BAM diagnosis. The lack of standardised protocols is a limitation identified in several studies, which translates into lower confidence in the results on the part of physicians (7,12). Recent studies have been designed to try and overcome these limitations and improve the usefulness of the test (26).

Acknowledgements

This work was supported by the Department of Nuclear Medicine at Addenbrooke's Hospital, CUH, Cambridge; by the Department of Nuclear Medicine at West Suffolk Hospital, Bury St. Edmunds; and by the Department of Nuclear Medicine and the Department of Clinical Physics and Bioengineering at Queen Elizabeth University Hospital, NHS Greater Glasgow and Clyde, Glasgow.

REFERENCES

1. Arasaradnam RP, Brown S, Forbes A, Fox MR, Hungin P, Kelman L, et al. Guidelines for the investigation of chronic diarrhoea in adults: British Society of Gastroenterology, 3rd edition. *Gut*. 2018 Aug;67(8):1380–99.
2. Kumar A, Al-Hassi HO, Jain M, Phipps O, Ford C, Gama R, et al. A single faecal bile acid stool test demonstrates potential efficacy in replacing SeHCAT testing for bile acid diarrhoea in selected patients. *Sci Rep*. 2022;12(1):8313–8313.
3. Fernandes DCR, Poon D, White LL, Andreyev HJN. What is the cost of delayed diagnosis of bile acid malabsorption and bile acid diarrhoea? *Frontline Gastroenterology* 2019;10:72–76.
4. Arasaradnam RP, Cullis J, Nwokolo C, Bardhan K, Williams N. Bile acid malabsorption and SeHCAT: the ‘Cinderella’ will be going to the Nuclear Medicine Ball! *Nucl Med Commun*. 2012 May;33(5):449–51.
5. Review article: bile acid diarrhoea – pathogenesis, diagnosis and management - NHS Education for Scotland [Internet]. [cited 2023 Jan 23]. Available from: https://nhs-scot-primo.hosted.exlibrisgroup.com/primo-explore/fulldisplay?docid=TN_cdi_swepub_primary_oai_gup_ub_gu_se_236003&context=PC&vid=44NHSS_VU1&lang=en_US&search_scope=default_scope&adaptor=primo_central_multiple_fe&tab=default_tab&query=any,contains,Review%20articles:%20Bile%20acid%20diarrhoea%20%E2%80%93%20pathogenesis,%20diagnosis%20and%20management&offset=0
6. Khalid U, Lalji A, Stafferton R, Andreyev J. Bile acid malabsorption: a forgotten diagnosis? *Clin Med Lond Engl*. 2010;10(2):124–6.
7. Overview | SeHCAT (tauroselcholic [75 selenium] acid) for diagnosing bile acid diarrhoea | Guidance | NICE [Internet]. NICE; [cited 2023 Jan 23]. Available from: <https://www.nice.org.uk/guidance/dg44>
8. Zanoni L, Fraccascia N, Tabacchi E, Bonfiglioli R, Stanghellini V, Barbara G, Fanti S. SeHCAT test for bile acid malabsorption may “the old” become “the gold one” in the diagnostic burden of chronic diarrhea. *Clinical and Translational Imaging* 2021;9:177–180.
9. Wright JW, Lovell LA, Gemmell HG, McKiddie F, Staff RT. SeHCAT retention values as measured with a collimated and an uncollimated gamma camera a method comparison study. *Nuclear Medicine Communications* 2013;34:718–721.
10. Bronte A, Bastidas JF, Rosales JJ, Zuaznabar J, Herraiz M, Ritcher JA. Variation of enterohepatic circulation observed with ⁷⁵SeHCAT images in the first three hours. Scintigraphic patterns and analysis of their association with the diagnosis of bile acid malabsorption. *Revista Española de Medicina Nuclear e Imagen Molecular* 2021;40:351–357.
11. Notghi A, O'Brien J, Low CS, Thomson W. Measuring SeHCAT retention: a technical note. *Nucl Med Commun*. 2011 Oct;32(10):960–6.
12. Fani B, Bertani L, Pagliantini I, Fantechi L, De Bortoli N, Costa F, et al. Pros and Cons of the SeHCAT Test in Bile Acid Diarrhea: A More Appropriate Use of an Old Nuclear Medicine Technique. *Gastroenterol Res Pract*. 2018;2018:2097359.
13. Farrugia A, Arasaradnam R. Bile acid diarrhoea: pathophysiology, diagnosis and management. *Frontline Gastroenterology* 2021;12:500–507.
14. Mena Bares LM, Carmona Asenjo E, García Sánchez MV, Moreno Ortega E, Maza Muret FR, Guiote Moreno MV, Santos Bueno AM, Iglesias Flores E, Benítez Cantero JM, Vallejo Casas JA. ⁷⁵SeHCAT scan in bile acid malabsorption in chronic diarrhea. *Revista Española de Medicina Nuclear e Imagen Molecular (English Edition)* 2017;36:37–47.
15. Baena García A, Partida Palma E, García Martínez S, De Bonilla Candau M, Pajares Vinardell M. ⁷⁵Se-Homocholeic acid taurine scintigraphy (⁷⁵SeHCAT®), a standard benchmark test in bile acid malabsorption? *Revista Española de Medicina Nuclear e Imagen Molecular (English Edition)* 2019;38:305–311.
16. GE HealthCare Canada Inc. Product Monograph SeHCAT (Tauroselcholic Acid) [pdf]. GE HealthCare 2016 [cited 2022 December 21]. Available from: https://pdf.hres.ca/dpd_pm/00036708.PDF.
17. National Isotope Development Center. Selenium-75 Product Information [internet]. Isotope Program, U.S. Department of Energy n.d. [cited 2022 December 21]. Available from: <https://www.isotopes.gov/sites/default/files/2019-09/Se-75.pdf>.
18. James G, Notghi A, O'Brien J, Thomson W. Error analysis of collimated and uncollimated SeHCAT retention measurement using a gamma camera. *Nuclear Medicine Communications* 2021;42:253–260.
19. Taylor JC, Hillel PG, Himsworth JM. Commissioning of a new SeHCAT detector and comparison with an uncollimated gamma camera. *Nuclear Medicine Communications* 2014;35:1071–1076.
20. Smith MJ, Perkins AC. A survey of the clinical use of SeHCAT in the UK. *Nucl Med Commun*. 2013 Apr;34(4):306–13.
21. Hames TK, Condon BR, Fleming JS, Philips G, Holdstock G, Smith CL, Howlett PJ, Ackery D. A comparison between the use of a shadow shield whole body counter and an uncollimated gamma camera in the assessment of the seven-day retention of SeHCAT. *The British Journal of Radiology* 1984;57:581–584.
22. Soares S, Heraghty N, Gulliver N, Peters AM. ⁷⁵SeHCAT whole body retention for unexplained chronic diarrhoea based on early first whole body counting. *Nuclear Medicine Communications* 2021;42:1285–1287.
23. Smout A, Scuffham J, Hinton P. Single scan SeHCAT studies: a model for the prediction of the 3-h counts. *Nuclear Medicine Communications* 2021;42:1209–1216.
24. Nuclear Power. Whole-Body Counter – Whole-Body Counting [internet]. Nuclear Power 2022 [cited 2022 November 29]. Available from: <https://www.nuclear-power.com/nuclear-engineering/radiation-dosimetry/radiation-dosimeter/dosimetry-in-nuclear-power-plants/whole-body-counter-whole-body-counting/>.
25. Colestyramine | Drugs | BNF content published by NICE [Internet]. [cited 2023 Jan 27]. Available from: <https://bnf.nice.org.uk/drugs/colestyramine/>
26. Reid F, Peacock J, Coker B, McMillan V, Lewis C, Keevil S, et al. A Multicenter Prospective Study to Investigate the Diagnostic Accuracy of the SeHCAT Test in Measuring Bile Acid Malabsorption: Research Protocol. *JMIR Res Protoc*. 2016;5(1):e13–e13.
27. Woolson KL, Sherfi H, Sulkin T, Palmer J, Murray IA. PTH-108 Sehcate: Nice Or Not Nice? *Gut*. 2014;63(Suppl 1):A258-.



SCINTIGRAPHY OF GASTRO-OESOPHAGEAL REFLUX, PULMONARY ASPIRATION AND GASTRIC EMPTYING IN CHILDREN

by Zvi Bar-Sever¹
Dr. Laura Drubach²

¹Department of Nuclear Medicine, Schneider Children's Medical Center,
Tel Aviv University, Israel

²Division of Nuclear Medicine, Department of Radiology, Boston's Children Hospital,
Harvard University

INTRODUCTION

Diseases of the gastrointestinal and respiratory tract are common in children and range from mild asymptomatic conditions to severe, life-threatening conditions. Nuclear medicine has an important role in the evaluation of these conditions. This chapter will focus on gastro-oesophageal reflux, pulmonary aspiration and gastric emptying evaluation in children. Clinical presentations, diagnostic modalities and a brief description of treatment principles will be presented. Nuclear medicine studies that are used for the diagnosis of these conditions will be discussed in detail, including subsections on the required preparations, radiopharmaceutical administration and dosimetry, imaging protocols, processing and interpretation.

GASTRO-OESOPHAGEAL REFLUX (GER) IN INFANTS AND CHILDREN

Definitions

GER implies retrograde passage of gastric contents from the stomach into the oesophagus.

Regurgitation suggests that refluxed gastric contents entered the oropharynx, whether or not they were expelled from the mouth. Vomiting is defined as expulsion of gastric contents from the mouth, and is typically a forceful action. Rumination refers to voluntary regurgitation of stomach contents into the mouth for

self-stimulation; may present at any age, including in infants (1).

GER is a common phenomenon encountered at all ages. It is most frequent during the first 18 months of life and is asymptomatic in most cases. Repetitive reflux episodes, however, might produce symptoms and complications in some infants and children, leading to a condition termed gastro-oesophageal reflux disease (GERD). Frequent episodes of regurgitation during infancy are associated with GERD symptoms in later childhood (2). It is thought that the frequency and duration of reflux, gastric acidity, gastric emptying, oesophageal clearing mechanisms, oesophageal mucosal barrier, airway hypersensitivity and genetic predisposition are contributing factors in the pathogenesis of GERD (3).

Epidemiology and clinical presentations

The prevalence of GER and GERD is difficult to establish because signs and symptoms are non-specific, especially in infants. GER is very common during the first months of life due to transient relaxations of the lower oesophageal sphincter, unrelated to swallowing and due to inadequate adaptation of the sphincter tone to changes in abdominal pressure (4). Most infants are healthy and thriving well. GER episodes can be completely asymptomatic or lead to regurgitation into the mouth. Sixty-one per cent of healthy 4-month-old infants had at least one reflux

episode, declining to 21% between 6 and 7 months (5).

Symptoms of GERD were found in 1.8–8.2% of children and in 3–5% of adolescents. Preterm infants, children with neurological disabilities, children with cystic fibrosis, Down's syndrome, repair of oesophageal atresia, hiatal hernia, increased intra-abdominal pressure (peritoneal dialysis, abdominal masses, etc.) and obese children have higher rates of GERD (6,7,8,9).

Clinical manifestations of GERD vary with age and are encountered in both gastrointestinal (GI) and respiratory systems. Infants with GERD may experience recurrent vomiting. A small percentage of them will present with complications of oesophagitis including dysphagia, feeding difficulties, irritability, anaemia, haematemesis and failure to thrive. Respiratory complications include wheezing, recurrent pneumonia, and, rarely, brief resolved unexplained events (BRUE) that include apnoea, bradycardia, cyanosis/pallor and sudden behavioural changes. It is thought that these mechanisms are related to laryngospasm, possibly triggered by a reflux episode. A clear association between GER and BRUE has not been convincingly established (10). In preschool children, GERD may present as food aversion, poor weight gain, and hyperactive airway disease. It is hypothesised that sudden drops in oesophageal pH due to acid reflux episodes trigger bronchoconstriction (11). Aspiration pneumonia is another serious complication

that is mainly encountered in children with congenital or acquired neurological impairments. Recurrent aspirations can lead to chronic lung disease with bronchiectasis and respiratory insufficiency. Chronic heartburn, regurgitation or both are the most common symptoms in school-aged children and adolescents (ATD 19). Additional, less common complications include nausea, oesophageal strictures with dysphagia and epigastric pain, Barrett's oesophagus, hoarseness due to reflux-induced laryngitis, chronic cough, dental disease, asthma, sinusitis, bronchiectasis and recurrent pneumonia (12). Some symptoms and complications attributed to GERD may, in fact, suggest a different, more serious medical condition requiring an accelerated diagnostic approach. Some of these red flags include projectile and bilious vomiting (suggesting bile obstruction), haematemesis, bloody stools, hepatosplenomegaly, abdominal distension and neurologic deficiencies. Systemic symptoms raise the possibility of infectious and metabolic conditions (10).

Diagnosis

Several imaging and non-imaging methods are available. Some demonstrate the presence of reflux episodes and others GER complications. Given the high incidence of asymptomatic, "benign" GER episodes, especially in infants, clinical judgement as well as the frequency and severity of the episodes should be carefully considered

when associating the reflux with the clinical symptoms and complications.

Diagnostic evaluations should be tailored according to the child's age, symptoms, and the presence of red flags suggesting a serious condition other than GERD (1).

The diagnosis is sometimes achieved following a favourable response to a therapeutic trial. For example, empirical treatment with proton pump inhibitors (PPIs) has been shown to be a cost-effective diagnostic technique in adults and may be useful in adolescents with uncomplicated heartburn (10). This approach was not found to be effective in infants and children, where the response to placebo and PPI trials was similar (13). Diagnostic tests include oesophageal pH monitoring, oesophageal multichannel intraluminal impedance monitoring, gastro-oesophageal reflux scintigraphy, barium contrast radiography and endoscopy with biopsy. Non-scintigraphic techniques will be described briefly in the following paragraph, followed by a detailed description of gastro-oesophageal reflux scintigraphy (GES).

Oesophageal pH and impedance monitoring

Twenty-four-hour oesophageal pH monitoring requires placement of a transnasal catheter with pH-sensitive electrodes in the distal oesophagus. These electrodes allow continuous recording of the oesophageal pH, which normally ranges from 5–7. A drop in the pH below 4 suggests

reflux of acid gastric contents. The “reflux index” is the percentage of time in which the oesophageal pH is less than four. It is the most important parameter of the test that sheds light on the cumulative oesophageal acid exposure and can be used to assess the effectiveness of anti-acid therapies (1). A major limitation of pH monitoring is its inability to detect non-acidic reflux episodes. These episodes occur mostly during the post-prandial period, when gastric acidity is neutralised in relation to the patient's age, meal volume and composition, and feeding frequency (14). Non-acidic reflux episodes are clinically significant. It has been shown in infants and children that irritability, sleep disorders, bronchitis, aspiration pneumonia, desaturation and apnoea episodes can be induced by both acidic and non-acidic reflux (15). The correlation between pH monitoring results, clinical symptoms, presence of oesophageal disease, and response to therapy was found to be weak (1).

Multichannel intraluminal impedance (MII) monitoring is a catheter-based technique that measures electrical impedance changes in the oesophagus induced by bolus transit. It can be performed in combination with oesophageal pH monitoring by placing the impedance and pH probes on the same catheter. It can also be combined with high resolution oesophageal manometry enabling quantification of the proportion of transient lower oesophageal sphincter relaxations associated with bolus movement into the

oesophagus (1). MII monitoring is capable of detecting both acidic and non-acidic reflux and is considered by many to be a gold standard. It should be kept in mind, however, that extended pH monitoring and MII monitoring, whether separately or combined, are invasive procedures requiring hospitalisation. The combination of 24-hour pH monitoring with intraluminal impedance monitoring detects more reflux episodes than the two separately and is more sensitive than GER scintigraphy (16, 17). The same study, which included 75 children, found slight or no agreement between impedance, pH monitoring and gastro-oesophageal scintigraphy results. When combined impedance and pH monitoring was considered to be the gold standard, the sensitivity of GER scintigraphy was over 80%.

Barium contrast radiography

Upper gastrointestinal (UGI) series with barium contrast, used in the past, is no longer considered a first-line study for the diagnosis of reflux because it has a lower sensitivity and specificity compared to oesophageal pH and impedance studies and compared with scintigraphy. This study is challenging in young, uncooperative children unwilling to swallow the contrast. Videofluoroscopy provides only a brief observation period to avoid excessive radiation exposure. However, unlike pH monitoring impedance and GER scintigraphy, barium studies provide anatomical details that may be relevant for

the diagnosis of alternative conditions such as bowel malrotation, annular pancreas and antral web (18). In cases of prominent dysphagia, these studies can demonstrate oesophageal strictures or other conditions such as achalasia or hiatal hernia.

Endoscopy with biopsies

Endoscopy cannot detect GER. Instead, it allows visualisation of the oesophageal mucosa to assess damage from reflux episodes. Biopsies increase the sensitivity of the procedure and help identify other conditions, unrelated to GER, such as eosinophilic oesophagitis, allergic gastritis and inflammatory bowel disease (9). The procedure is invasive, requiring anaesthesia, but it is considered safe in infants and children.

Gastro-oesophageal reflux scintigraphy

GER scintigraphy is a nuclear medicine study, also known by the name “milk scan”. It is designed to detect GER and pulmonary aspiration of gastric contents. It can also measure gastric emptying.

The patient is fed with his/her regular milk or milk formula-based meal mixed with a small amount of radiotracer. Dynamic images of the chest, recorded for one hour, may detect GER episodes by showing tracer activity in the oesophagus. Tracer activity in the bronchi or lung parenchyma indicates pulmonary aspiration. Static images of the chest obtained at 1 and 4 hours (rarely at 24 hours as well) can detect subtle aspiration

that was not evident on the dynamic images as well as “late” aspiration that might have occurred between the end of the dynamic acquisition and the “late” static image. Including both chest and abdomen in the field of view enables calculation of gastric emptying.

This section will describe the study protocol and its ability to detect GER. The role of the study in the detection of pulmonary aspiration and the assessment of gastric motility will be described in the following sections on pulmonary aspiration and gastric emptying, respectively.

Study protocol

There is no universally accepted protocol for the “milk scan”. Most techniques share the same basic principles. A common protocol used in the authors’ departments will be described as a general reference.

Preparations

It is important to exclude milk allergy. Infants with this condition should be fed with their regular, non-allergenic milk formula. A 4–6-hour fast is required. For young infants, it is recommended to schedule the study so it can replace a regular meal. Parents and caregivers are instructed to bring the child’s regular meal (human milk, cow milk, milk formula) in his/her feeding bottle and an additional empty bottle. The volume of the meal should be similar to the volume of a regular meal ingested at home. However, it is recommended that the meal volume should

exceed 50 ml, because inadequate filling of the stomach might reduce the sensitivity of the study. The radiopharmaceutical is mixed with the milk or milk formula in the first bottle containing one third of the total meal volume. The second bottle contains the remaining, unlabelled, portion of the meal. The child is first fed with the bottle containing the labelled milk/milk formula. He/she is then offered the second bottle with the unlabelled milk to complete the desired meal volume and to wash all remaining activity from the mouth and oesophagus (or from the nasogastric or gastric tubes, when used). Oral feeding is the preferred route for tracer administration, but if necessary the meal can be administered through a pre-existing gastric tube or through a nasogastric tube that should be removed after feeding. It is best to complete the feeding within 10–15 minutes. Infants should be held upright and burped prior to imaging. Spillage of the meal during feeding, and regurgitation or vomiting during feeding or acquisition result in significant contamination artefacts that can result in interpretation errors, especially when they involve the chest. It is recommended to cover the child during feeding and imaging with disposable absorbent sheaths to prevent the hazard of contamination artefacts.

Radiopharmaceutical

The recommended radiopharmaceutical is [^{99m}Tc]-sulphur colloid that remains stable in the acidic medium of the stomach and

is not absorbed from the GI or respiratory mucosa. Absorption through the mucosa could increase background activity, reduce the available tracer in the stomach and hinder the study sensitivity. The recommended activity according to the EANM dosage calculator ranges from 10 MBq for a 3 kg infant up to 39 MBq for a 68 kg patient. Typical activities and effective doses (in brackets) for 1, 5, 10 and 15-year-old children are 10 MBq (1.4 mSv), 13 MBq (0.99 mSv), 20 MBq (0.98 mSv) and 33 MBq (1.01 mSv) respectively. The critical organ is the large bowel (19). Recommended activities can be obtained from online calculators available on the EANM, SNMMI and Image Gently websites.

Sedation

Sedation and anaesthesia can alter the performance of the swallowing mechanism, increasing the risk of aspiration. They are therefore prohibited in studies involving administration of a test meal, such as GER and gastric emptying scintigraphy.

Acquisition

The child is placed in the supine position and secured to the camera bed. Posterior view dynamic images, 30 seconds per frame on a 128x128 matrix are acquired for 60 minutes. The imaging zoom should be adjusted to the size of the child. The field of view extends from the mouth to the upper abdomen, or the entire abdomen if gastric emptying calculations

are required. Dynamic imaging is followed by anterior and posterior static images of the chest over 3–5 minutes on a 256 × 256 matrix. A second set of similar static images is obtained 4 hours from the start of acquisition. Twenty-four-hour images are optional and may be too count poor for diagnostic purposes. Some centres perform a high-count, “baseline” static image of the chest and upper abdomen at the beginning, before the dynamic sequence. This image can sometimes demonstrate aspiration that occurred during feeding. Positioning cobalt-57 markers over the xiphoid and suprasternal notch can enhance spatial orientation. In selected cases, a Co-57 flood source transmission image of the chest, superimposed on the static emission image, is helpful in localisation of ectopic activity over the chest (20).

Variations from this protocol have been reported over the years. Some centres prefer anterior view imaging to decrease the patient-to-collimator distance and prevent oesophageal count attenuation by the spine and the imaging table in general. This approach, however, means that the collimator is positioned very close to the child’s face throughout the study. This is frightening to the non-sedated child, prevents eye contact with his/her caregivers and is likely to cause many motion artefacts. We prefer imaging from the posterior view, with an unobstructed approach to the child. This set-up also allows distracting entertainment from overhead video screens.

One study actually found that the ability to detect reflux did not differ between anterior and posterior dynamic views (21). A study that examined the effect of the patient's position on GER detection rate found that the supine position was more sensitive than the prone and lateral decubitus positions (22). Another study showed that shifting the imaging positions during the study yielded more reflux episodes than the traditional supine position (23). Repetitive immobilisations in the different positions could be more intimidating to the young child, resulting in motion artefacts. An attempt to shorten the dynamic acquisition time from 60 to 30 minutes resulted in missing 25% of the reflux episodes (22). Some authors use shorter frame times of

5–10 seconds in dynamic imaging. They claim that reflux detection is still possible despite the reduced count density in each frame, allowing detection of brief reflux episodes that cannot be captured with longer frame times and thus providing a more precise estimation of the total number of reflux episodes (24).

Processing and interpretation

Interpretation of GER scintigraphy is mainly based on careful visual assessment of the images. Adjustments of the image window and cinematic display are useful manipulations that may help detect subtle reflux and aspiration episodes. A reflux episode is identified when new tracer activity is seen in the oesophagus (Figure 1).

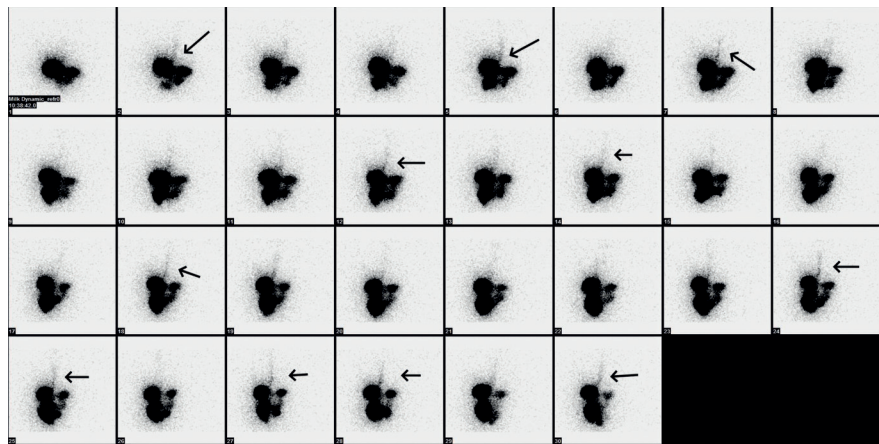


Figure 1 – (Gastro-oesophageal reflux)
Milk scan of a 6-year-old boy with cerebral palsy, psychomotor retardation and chronic lung disease with pulmonary hypertension. Selected frames from his study show multiple episodes of gastro-oesophageal reflux (arrows) without aspiration.

The number of episodes and the level of the refluxed tracer (distal, proximal oesophagus, oropharynx) should be noted. A crude reflux residence time in the oesophagus can be obtained by dividing the number of frames showing activity in the oesophagus by the total number of frames. Time-activity curves can provide a graphic representation of GER episodes. Regions of interest (ROIs) are positioned over the oesophagus and stomach. Reflux episodes appear as sharp peaks in the oesophageal curve. Motion artefacts, causing gastric counts to be included in the oesophageal ROI, adversely affect the curve and introduce errors. Applying motion correction software can sometimes prevent these errors. Tracer activity in the trachea, proximal or distal bronchi or lung parenchyma suggest pulmonary aspiration. Some centres process the raw image data in order to establish a semi-quantitative analysis that can augment the interpretation. These include advanced techniques attempting to quantify GER by taking into account the volume of the reflux in each episode, the reflux frequency and the clearing rate of the refluxate from the oesophagus. Some centres use indices that normalise oesophageal activity during the reflux to the initial gastric activity (22,25). Creation of a condensed image can also improve reflux detectability (26). One study found visual interpretations to be superior to interpretations based on time-activity curves and on condensed images (27).

GER scintigraphy is a non-invasive, easy-to-perform study that does not require significant patient cooperation. Radiation exposure is low. Unlike other imaging and non-imaging techniques, it imitates physiological conditions. It is a sensitive method to detect GER (17). A unique feature of the study is the combined assessment of GER, pulmonary aspiration and gastric emptying.

Treatment

Treatment principles for infants and children with symptomatic reflux and GERD will now be briefly mentioned. In cases of well thriving babies with frequent regurgitation episodes, reassuring the parents and explaining the benign nature of this phenomenon is usually sufficient. Infants should not be placed in the prone position because this position has been associated with increased risk of sudden infant death. Keeping an infant upright for 20–30 minutes after a feed can reduce the likelihood of regurgitation. Simple lifestyle changes might improve the condition. It is important to avoid tobacco smoke exposure because it might increase reflux episodes (28). Wherever possible avoid switching from breastfeeding to milk formula feeding, because breastfeeding may have a protective effect on regurgitation in infants (29, 30). Overfeeding should be avoided. A trial of thickening the feeds is worthwhile, but this strategy is cumbersome for mothers who are breastfeeding and the overall

success of this strategy is modest (1). In infants with poor weight gain and irritability, milk protein allergy should be excluded and an empirical trial of removing cow's milk from the diet is suggested (31, 32, 33).

In older children and adolescents, beneficial lifestyle changes include weight loss in obese individuals and avoidance of tobacco smoke exposure, caffeine, chocolate, spicy foods and alcohol. Pharmacological therapy with acid-suppressing medications such as histamine-2 receptor blockers or proton pump inhibitors is initiated when dietary and lifestyle changes fail. The effect of these pharmacological interventions should be closely monitored. Refractory cases of GERD may be referred to surgery for a fundoplication procedure (1, 10).

PULMONARY ASPIRATION

Definition and risk factors

Pulmonary aspiration is defined as entry of foreign materials into the respiratory system below the level of the true vocal cords. Aspirated substances include gastric contents (following gastro-oesophageal reflux, regurgitation or vomiting), solids and liquids during feeding, and salivary secretions. Foreign body aspiration will not be discussed in this chapter. Swallowing dysfunction is the common mechanism leading to aspiration. Swallowing is a complex mechanism that consists of voluntary and involuntary elements. It begins in utero with suckling and

swallowing of amniotic fluid (34). The ability to form a bolus and to propel the food into the oesophagus (deglutition) develops gradually and continues to improve until 2 years of age. Many morphological and functional abnormalities are considered to be risk factors for swallowing dysfunction and consequent aspiration. Conditions indicative of an anatomical predisposition include cleft lip and palate, choanal atresia, micrognathia, pharyngeal masses (cysts and tumours), laryngeal clefts and webs, trachea-oesophageal fistula, vascular rings, oesophageal strictures and achalasia. Surgery of the upper aerodigestive tract is an additional risk factor. Functional abnormalities include a wide range of congenital or acquired neurological disabilities (with or without CNS malformations), neuromuscular disorders, vocal cord paralysis, medications that alter the level of consciousness, respiratory syncytial virus bronchiolitis and other conditions causing respiratory insufficiency with tachypnoea (35).

Clinical presentations

In infants, swallowing dysfunction and aspiration appear as choking and gagging episodes during meals, apnoeic episodes and cyanosis. Stridor is another presentation in young infants. Poor weight gain and failure to thrive may be additional complications due to poor caloric intake. Some infants and children present with "wet breathing" or "rattling" due to

laryngeal penetration. Cough is a common sign unless the cough reflex is blunted. These children might experience "silent" aspirations. Recurrent aspirations may cause wheezing, asthma, hoarseness, recurrent pneumonias, bronchiectasis and interstitial lung disease (35). Ultimately, repeated severe lung aspirations will cause respiratory insufficiency and death.

Diagnosis

Diagnosis of pulmonary aspiration is based on clinical evaluation supplemented by imaging and non-imaging studies that provide direct and indirect evidence for swallowing dysfunction and aspiration. Clinical examination includes observation of the child during ingestion of liquids and solids of various thicknesses and textures. A neurological examination searches for possible neurological deficiencies. Chest radiographs and CT are obtained to evaluate lung disease resulting from aspiration as well as congenital anomalies that predispose to aspiration.

Videofluoroscopic swallow study (modified barium swallow)

This study evaluates the integrity of the swallowing mechanism and the presence of aspiration. It is the most common test used in children (36, 37, 38). Videofluoroscopy is performed while offering the patient a variety of food and liquid textures mixed with barium or other contrast. The study requires multiple swallows because

aspiration is an intermittent phenomenon and because swallowing abnormalities may first be evident only after the child fatigues (especially in infants). Swallowing dysfunction may present as pooling of contrast in the vallecular and pyriform sinuses and in the pharyngeal recesses. When aspiration occurs, contrast is seen in the tracheobronchial tree. Cricopharyngeal dysfunction and laryngeal penetration might reflect physiological immaturity in young infants. They are considered pathological in children older than one year of age.

Fibre-optic endoscopy

This invasive technique is not frequently used in children. It involves placement of a fibre-optic laryngoscope above the palate, enabling the endoscopist to observe laryngeal elevation and closure during swallowing. Adding colour to the food helps in detecting residual pooling and aspiration (36, 39).

SCINTIGRAPHIC TECHNIQUES FOR THE EVALUATION OF ASPIRATION

GER scintigraphy

This study can demonstrate pulmonary aspiration of gastric contents due to GER, regurgitation or vomiting (Fig 2). The technical details of the study were described in the previous section. In practice, it has been the experience of many nuclear medicine practitioners that the sensitivity

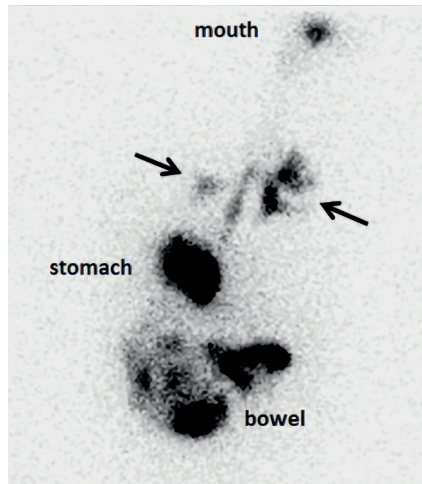


*Figure 2 – (Aspiration on milk scan)
A 3-year-old girl with cerebral palsy experienced repeated pulmonary infections despite measures to prevent aspiration that included Nissen fundoplication and gastrostomy tube feedings. Her salivagram was negative. The milk scan demonstrated multiple episodes of GER reaching the oropharynx and thereby indicating malfunction of the fundoplication. Additionally, a large amount of tracer was noted in the lung fields (arrows) suggesting pulmonary aspiration. (Courtesy: Dr. Anita Brink, Red Cross Memorial Hospital, Cape Town.)*

of the study for detection of pulmonary aspiration is relatively low, ranging from 1–26% in various studies (40, 41). The wide range of sensitivities is thought to reflect variabilities in patient selection, study protocols and the use of different clinical and imaging tests as a reference for aspiration. The low sensitivity of milk scans in the detection of lung aspirations is supported by the observation that anti-reflux treatment reduces the incidence of pulmonary disease in children who were negative for aspiration

on GER scintigraphy (42). The low detection rates may also reflect the intermittent nature of pulmonary aspiration. Rapid clearance of aspirated tracer from the large airways by pulmonary defence mechanism and low tracer concentration in the aspirate might be additional causes for the low detection rate (43). Of the two imaging studies that can directly demonstrate aspiration of gastric contents, GER scintigraphy was more sensitive than barium upper GI series (44).

The radionuclide salivagram

The radionuclide salivagram is a scintigraphic technique specifically designed to image aspiration of saliva.

Subtle, inconsequential aspiration of small amounts of saliva can occur in normal individuals, especially when airway protective mechanisms are stressed while talking, laughing and eating, or during sleep. These salivary secretions are rapidly cleared from the tracheobronchial tree by pulmonary defence mechanisms that include the cough and the mucociliary transport mechanisms. Frequent, repetitive aspiration of salivary secretions and failure to clear the aspirates from the tracheobronchial tree lead to recurrent pulmonary infections.

Aspirated saliva transports bacteria from the normal flora of the oral cavity into the different microenvironment of the lower respiratory tract. These bacteria are pathogenic to the lungs and cause recurrent lung infections. This hypothesis is supported by bacteriological studies

showing that bacteria isolated from the lungs in aspiration pneumonia are similar to the bacteria in the oropharyngeal flora (45, 46). Repeated aspiration of salivary secretions is responsible for ongoing lung infections in children in whom oral feeding was discontinued to prevent aspiration while eating or drinking and anti-reflux surgery was carried out to prevent retrograde aspiration of gastric contents (47, 48, 49). Aspiration of saliva should be considered in all children with symptoms of recurrent pulmonary aspirations.

Study protocol

As with GER scintigraphy, there is no universally accepted protocol for this study. A common protocol used in the authors' departments will be presented as a general reference (20).

Preparations

No fasting or other preparations are required. Anaesthesia and sedation can adversely affect the swallowing and pulmonary defence mechanisms and should therefore be avoided.

Radiopharmaceutical administration

The radiopharmaceutical is [^{99m}Tc]-sulphur colloid. A fixed (non-weight-based) activity of 9.25–11.1 MBq (0.25–0.3 mCi) is recommended. The effective dose is similar to the effective dose from GER scintigraphy for similar tracer activities. The tracer volume should not exceed 1 drop (approximately 100

μL). The radiopharmaceutical is placed under or over the tongue. The small volume is a key element of the study. It should not initiate the swallowing process, thus allowing time for the tracer to mix with the salivary secretions.

Acquisition

The child is secured to the imaging bed in the supine position. Imaging begins immediately following tracer administration. Posterior view dynamic images, 30 seconds per frame are recorded on a 128X128 matrix for 60 minutes. A low-energy high or ultra-high resolution collimator is used and the imaging zoom is adjusted to the size of the child. The field of view includes the oropharynx, neck and thorax. At the end of the dynamic acquisition, 3–5 minutes anterior and posterior static images of the chest are recorded on a 256X256 matrix. If no aspiration is seen and significant tracer activity remains in the oral cavity, additional delayed static images are acquired at 120 minutes. Regurgitation and drooling can produce contamination artefacts. It is recommended to cover the child with absorbent sheaths with plastic lining on one side. Spatial orientation and localisation of ectopic activities can be enhanced by placing Co-57 markers on the suprasternal notch and xiphoid process. In selected cases, a Co-57 flood source transmission image of the chest, superimposed on the emission image, can be helpful.

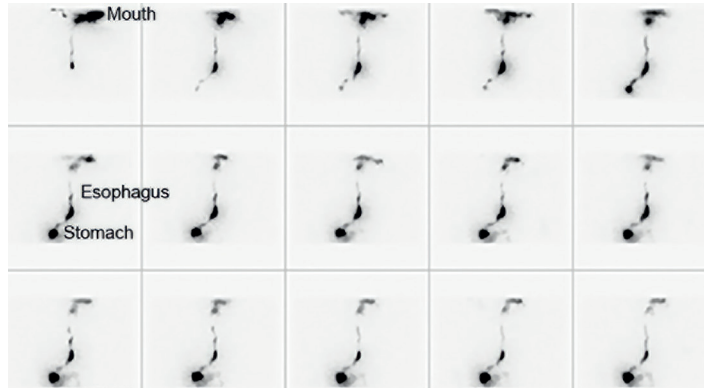


Figure 3 – (Normal salivagram) Salivagram in a 13-year-old with cerebral palsy showing passage of the radiopharmaceutical from the mouth to the oesophagus and into the stomach. No bronchopulmonary aspiration of saliva detected during the one hour of imaging.

Some authors have reported variations from the proposed protocol. For instance, some centres use shorter frame times for the dynamic imaging (50). SPECT/CT improved localisation of aspirated saliva in a study on 53 adults with acute exacerbations of chronic obstructive lung disease who underwent salivagrams (51). Some investigators reported a different tracer administration method in which the tracer is mixed in 10 ml of normal saline in a syringe. The syringe is placed in a syringe pump and the solution is delivered into the mouth through a feeding tube at a constant rate over 60 minutes (52, 53). This method of administration may be more challenging to the swallowing mechanisms, accounting for higher rates of positive studies (41, 53).

Interpretation

A normal salivagram shows tracer transit from the oral cavity through the oesophagus into the stomach without any uptake in the airways or lung parenchyma (Fig 3). Tracer activity in the tracheobronchial tree or lung parenchyma indicates aspiration of saliva (Fig 4). Detectability can be enhanced by manipulation of the image grey scale window and by cinematic display. Distal aspirations in the smaller bronchi and lung parenchyma are assumed to represent more severe cases of aspiration than aspiration into the trachea and large main bronchi. One study proposed a 4-point classification system to better describe the aspiration pattern and to grade the severity of aspirations, thus improving the ability to compare follow-up studies. No clear correlation was found between the presence and type of clinical symptoms and

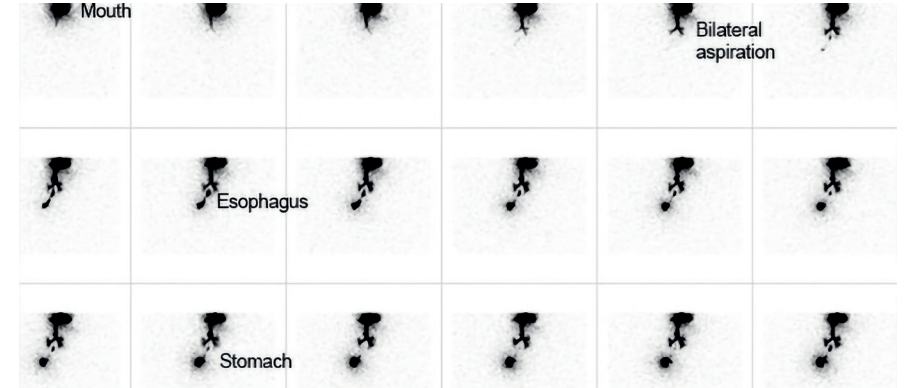


Figure 4 – (Aspiration of saliva) Salivagram in an 8-year-old with neuromuscular disorder and history of multiple episodes of pneumonia. There is rapid bilateral aspiration of the radiopharmaceutical into the proximal bronchi.

the aspiration grade (50). Another group proposed an aspiration index to optimise the classification of pulmonary aspiration detected by salivagrams. They divided the counts in the respiratory tract by the total counts in the field of view. Higher values were encountered in more severe grades of aspiration (54). Occasionally the dynamic images show clearance of aspirated tracer from the tracheobronchial tree. This observation requires continuation of the acquisition for the entire 60 minutes, even when there is earlier evidence of aspiration. The ability of the radionuclide salivagram to demonstrate clearance of aspirated tracer provides an important insight into the functional integrity of pulmonary defence mechanisms. Malfunction of these mechanisms increases the likelihood of lung disease in patients who aspirate (45).

Clinical experience

Positive salivagrams reported in the literature range from 16%–56%, (41, 53, 55, 56), reflecting differences in patient selection and study technique. Salivagrams detect more aspirations than GER scintigraphy. In 266 children who underwent both procedures, salivagrams were positive in 22% and milk scans in 1.9% for pulmonary aspiration. The authors concluded that anterograde aspiration was more common than retrograde aspiration in their study population (57). Pulmonary aspiration was evaluated in 63 children with cerebral palsy. Salivagrams detected aspiration in 56%, barium videofluoroscopy swallowing test in 39% and milk scans in 6%. It should be kept in mind, however, that these studies detect different types of aspiration (41). In a study on 222 children that compared salivagrams with chest

radiographs, positive salivagrams were encountered in 25% and chest X-ray abnormalities in 24%. The authors found a strong correlation between positive salivagrams and chest radiographic abnormalities. The odds of positive salivagrams in neurologically impaired children were 5.6 times higher than in other conditions. They concluded that salivagrams are valuable tools to determine the presence of pulmonary aspiration and the likelihood of identifiable radiographic consequences. Salivary aspiration is clinically significant and can cause structural lung changes. They noted that positive salivagrams led to management changes in all patients (55). Another study reported that positive salivagrams were strongly associated with chronic respiratory infections, developmental delay, reactive airway exacerbations and prescription of anti-reflux medications (58).

Some centres perform scintigraphy with a labelled liquid bolus of 5–10 ml. These are not salivagrams, but rather radionuclide swallowing studies. They can demonstrate aspiration of liquids in a similar way to the barium swallow studies, but not aspiration of saliva (59). The relation between swallowing dysfunction and the swallowed volume is complex. A study performed on adults with brain lesions who underwent salivagrams found a significantly higher aspiration rate when the tracer was administered in a volume of 0.5 cc versus 0.1 cc (60).

Treatment of pulmonary aspiration in children

Management is individualised according to the suspected source of aspiration, the cause of the swallowing dysfunction and the severity of the associated complications. In mild cases, treatment is based on modifications of the bolus size, food consistency and texture, frequency of feeding and feeding position (35). More severe cases of swallowing dysfunction require temporary or permanent discontinuation of oral feeding with placement of a percutaneous gastrostomy tube to provide nutrition. When the aspiration source is gastric contents, and conservative anti-reflux strategies fail, fundoplication surgery is performed. Prevention of saliva aspiration is more complex. Measures may include administration of anticholinergic agents to reduce excessive salivation. More radical measures are used in children with intractable aspiration of saliva and life-threatening pulmonary disease. These measures include salivary gland excision, salivary duct ligation, injection of the parotid and submandibular glands with botulinum toxin, and, rarely, laryngotracheal separation with construction of a permanent tracheostomy (35).

SCINTIGRAPHY OF GASTRIC DYSMOTILITY IN CHILDREN

Clinical background

Gastric dysmotility refers to delayed gastric emptying (gastroparesis) and to the rare cases of rapid gastric emptying. Gastroparesis is defined as delayed gastric emptying of fluids or solids in the absence of mechanical obstruction (61,62). The literature on paediatric gastroparesis is sparse, and given the non-specific signs and symptoms of this condition the overall incidence and prevalence in children is unknown (63). Gastroparesis in children is most often idiopathic. About 40% of paediatric patients with gastroparesis have associated comorbidities including epilepsy, cerebral palsy, developmental delay and prematurity (64). Another study reported that 18% of paediatric gastroparesis cases were of post-viral origin, 18% due to medications, 12.5% post-surgery, 8% mitochondrial diseases and 2–4% due to diabetes (65). Diabetes mellitus is among the most common aetiologies of gastroparesis in adults. Adults with gastroparesis may have associated psychiatric and/or abuse comorbidities in up to 62% of cases (66). This association is less common in children. A study on 239 paediatric patients with gastroparesis found psychiatric comorbidities in 28% (64).

Clinical symptoms of delayed gastric emptying in the paediatric population are age dependent. In infants the leading symptom is vomiting, which can be

associated with weight loss. Vomiting is also common in children 1–10 years old, with the additional symptom of abdominal pain. In older children abdominal pain is the leading symptom, followed by nausea and vomiting. (66). The outcome of gastroparesis in children appears to be more favourable than in adults. In a study on 239 children with gastroparesis, 60% reported significant improvement in nausea, vomiting, abdominal pain, early satiety, bloating and weight loss at a 2-year follow-up (64). Paediatric cases of gastric dysmotility presenting with rapid emptying, also known as the “dumping syndrome”, are most often secondary to gastric surgery. Dumping syndrome can also be encountered in Zollinger-Ellison syndrome (one or more gastrinomas). Overall, rapid emptying is uncommon in children. Symptoms include post-prandial diarrhoea, hypoglycaemia, flushing, sweating, tachycardia and abdominal cramps (67).

DIAGNOSTIC TESTS

Gastric emptying scintigraphy

Gastric emptying scintigraphy is considered the gold standard for gastric emptying evaluation (63). Scintigraphy can assess both solid and liquid emptying. Solid emptying is considered more reliable. A standardised egg-based meal and normal reference values have been established for adults. This meal can also be used for older children and adolescents. For infants and young children who cannot consume solids

the only option is liquid gastric emptying. The diet of infants is based on milk or milk formulas, which is the only practical choice for a test meal. The milk-based meal is also used in young children because it is more acceptable to them than the standardised solid meal. Milk and milk formulas are actually transformed into semi-solid chime in the acidic environment of the stomach, so their clearance does not truly represent liquid gastric emptying (20). Gastric emptying scintigraphy is a physiological, non-invasive, inexpensive and widely available technique that provides both visual and quantitative assessment of gastric emptying. It requires standardisation of the test meal composition and study protocol in order to derive any meaningful comparison between studies and establish normal reference values. These requirements are especially challenging in infants and children. The test meal should be palatable to children, yet standardised. Normal values for gastric emptying require testing of healthy volunteers. Most centres will not perform studies that involve ionising radiation on healthy children due to ethical considerations, resulting in a lack of universally accepted normal reference values. Given these circumstances, centres performing gastric emptying scintigraphy in children use their own “in-house” test meals and their own reference values for normal emptying. These measures are not validated or universally accepted. In recent years, attempts have been made to standardise the paediatric test meal and establish normal

reference values. More details of paediatric gastric emptying techniques, protocols and reference values will be described in the following sections.

Alternative, non-scintigraphic methods for assessment of gastric emptying are also available and their principles will be briefly outlined.

C-13 gastric emptying breath tests

This test uses mass spectrometry to measure concentrations of non-radioactive C-13 in expired air following a test meal containing C-13. The test meal for liquid emptying contains C-13 acetate, and the solid emptying meal contains C-13 octanoic acid or spirulina platensis. The meal is absorbed from the gut and metabolised in the liver, creating $^{13}\text{CO}_2$ molecules that are eliminated in the lungs with the expired air (68). This is a non-invasive test without radiation exposure and with a good correlation to gastric emptying scintigraphy results (69). One study established normal breath test reference values for a standardised milk-based meal containing C-13 acetate for children 1–17 years old (70). Breath tests have their limitations, however. C-13 build-up in expired air not only depends on the gastric emptying rate but also on gut absorption and the function of the liver and lungs. Physical activity, dietary factors, concurrent diseases and medications also influence results (71).

Barium swallow and endoscopy

These studies do not measure gastric emptying. They provide direct and indirect visualisation of the oesophagus, stomach and duodenum and are important in detecting anatomical obstructions affecting gastric emptying (e.g. pyloric stenosis, obstructing masses, antral web, etc.). They can also detect other conditions with similar presentation to gastroparesis (e.g. gastritis, peptic disease, etc.).

US and MRI techniques

These are non-invasive imaging studies. US can determine gastric volumes and trans-pyloric flow. It can also assess gastric accommodation (72). Time-sequenced magnetic resonance imaging (MRI) of the stomach is an emerging technique for non-invasive assessment of gastric emptying and motility. MRI processing creates 3D models of the stomach. This tool can be used for evaluating gastric volumes, surface geometry, and wall tension in response to filling and emptying (73, 74).

US and MRI techniques require additional validation and standardisation and are not employed in routine clinical practice in most centres.

Electrogastrography

External electrodes record the electrical activity of the stomach. This non-invasive technique can be used to evaluate abnormalities in myoelectrical activity and gastric contractions (75). The

technique requires further standardisation and is uncommon in routine clinical practice.

Wireless motility capsule

The wireless motility capsule is a non-digestible, orally ingested capsule that measures intraluminal pressure, temperature, pH, and allows calculation of transit times in the GI tract. It has been FDA approved in adults. Application of this technique in young children can be challenging, and the reported paediatric experience is very limited (76).

Solid gastric emptying scintigraphy

This test is based on the low-fat standardised adult meal and is therefore only applicable to older children and adolescents. This meal includes 120 grams of egg white (approximately equivalent to the egg whites of 2 large eggs or 118 ml (4 oz) of liquid egg whites), 2 slices of toasted white bread, 30 grams of strawberry jam and 120 grams of water (77).

It is important for the radioactive label to remain firmly attached to the solid component of the meal. The radiopharmaceutical [$^{99\text{m}}\text{Tc}$]-sulphur colloid cooked with egg whites is 95% bound at 3 hours. The standardised water component of the meal is also important, because liquids affect the emptying of solids. Alternative solid meals have been proposed in cases of egg or gluten allergies and in order to make the meal more appealing to children.

Some test meals were based on different solid components such as bran, oatmeal, peanut butter, melted cheese, etc. These meals vary in their caloric and fat contents and their labelling efficiency. They also lack normal reference values. It is therefore recommended to adhere to the adult egg-based standardised meal and imaging protocol whenever possible. At times, this recommendation can be challenging. Some children will refuse to comply because the meal is not palatable to them. Others might only consume part of the meal. Egg or gluten allergies could also prohibit the use of this test meal. Moreover, it is also uncertain if the adult normal reference values are applicable to children across all age groups. A study on 216 children, 4–18 years old, evaluated the applicability of the adult egg-based solid gastric emptying protocol. Delayed gastric emptying was defined as a gastric residual greater than 10% at 4 hours. Thirteen per cent were unable to consume the full meal. Children with delayed gastric emptying were significantly younger than those with normal emptying. Age- or size-related differences in gastric emptying rates were more evident at the 3 and 4-hour time points. The authors concluded that the normal adult reference values may not be adequate for children younger than 10 years (78). A more recent study analysed 1151 solid gastric emptying studies in children older than 6 years. Delayed emptying was defined as gastric residual greater than 10% at 4 hours. Children were stratified into normal and

delayed emptying, egg-based or cheese-based meals, and complete or partial meals. Good agreement was found between those defined as normal versus delayed, based on adult reference values and data-driven k-means clustering in all cohorts, across all ages and regardless of sex. Additionally, good concordance in gastric emptying rates was found between the standard egg-based meal and the non-standard cheese-based meal. Good concordance was also present between gastric emptying rates of children who consumed part of the egg-based meal (50–100% of the meal) and those who completed the meal. The authors concluded that the adult consensus normative standards for solid gastric emptying are applicable for use in children, and that the same reference values can be applied to the non-standard cheese-based meal and to partial standard meals (79).

SOLID GASTRIC EMPTYING PROTOCOL

Preparations

The procedure should be thoroughly explained and the possibility of egg or gluten allergies ruled out. The likelihood of the child being able to ingest the test meal should be verified. Instruct diabetic patients to bring their glucose monitors and insulin with them and to make the necessary adjustment to their morning dose of insulin to account for the test meal. Blood glucose levels should be below 200 mg/dL. It is important to check if

the child is taking any medications. Prokinetic medications such as metoclopramide, tegaserod, domperidone, erythromycin, etc. should be discontinued 2 days before the test, with the approval of the referring physician, unless the test is being done to assess the efficacy of these drugs. Other medications that might affect the gastric emptying rate should also be stopped, generally 2 days before the study. These include atropine, nifedipine, progesterone, octreotide, theophylline, benzodiazepine and phentolamine. The study should be delayed for at least 48 hours after barium radiography. A four- to six-hour fast is required.

Radiopharmaceutical administration

[^{99m}Tc]-sulphur colloid, which is not absorbed by the GI and respiratory mucosa, is the tracer of choice. The activity according to the EANM dosage card in children 5–15 years old varies from 13 to 33 MBq and can be obtained using the online administered activity calculator on the EANM website. The associated effective dose ranges from 1.01 mSv in 15-year-old children to 0.99 mSv in 5-year-olds. The North American consensus guidelines for administered activities in children recommend a fixed activity of 9.25 MBq for children younger than 10 years old and 18.5 MBq for older children and adults. The associated effective doses range from 0.70–0.57 mSv (19). The radiopharmaceutical is mixed and cooked with the egg whites, adhering to the radiation safety regulations and taking

care to avoid contamination. Feeding time should not exceed 15 minutes.

Acquisition

Imaging is performed in the supine position using a low-energy high or ultra-high resolution collimator and a size-appropriate zoom. The field of view should extend from the distal oesophagus to the proximal bowel. Simultaneous anterior and posterior images of 60 seconds' duration are obtained immediately after completion of the meal. Additional images with the same camera and acquisition parameters are obtained at 1, 2, 3 and 4 hours. Instruct the child to maintain an upright position between the imaging sessions. For children younger than 8 years and lighter than 30 kg, imaging can be performed from the posterior view only. In young children, a good correlation was found between gastric emptying calculations performed from the posterior view image and calculations based on the geometrical mean of counts from anterior and posterior images (81).

Processing

Regions of interest including the entire stomach and excluding any bowel activity are drawn on all images. When simultaneous anterior and posterior images are acquired, the geometric mean should be calculated for each time point. The geometric mean is the square root of the product of anterior and posterior counts derived from the ROIs.

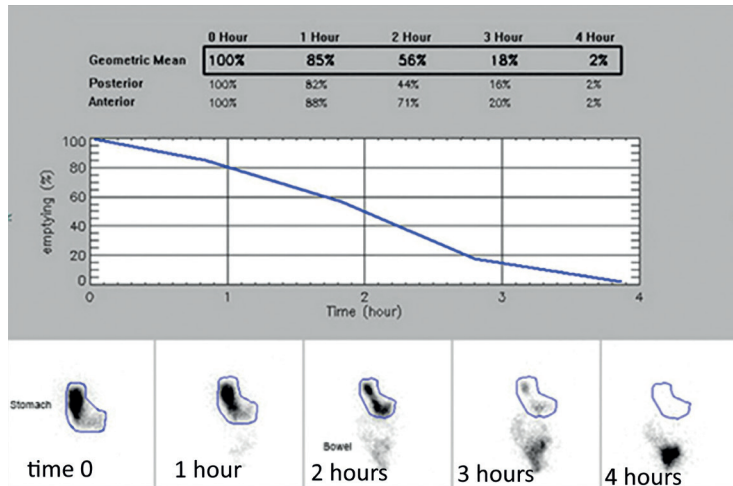


Figure 5 – (Normal gastric emptying)
Gastric emptying images in a 12-year-old with symptoms of nausea and epigastric pain. The patient ingested a standard meal in 6 minutes. Conjugate anterior and posterior images

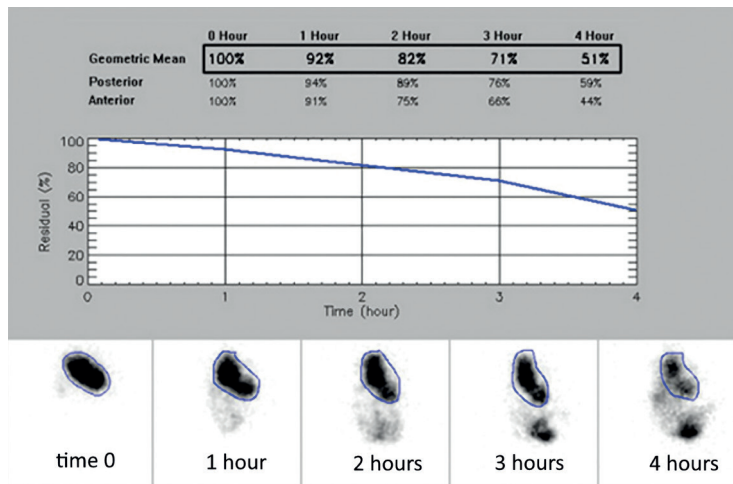


Figure 6 – (Delayed gastric emptying)
Gastric emptying in a 15-year-old who is recovering from a viral infection and complains of nausea and abdominal fullness. The patient ingested a standard meal in 10 minutes. There is delayed gastric emptying at 4 hours, with a residual of 51% of initial activity.

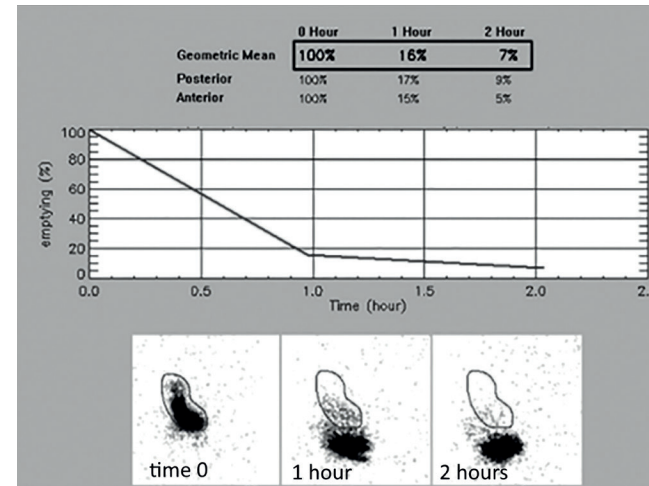


Figure 7 – (Rapid gastric emptying)
Gastric emptying in a 9-year-old with symptoms of dyspepsia. After ingestion of a standard meal, there is rapid emptying of the stomach. Residual of 16% at 1 hour and 7% at 2 hours is consistent with rapid gastric emptying.

Creating a time-activity curve from the geometric mean or posterior view counts is optional. The percentage of residual stomach activity at 1, 2, 3 and 4 hours (gastric residuals) is calculated by dividing the decay-corrected stomach counts at each time point by the initial stomach counts (time 0) and multiplying by 100.

Interpretation

The upper limits for normal gastric residuals (adult criteria) are 90%, 60%, 30% and 10% at 1, 2, 3 and 4 hours, respectively. Figure 5 shows normal solid gastric emptying. Residuals exceeding these limits suggest delayed gastric emptying (Figure 6). A gastric residual greater than 10% is the most robust criteria for delayed emptying at 4 hours.

Rapid gastric emptying is suggested when gastric residuals are less than 70% at 0.5 hours and less than 30% at 1 hour (Figure 7).

Some interpretation pitfalls should be mentioned. Vomiting that occurs at any point during the study may reduce gastric activity and result in erroneous gastric residual calculations. Poor labelling and non-standard meals are additional sources of error (20, 80).

Liquid gastric emptying scintigraphy

Gastro-oesophageal scintigraphy (the “milk scan”) is employed for gastric emptying assessment in infants and young children. Preparations, radiopharmaceutical administration and the acquisition protocol were described in detail in the previous section.

When the scan is performed for gastric emptying assessment, medications affecting gastric emptying should be discontinued, unless the scan is being used to evaluate the effect of specific drug regimens (see section on solid gastric emptying). If barium contrast radiography was performed, schedule the scan at least 48 hours later. Glycaemic control is also important because hyperglycaemia can delay gastric emptying (82). In the case of young children, it is advised to schedule the study so it replaces a regular meal.

The field of view should include the chest and the entire abdomen. Age-dependent normative data for liquid (milk-based) gastric emptying in infants and children was previously lacking due to ethical issues regarding administration of radioactive tracers to healthy children. Each centre devised its own upper and lower limits for normal emptying. However, a recent important retrospective study on a huge patient cohort established “pseudo-normal” reference values for milk-based gastric emptying in infants and children younger than 5 years of age (83). This was achieved by reviewing 5136 GER scans performed over 22 years using the same protocol in a single medical centre. Studies of patients with risk factors for abnormal gastric emptying were excluded. Children with the following conditions were excluded: prematurity, chromosomal aberrations/syndromes, neurological disorders, congenital and acquired heart,

lung and renal diseases, malignancies, abdominal surgeries, bowel pathologies, gastric tubes and vomiting during acquisition. The remaining 2273 scans, of presumably healthy children with no risk factors for gastric dysmotility, were analysed. The mean age was 9 months. The imaging protocol was slightly different from the one described earlier for GER scintigraphy. Feeding was carried out on the camera bed in the supine position. Posterior images of the chest (5 seconds per frame) were obtained for 2.5 min during oral administration of a few millilitres of labelled milk/formula, to evaluate for aspiration. Following administration of the remainder of the meal, 10-second posterior view images of the chest and abdomen were recorded for 60 minutes. Upon completion of the dynamic sequence, an anterior view image of the abdomen was obtained for calculation of the percentage of gastric emptying. A similar anterior image of the abdomen was repeated at 3 hours from the start of the study. A final posterior view image of the chest was then obtained to check for late aspiration. The percentage of gastric emptying was calculated from the 1- and 3-hour static images. Separate regions of interest were manually drawn over the stomach and the bowel (Figure 8). The percentage of gastric emptying was defined as the counts in the bowel ROI divided by the counts in the bowel plus stomach ROIs multiplied by 100. Significant emptying may occur during feeding (84). This is accounted

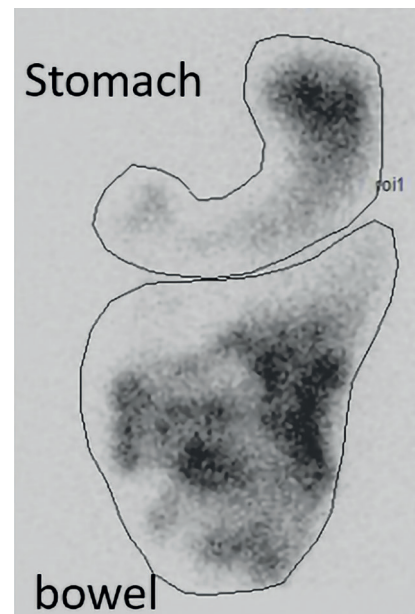


Figure 8 – (Regions of interest)
Calculation of the percentage of gastric emptying requires drawing of regions of interest over the stomach and bowel on the 1- and 3-hour anterior images of the abdomen.

for in the calculations because at any time point the activity in the bowel was divided by the total ingested activity, expressed as the sum of the stomach and bowel counts. The mean gastric emptying percentage at one hour was 43%, and at 3 hours 91%. Further statistical analysis established cut-off values for normal emptying. Normal emptying was defined as a percentage of emptying greater than 50% at 1 hour and greater than 80% at 3 hours. The 3-hour cut-off was considered more robust. Abnormal gastric emptying is shown in Figure 9. Additional results showed that the gastric

emptying rate decreased with larger meal volumes. Interestingly, gastric emptying was faster in infants younger than 6 months, in contradiction of other reports that found slower emptying rates in infants younger than 1 year compared to older children (85, 86). Gastric emptying was faster in patients fed through combined nasogastric tube and oral routes as compared with those fed exclusively orally. Sex did not affect gastric emptying rates and there was no significant difference in gastric emptying between children with or without gastro-oesophageal reflux (83).

Interpretation of milk-based gastric emptying scans

Given the lack of universally accepted normative data for milk-based gastric emptying in infants and children, we recommend using the percentage of gastric emptying at 1 and 3 hours, as described in the previous section, as normal reference values using the above-mentioned calculation method (83).

Simultaneous assessment of solid and liquid gastric emptying

Simultaneous assessment of liquid and solid gastric emptying in a single study is possible but uncommon in clinical practice in children. The solid is labelled with [^{99m}Tc]-sulphur colloid, and the liquid (water) with ¹¹¹In. Maintaining a ratio of at least 6:1 between the ^{99m}Tc and ¹¹¹In activities reduces down-scatter from ¹¹¹In into the

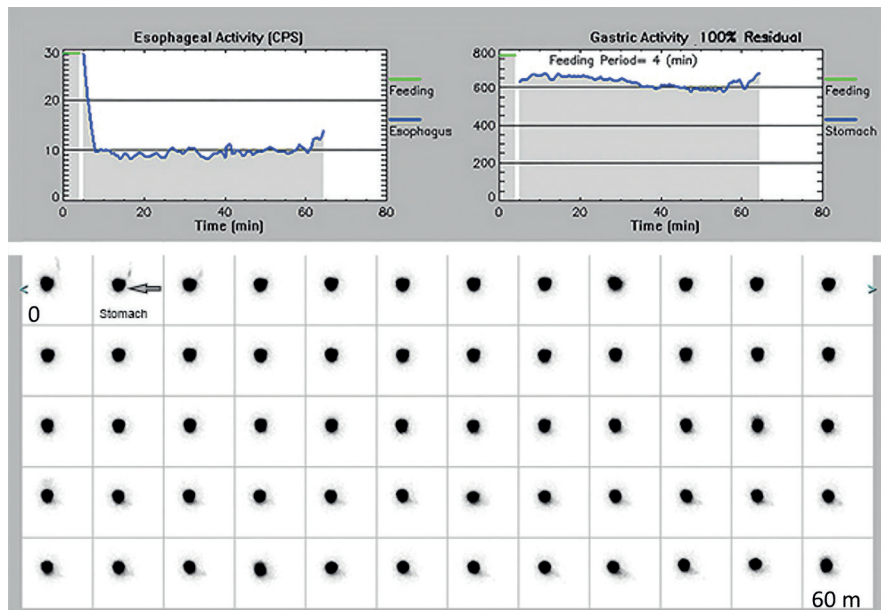


Figure 9 – (Delayed gastric emptying on milk scan)
Milk scan in an 8-month-old with failure to thrive and a G-tube in place. The patient received 90 ml of milk formula by mouth. Initial images show a small amount of formula within the oesophagus, reflecting residual activity from the oral feeding. After 1 hour of imaging there is no emptying of the stomach. No gastro-oesophageal reflux seen.

^{99m}Tc window. Recommended paediatric activities for this dual isotope study are 11.1 MBq (0.3 mCi) for [^{99m}Tc]-sulphur colloid and 1.85 MBq (50 microCuries) for ^{111}In (20).

Treatment principles for gastric dysmotility

Dietary and lifestyle changes are the first line of treatment for delayed gastric emptying. Patients should avoid fatty and high-fibre meals since these might delay gastric emptying. Small frequent meals may be helpful. In severe cases with intolerance

of solid food, nutrition is given in liquid form. Liquid emptying is often preserved despite delayed emptying of solids. In cases of severe vomiting, nutrition is provided via nasojejun tube or through a jejunostomy tube. IV parenteral nutrition is given in selected cases of enteral feeding failure. Drug therapy is often administered in children in addition to dietary modifications. There are several prokinetic drugs that improve gastric emptying. These include macrolide antibiotics (e.g. erythromycin), metoclopramide, domperidone and

cisapride. Metoclopramide has CNS side effects and appears to be less effective in children than in adults. Based on the limited data, domperidone is more effective in children than metoclopramide. It is associated, however, with side effects of cardiac arrhythmias and has limited availability in some countries. More invasive procedures are reserved for selected cases who fail to respond adequately to dietary and drug therapies. Injection of botulinum toxin into the pylorus muscle is used in cases of pyloric dysfunction. It reduces the pyloric contractility and acetylcholine release. Implantation of a gastric neurostimulator is another invasive procedure that delivers high-frequency, low-amplitude current to the smooth muscle of the stomach, improving gastric relaxation and accommodation. Very limited paediatric data report some success with these procedures (63).

Rare cases of rapid gastric emptying associated with dumping syndrome are treated with dietary changes (frequent small meals, high in fibre and protein and low in carbohydrates and avoidance of specific foods that aggravate the symptoms). In selected severe cases, octreotide therapy can be helpful. Surgical repairs and reconstructions relating to the primary surgery that initiated the dumping syndrome are performed as a last resort (87).

CONCLUSION

Nuclear medicine studies provide important diagnostic information for children with suspected GER, pulmonary aspiration and gastric dysmotility. This information can complement results from other imaging or non-imaging diagnostic procedures. Sometimes scintigraphy is the only imaging-based diagnostic method (e.g. salivagram for detection of salivary aspiration). Nuclear medicine scans of the GI system are non-invasive and physiological. The ingested radiopharmaceutical does not affect the physiology or pathophysiology of the system, and labelled meals for GER scintigraphy and liquid gastric emptying are similar in volume and composition to the child's regular meals at home. The radiation exposure associated with these scans is very low and should not prohibit performing the scans when indicated. The value of these tests should be explained to clinicians caring for the children, because unfortunately these procedures are underrepresented in the clinical literature and guidelines.

REFERENCES

- Rosen R, Vandenplas Y, Singendonk M, Cabana M, DiLorenzo C, Gottrand F, et al. Pediatric Gastroesophageal Reflux Clinical Practice Guidelines: Joint Recommendations of the North American Society for Pediatric Gastroenterology, Hepatology, and Nutrition and the European Society for Pediatric Gastroenterology, Hepatology, and Nutrition. *J Pediatr Gastroenterol Nutr.* 2018;66(3):516-554.
- Martin AJ, Pratt N, Kennedy JD, Ryan P, Ruffin RE, Miles H, et al. Natural history and familial relationships of infant spilling to 9 years of age. *Pediatrics.* 2002;109(6):1061-7.
- Lightdale JR, Gremse DA. Section on Gastroenterology, Hepatology, and Nutrition. Gastroesophageal reflux: management guidance for the pediatrician. *Pediatrics.* 2013;131(5):e1684-95.
- Kawahara H, Dent J, Davidson G. Mechanisms responsible for gastro-esophageal reflux in children. *Gastroenterology.* 1997;113:399-408.
- Nelson SP, Chen EH, Syniar GM, Christoffel KK. One-year follow-up of symptoms of gastroesophageal reflux during infancy. *Pediatric Practice Research Group.* *Pediatrics.* 1998;102:E67.
- Vandenplas Y, Rudolph CD, Di Lorenzo C, Hassall E, Liptak G, Mazur L, et al. Pediatric gastroesophageal reflux clinical practice guidelines: Joint recommendations of the North American Society for Pediatric Gastroenterology, Hepatology, and Nutrition (NASPGHAN) and the European Society for Pediatric Gastroenterology, Hepatology, and Nutrition (ESPGHAN). *J Pediatr Gastroenterol Nutr.* 2009;49:498-547.
- Macchini F, Leva E, Torricelli M, Valadè A. Treating acid reflux disease in patients with Down syndrome: Pharmacological and physiological approaches. *Clin Exp Gastroenterol.* 2011;4:19-22.
- Malaty HM, Fraley JK, Abudayyeh S, Fairly KW, Javed US, Aboul-Fotouh H, et al. Obesity and gastroesophageal reflux disease and gastroesophageal reflux symptoms in children. *Clin Exp Gastroenterol.* 2009;2:31-36.
- Zevit N, Shamir R. Regurgitation and gastroesophageal reflux. *World Rev Nutr Diet.* 2015;113:203-208.
- Davies I, Burman-Roy S, Murphy MS. Guideline Development Group. Gastro-oesophageal reflux disease in children: NICE guidance. *BMJ.* 2015;14:350:g7703.
- Harding S.M. Recent clinical investigations examining the association of asthma and gastroesophageal reflux. *Am J Med.* 2003;115: 39s-44s. (suppl 3A)
- Rybak A, Pesce M, Thapar N, Borrelli O. Gastro-Esophageal Reflux in Children. *Int J Mol Sci.* 2017;18(8):1671.
- Orenstein SR, Hassall E, Furmaga-Jablonska W, Atkinson S, Raanan M. Multicenter, double-blind, randomized, placebo-controlled trial assessing the efficacy and safety of proton pump inhibitor lansoprazole in infants with symptoms of gastroesophageal reflux disease. *J Pediatr.* 2009;154: 514-520.e4.
- Mitchell DJ, McClure BG, Tubman TR. Simultaneous monitoring of gastric and oesophageal pH reveals limitations of conventional oesophageal pH monitoring in milk fed infants. *Arch Dis Child.* 2001; 84:273-276.
- Thomson M. The pediatric esophagus comes of age. *J Pediatr Gastroenterol Nutr.* 2002;34:S40-S45 (suppl 1).
- Safe M, Cho J, Krishnan U. Combined Multichannel Intraluminal Impedance and pH Measurement in Detecting Gastroesophageal Reflux Disease in Children. *J Pediatr Gastroenterol Nutr.* 2016;63(5):e98-e106.
- Uslu Kizilkan N, Bozkurt MF, Saltik Temizel IN, Demir H, Yüce A, Caner B, et al. Comparison of multichannel intraluminal impedance-pH monitoring and reflux scintigraphy in pediatric patients with suspected gastroesophageal reflux. *World J Gastroenterol.* 2016;22(43):9595-9603.
- Valusek PA, St Peter SD, Keckler S, Laituri CA, Snyder CL, Ostlie DJ, et al. Does an upper gastrointestinal study change operative management for gastroesophageal reflux? *J Pediatr Surg.* 2010; 45:1169-1172.
- Lassmann M, Treves ST. EANM/SNMMI Paediatric Dosage Harmonization Working Group. Paediatric radiopharmaceutical administration: harmonization of the 2007 EANM paediatric dosage card (version 1.5.2008) and the 2010 North American consensus guidelines. *Eur J Nucl Med Mol Imaging.* 2014;41(5):1036-41.
- Bar-Sever Z. Gastroesophageal reflux, gastric emptying, esophageal transit and pulmonary aspiration; in Treves ST, editor. *Pediatric Nuclear Medicine and Molecular Imaging 4th edition.* NY (US) Heidelberg (GE), Dordrecht (NL), London (UK): Springer; 2014. p.203-234.
- Reyhan M, Yapar AF, Aydin M, Sukan A. Gastroesophageal scintigraphy in children: A comparison of posterior and anterior imaging. *Ann Nucl Med.* 2005;19:17-21.
- Piepsz A, Georges B, Rodesch P, Cadranet S. Gastroesophageal scintiscanning in children. *J Nucl Med.* 1982;23:631-632.
- Othman S. Gastroesophageal reflux studies using milk in infants and children—The need for multiple views. *Nucl Med Commun.* 2011;32:967-971.
- Codreanu I, Chamroonrat W, Edwards K, Zhuang H. Effects of the frame acquisition rate on the sensitivity of gastro-oesophageal reflux scintigraphy. *Br J Radiol.* 2013; 86(1026):20130084.
- Fisher RS, Malmud LS, Roberts GS, Lobis IF. Gastroesophageal (GE) scintiscanning to detect and quantitate GE reflux. *Gastroenterology.* 1976;70:301-308.
- Klein HA. Applications of condensed dynamic images. *Clin Nucl Med.* 1986;11:178-182.
- Tuncel M, Kiratli PO, Aksoy T, Bozkurt MF. Gastroesophageal reflux scintigraphy: Interpretation methods and inter-reader agreement. *World J Pediatr.* 2011;7:245-249.
- Djeddi D, Stephan-Blanchard E, Léké A, Ammari M, Delanaud S, Lemaire-Hurtel AS et al. Effects of Smoking Exposure in Infants on Gastroesophageal Reflux as a Function of the Sleep-Wakefulness State. *J Pediatr.* 2018;201:147-153.
- Heacock HJ, Jeffery HE, Baker JL, Page M. Influence of breast versus formula milk on physiological gastroesophageal reflux in healthy, newborn infants. *J Pediatr Gastroenterol Nutr.* 1992;14(1):41-6.
- Billeaud C, Guillet J, Sandler B. Gastric emptying in infants with or without gastro-oesophageal reflux according to the type of milk. *Eur J Clin Nutr.* 1990;44(8):577-83.
- Forget P, Arends JW. Cow's milk protein allergy and gastro-oesophageal reflux. *Eur J Pediatr.* 1985;144(4):298-300.
- Cavataio F, Iacono G, Montalto G, Soresi M, Tumminello M, Campagna P, et al. Gastroesophageal reflux associated with cow's milk allergy in infants: which diagnostic examinations are useful? *Am J Gastroenterol.* 1996;91(6):1215-20.
- Hill DJ, Heine RG, Cameron DJ, Catto-Smith AG, Chow CW, Francis DE, et al. Role of food protein intolerance in infants with persistent distress attributed to reflux esophagitis. *J Pediatr.* 2000;136(5):641-7.
- Kakodkar K, Schroeder JW. Pediatric dysphagia. *Pediatr Clin North Am.* 2013;60(4):969-77.
- Das Shailendra, Boesch PR. Aspiration due to swallowing dysfunction in children. Mallory GB, Hoppin AG editors, UpToDate 2022, Waltham, MA.
- Darrow DH, Harley CM. Evaluation of swallowing disorders in children. *Otolaryngol Clin North Am.* 1998;31(3):405-18.
- DeMatteo C, Matovich D, Hjartarson A. Comparison of clinical and videofluoroscopic evaluation of children with feeding and swallowing difficulties. *Dev Med Child Neurol.* 2005;47(3):149-57.
- Hiorns MP, Ryan MM. Current practice in paediatric videofluoroscopy. *Pediatr Radiol.* 2006;36: 911-919.
- da Silva A.P., Lubianca Neto J.F., Santoro P.P.: Comparison between video fluoroscopy and endoscopic evaluation of swallowing for the diagnosis of dysphagia in children. *Otolaryngol Head Neck Surg.* 2010;143(2):204-9.
- Berdon WE, Mellins RB, Levy J. On the following paper by H.D. Fawcett, C.K. Hayden, J.C. Adams and L.E. Swischuk: How useful is gastroesophageal reflux scintigraphy in suspected childhood aspiration?. *Pediatr Radiol.* 1988;18:309-310.
- Baikie G, South MJ, Reddihough DS, Cook DJ, Cameron DJ, Olinsky A. Agreement of aspiration tests using barium videofluoroscopy, salivagram, and milk scan in children with cerebral palsy. *Dev Med Child Neurol.* 2005;47(2):86-93.
- Fawcett HD, Hayden CK, Adams JC, Swischuk LE. How useful is gastroesophageal reflux scintigraphy in suspected childhood aspiration? *Pediatr Radiol.* 1988;18:311-313.
- Heyman S, Eicher PS, Alavi A. Radionuclide studies of the upper gastrointestinal tract in children with feeding disorders. *J Nucl Med.* 1995;36:351-354.

44. McVeagh P, Howman-Giles R, Kemp A. Pulmonary aspiration studied by radionuclide milk scanning and barium swallow roentgenography. *Am J Dis Child.* 1987;141: 917-921.
45. Lorber B, Swenson RM. Bacteriology of aspiration pneumonia. A prospective study of community- and hospital-acquired cases. *Ann Intern Med.* 1974;81:329-331.
46. Bartlett JG, Gorbach SL, Finegold SM. The bacteriology of aspiration pneumonia. *Am J Med.* 1974; 56:202-207.
47. Heyman S. The radionuclide salivagram for detecting the pulmonary aspiration of saliva in an infant. *Pediatr Radiol.* 1989;19:208-209.
48. Bauer ML, Figueroa-Colon R, Georgeson K, Young DW. Chronic pulmonary aspiration in children. *South Med J.* 1993; 86:789-795.
49. Bui HD, Dang CV, Chaney RH, Vergara LM. Does gastrostomy and fundoplication prevent aspiration pneumonia in mentally retarded persons? *Am J Ment Retard.* 1989;94:16-19.
50. Wu H, Zhao R. Image characteristics and classification of salivagram in the diagnosis of pulmonary aspiration in children. *Nucl Med Commun.* 2017;38(7):617-622.
51. Hou P, Deng H, Wu Z, Liu H, Liu N, Zheng Z, et al. Detection of salivary aspiration using radionuclide salivagram SPECT/CT in patients with COPD exacerbation: a preliminary study. *J Thorac Dis.* 2016;8(10):2730-2737.
52. Silver KH, Van Nostrand D. Scintigraphic detection of salivary aspiration: Description of a new diagnostic technique and case reports. *Dysphagia.* 1992;7(1):45-9.
53. Somasundaram VH, Subramanyam P, Palaniswamy S. Salivagram revisited: Justifying its routine use for the evaluation of persistent/recurrent lower respiratory tract infections in developmentally normal children. *Ann Nucl Med.* 2012; 26:578-585.
54. Shao F, Zhao X, Toyama H, Ichihara T, Zhuang H, Zhao R, et al. Semi-quantitative assessment optimized the grading of pulmonary aspiration on salivagram in children. *Ann Nucl Med.* 2021;35(3):321-327.
55. Drubach LA, Zurakowski D, Palmer EL 3rd, Tracy DA, Lee EY. Utility of salivagram in pulmonary aspiration in pediatric patients: Comparison of salivagram and chest radiography. *AJR Am J Roentgenol.* 2013;200:437-441.
56. Bar-Sever Z, Connolly LP, Treves ST. The radionuclide salivagram in children with pulmonary disease and a high risk of aspiration. *Pediatr Radiol.* 1995;25 Suppl 1:5180-3.
57. Yang J, Codreanu I, Servaes S, et al. Radionuclide salivagram and gastroesophageal reflux scintigraphy in pediatric patients: Targeting different types of pulmonary aspiration. *Clin Nucl Med.* 2015; 40:559-563.
58. Simons JP, Rubinstein EN, Mandell DL. Clinical predictors of aspiration on radionuclide salivagrams in children. *Arch Otolaryngol Head Neck Surg.* 2008;134:941-944.
59. Shaw DW, Williams RB, Cook IJ, et al. Oropharyngeal scintigraphy: A reliable technique for the quantitative evaluation of oral-pharyngeal swallowing. *Dysphagia.* 2004;19:36-42.
60. Lee DH, Kim JM, Lee Z, Park D. The effect of radionuclide solution volume on the detection rate of salivary aspiration in the radionuclide salivagram: A STROBE-compliant retrospective study. *Medicine (Baltimore).* 2018;97(30):e11729.
61. Camilleri M. Novel Diet, Drugs, and Gastric Interventions for Gastroparesis. *Clin Gastroenterol Hepatol.* 2016;14(8):1072-80.
62. Islam S. Gastroparesis in children. *Curr Opin Pediatr.* 2015;27(3):377-82.
63. Febo-Rodriguez L, Chumpitazi BP, Shulman RJ. Childhood gastroparesis is a unique entity in need of further investigation. *Neurogastroenterol Motil.* 2020;32(3):e13699.
64. Waseem S, Islam S, Kahn G, Moshiree B, Talley NJ. Spectrum of gastroparesis in children. *J Pediatr Gastroenterol Nutr.* 2012;55(2):166-72.
65. Rodriguez L, Irani K, Jiang H, Goldstein AM. Clinical presentation, response to therapy, and outcome of gastroparesis in children. *J Pediatr Gastroenterol Nutr.* 2012;55(2):185-90.
66. Soykan I, Sivri B, Sarosiek I, Kiernan B, McCallum RW. Demography, clinical characteristics, psychological and abuse profiles, treatment, and long-term follow-up of patients with gastroparesis. *Dig Dis Sci.* 1998; 43(11):2398-404.
67. Bufler P, Ehringhaus C, Koletzko S. Dumping syndrome: a common problem following Nissen fundoplication in young children. *Pediatr Surg Int.* 2001;17(5-6):351-5.
68. Keller J, Hammer HF, Hauser B. 13 C-gastric emptying breath tests: Clinical use in adults and children. *Neurogastroenterol Motil.* 2021;33(6):e14172.
69. Bharucha AE, Camilleri M, Veil E, Burton D, Zinsmeister AR. Comprehensive assessment of gastric emptying with a stable isotope breath test. *Neurogastroenterol Motil.* 2013; 25(1):e60-9.
70. Hauser B, Roelants M, De Schepper J, Veereman G, Caveliers V, Devreker T, et al. Gastric Emptying of Liquids in Children. *J Pediatr Gastroenterol Nutr.* 2016;62(3):403-408.
71. Keller J, Hammer HF, Afolabi PR, Benninga M, Borrelli O, Dominguez-Munoz E, et al. European guideline on indications, performance and clinical impact of 13 C-breath tests in adult and pediatric patients: An EAGEN, ESNM, and ESPGHAN consensus, supported by EPC. *United European Gastroenterol J.* 2021;9(5):598-625.
72. Minella R, Minelli R, Rossi E, Cremonese G, Tozzi A. Gastroesophageal and gastric ultrasound in children: the state of the art. *J Ultrasound.* 2021;24(1):11-14.
73. Bertoli D, Mark EB, Liao D, Brock C, Frøkjær JB, Drewes AM. A novel MRI-based three-dimensional model of stomach volume, surface area, and geometry in response to gastric filling and emptying. *Neurogastroenterol Motil.* 2022;23:e14497.
74. Lu KH, Liu Z, Jaffey D, Wo JM, Mosier KM, Cao J, et al. Automatic assessment of human gastric motility and emptying from dynamic 3D magnetic resonance imaging. *Neurogastroenterol Motil.* 2022;34(1):e14239.
75. Bhat S, Varghese C, Carson DA, Hayes TCL, Andrews CN, Mousa H, et al. Electrogastrography Abnormalities in Pediatric Gastrointestinal Disorders: A Systematic Review and Meta-analysis. *J Pediatr Gastroenterol Nutr.* 2021;73(1):9-16.
76. Green AD, Belkind-Gerson J, Surjanhata BC, Mousa H, Kuo B, Di Lorenzo C. Wireless motility capsule test in children with upper gastrointestinal symptoms. *J Pediatr.* 2013;162(6):1181-7.
77. Abell TL, Camilleri M, Donohoe K, Hasler WL, Lin HC, Maurer AH, et al. Consensus recommendations for gastric emptying scintigraphy: a joint report of the American Neurogastroenterology and Motility Society and the Society of Nuclear Medicine. *J Nucl Med Technol.* 2008;36(1):44-54.
78. Wong GK, Shulman RJ, Chumpitazi BP. Gastric emptying scintigraphy results in children are affected by age, anthropometric factors, and study duration. *Neurogastroenterol Motil.* 2015;27(3):356-362.
79. Ng TSC, Putta N, Kwatra NS, Drubach LA, Rosen R, Fahey FH, et al. Pediatric Solid Gastric Emptying Scintigraphy: Normative Value Guidelines and Nonstandard Meal Alternatives. *Am J Gastroenterol.* 2020;115(11):1830-1839.
80. Donohoe KJ, Maurer AH, Ziessman HA, Urbain JL, Royal HD, Martin-Comin J. Procedure guideline for adult solid-meal gastric-emptying study 3.0. *J Nucl Med Technol.* 2009;37(3):196-200.
81. Drubach LA, Kourmouzi V, Cao X, Zurakowski D, Fahey FH. Gastric emptying in children what is the best acquisition method? *J Pediatr Gastroenterol Nutr.* 2012;55(2):191-3.
82. Fraser R, Horowitz M, Maddox A, Harding PE, Chatterton BE, Dent J. Hyperglycemia slows gastric emptying in type 1 diabetes mellitus. *Diabetologia.* 1990;30:675-80.
83. Kwatra NS, Shalaby-Rana E, Andrich MP, Tsai J, Rice AL, Ghelani SJ, et al. Gastric emptying of milk in infants and children up to 5 years of age: normative data and influencing factors. *Pediatr Radiol.* 2020;50(5):689-697.
84. Lin E, Connolly LP, Drubach L, Zurakowski D, DiCanzio J, Mitchell K, et al. Effect of early emptying on quantitation and interpretation of liquid gastric emptying studies of infants and young children. *J Nucl Med.* 2000;41(4):596-599.
85. Seibert JJ, Byrne WJ, Euler AR. Gastric emptying in children: unusual patterns detected by scintigraphy. *AJR Am J Roentgenol.* 1983;141(1):49-51.
86. Di Lorenzo C, Piepsz A, Ham H, Cadranel S. Gastric emptying with gastro-oesophageal reflux. *Arch Dis Child.* 1987;62(5):449-453.
87. Berg P, McCallum R. Dumping Syndrome: A Review of the Current Concepts of Pathophysiology, Diagnosis, and Treatment. *Dig Dis Sci.* 2016;61(1):11-18



ONCOLOGICAL STUDIES (SPECT & PET)

*by Raquel Massa¹
Prakash Manoharan²*

¹Senior Clinical Technologist and Nuclear Medicine Clinical Trials, Department of Nuclear Medicine, Christie Medical Physics and Engineering, The Christie NHS Foundation Trust, Manchester, UK

²Consultant Radiologist and Nuclear Medicine Physician, Departments of Radiology and Nuclear Medicine, The Christie NHS Foundation Trust, Manchester, UK

INTRODUCTION

Gastrointestinal (GI) cancers arise from cells within the GI tract that proliferate in an uncontrolled, abnormal manner. Major types include gastric, oesophageal, colorectal, pancreatic, liver, and, more rarely, but with an increasing incidence, gastroenteropancreatic neuroendocrine tumours (GEP-NET). GI malignancies have a poor prognosis, accounting for 35% of all cancer-related deaths with major risk factors associated with lifestyle behaviours such as smoking, alcohol consumption, physical inactivity or sedentarism (1,2).

Positron emission tomography/computerised tomography (PET/CT) and single-photon emission computerised tomography/computerised tomography (SPECT/CT) are valuable molecular imaging modalities in the diagnosis, staging and management of cancer, including GI malignancies. This chapter will summarise a number of molecular imaging studies that have shown diagnostic value in GI malignancies, including their applicability and effectiveness, specific preparation, and considerations associated with performing the study, as well as the radiopharmaceutical administration, imaging protocol and processing (Tables 1 and 2).

General considerations in hybrid molecular imaging

Considerations associated with all molecular imaging studies discussed here include: confirmation of patient's

identity, adherence to legal and regulatory requirements for the safe use of radioactive substances for medical applications, determining pregnancy status in patients of childbearing age before radiopharmaceutical administration, obtaining written and oral consent to perform the examination, and providing individualised advice on precautions in respect of radiation protection (3–6). In cases of cognitive impairment where the patient is unable to consent to the procedure, capacity assessment should preferably be performed in advance by a member of the referring clinical team.

Patients should receive written confirmation regarding the appointment time along with information about what the procedure entails and its duration. To minimise the risk of wasted radiopharmaceutical and cancellations, patients should be asked to confirm their attendance, whereupon the importance of arriving on time should be emphasised. The information leaflet should request that patients notify the department if they are claustrophobic, pregnant, breastfeeding, have poor venous access or difficulty lying supine for a duration of at least 30 minutes. Patients who suffer from severe claustrophobia/anxiety or are unable to lie still for the duration of the scan may benefit from visiting the department to look at the scanner prior to their appointment. This will reduce the risk of cancellations and non-diagnostic scans and facilitate

planning. For some patients, an effective method to reduce anxiety may simply require communicating with the patient over the intercom. For others, wearing an eye mask, listening to relaxing music, taking oral medication (e.g. short-acting benzodiazepines) or having a family member present for the duration of the scan may be preferred (providing this is risk-assessed by the responsible technologist). The latter is less desirable due to potential radiation exposure and is not possible during CT acquisition.

The technologist acts as the operator, and is therefore responsible for carrying out the imaging procedure whilst providing patient-centred care. It is important that

a clear explanation of the procedure is provided, and that reassurance is given to the patient as well as an opportunity for them to ask questions. For optimal imaging, the patient should be instructed to remove all metallic objects from clothing and the body wherever possible, void their bladder, and be positioned on the scanner table with the arms raised over the head to prevent truncation artefacts and beam-hardening artefacts in the abdominal and pelvic areas. Sufficient support should be provided with the aid of immobilisation devices (e.g. foam wedges to support the arms, shoulders, and knees) to enhance the patient's comfort and reduce the risk of motion artefacts (Figure 1).



Figure 1 – Patient positioning with arms raised over the head for a whole-body PET/CT scan. This is important for preventing truncation and beam hardening artefacts in the abdominal and pelvic areas. Careful patient positioning supported by arm and knee rest, to enhance patient's comfort and reduce the risk of motion artefacts. An eye mask may be worn to reduce anxiety. Courtesy of the Department of Nuclear Medicine, The Christie NHS Foundation Trust, Manchester.

PET/CT IMAGING IN GASTROINTESTINAL CANCERS

PET/CT is a dual modality imaging system that allows sequential acquisition of CT images, then PET images, through the detection of 511keV photons resulting from positron/electron annihilation following positron emission. The most commonly utilised PET radionuclides for GI cancers are fluorine-18 and gallium-68. As a result, a three-dimensional image combining metabolic mapping with anatomic localisation is generated (7–9). This enables accurate localisation of malignant lesions and their differentiation from regions of normal physiological uptake (9). Standardised uptake value (SUV) is a semi-quantitative tool valuable in PET/CT imaging for staging and therapy response assessment. SUV provides an estimation of tumour metabolism in a region of interest normalised to a distribution volume, usually body weight (3,10). Hence, the patient's body weight and injected activity (MBq) must be recorded accurately prior to PET radiopharmaceutical administration.

Contrast-enhanced (CE) CT scan as an additional part of the PET/CT scan, also known as a one-stop-shop imaging approach, can be beneficial for more detailed anatomical localisation and diagnosis. For example, 2-[¹⁸F]FDG PET/CT with intravenous contrast, in assessing recurrence of pancreatic cancer, demonstrated improved sensitivity (92%), specificity (95%) and accuracy (93%) compared to 2-[¹⁸F]

FDG PET non-enhanced CT (83%, 91% and 87%, respectively) (11). Because iodinated contrast has an associated risk of causing an allergic or adverse reaction, the provision of specific additional information needs to be taken into consideration and written consent should be obtained after a full explanation of the procedure. Standard safety questions include previous reaction to iodinated contrast agents, history of allergy to iodine, known allergies or eczema, and asthma. Risk factors for contrast-induced nephropathy should be documented, including heart disease, thyroid disease, diabetes mellitus, myeloma, nephrotoxic medication and renal impairment. A local protocol should be followed for the administration of iodinated contrast after renal impairment assessment based on estimated glomerular filtration rate. Patients undergoing metformin therapy who have compromised renal function are at increased risk of developing a form of lactic acidosis known as MALA (metformin-associated lactic acidosis). In these cases, instructions should be given to discontinue metformin for at least 48 hours after the CE-CT scan.

The reporting imaging experts utilise the hybrid PET/CT data along with available previous diagnostic CT, MRI and other relevant imaging scans during the analysis of the PET/CT. This ensures that a comprehensive report is compiled for the individual patient.

The following section focuses on tracers for PET/CT imaging with an important role

in the detection of GI cancers, including the widely used 2-[¹⁸F]FDG and [⁶⁸Ga]Ga-DOTA-somatostatin receptor targeting peptides. [⁶⁸Ga]Ga-FAPI will also be discussed (Table 1).

Imaging with 2-[¹⁸F]FDG

2-deoxy-2-[¹⁸F] fluoro-D-glucose (2-[¹⁸F] FDG) is the most established PET

radiopharmaceutical in the oncology setting. In respect of cellular uptake, 2-[¹⁸F] FDG is a glucose analogue and, as such, its uptake reflects the increased glucose metabolism that characterises tumour cells of most cancer types. Therefore, 2-[¹⁸F]FDG PET/CT is considered to be an effective imaging modality in the diagnosis, staging/re-staging and assessment of therapy

Imaging of gastrointestinal cancer with the various PET/CT agents.

Radiopharmaceutical	Patient Preparation	Recommended Activity	Imaging Protocol
2-[¹⁸ F]FDG	4–6 hours fasting. Intense physical activity should be avoided 24 hours before the scan. Adequate pre-hydration.	370–740 MBq, depending on patient's weight, acquisition time per bed position and bed overlap (3,6).	Imaging at 60 minutes, base of the skull to proximal femur. Patient in supine position with arms raised over the head.
[⁶⁸ Ga]Ga-DOTA-TOC [⁶⁸ Ga]Ga-DOTA-NOC [⁶⁸ Ga]Ga-DOTA-TATE	Withdrawal of SSAs for 1 day for short-lived analogues and 3–4 weeks for long-acting analogues. Adequate pre-hydration.	100–200 MBq (22).	Imaging at 60 minutes, vertex to proximal femur. Patient in supine position with arms raised over the head.
[⁶⁸ Ga]Ga-FAPI-02 [⁶⁸ Ga]Ga-FAPI-04 [⁶⁸ Ga]Ga-FAPI-46	Adequate pre-hydration.	1.8 – 2.2 MBq/kg (34,37,39,41,45).	Imaging at 60 minutes, vertex to proximal femur. Early imaging 10 minutes post-injection may be possible. Patient in supine position with arms raised over the head.
SSAs: somatostatin analogues			

Table 1 – Imaging of gastrointestinal cancer with the various PET/CT agents.

response in many cancers, including GI malignancies (Figure 2) (3,6,11–14). For example, 2-[¹⁸F]FDG PET/CT outperforms morphological imaging for the detection of distant metastases in oesophageal cancer (13). Furthermore, 2-[¹⁸F]FDG PET/CT is particularly valuable for the detection of liver metastases in colorectal cancer, with both sensitivity and specificity greater than 90%, and also for the evaluation of extra-hepatic disease (12,13). That said, the sensitivity and specificity of 2-[¹⁸F]FDG PET imaging can be affected where increased physiological uptake of the radiopharmaceutical can be seen in abdominal organs, e.g. heterogenous liver uptake and diffuse bowel uptake caused by drugs (e.g. metformin) and by abdominal inflammatory and infectious conditions, e.g. diverticulitis and pancreatitis. Instances such as these may lead to false-positive interpretation (3).

Patient preparation

Patient preparation aims to minimise radiopharmaceutical uptake in normal tissues (urinary tract, skeletal muscle, myocardium, brown fat) that may cause false-positive results, while optimising uptake in target tissues (3). Before arrival in the department patients are instructed to fast for 6 hours before the administration of 2-[¹⁸F]FDG, stay well hydrated and where necessary to discontinue intravenous fluids containing glucose or parenteral feedings at least 4 to 6 hours before the time of injection.



Figure 2a – Patient with proven pancreatic mass/cancer (a-MIP), (b- axial fused), (c-sagittal) and (d -coronal fused) demonstrating the pancreatic body mass (red arrow) with increased uptake of 2-[¹⁸F]FDG

Courtesy of the Department of Nuclear Medicine, The Christie NHS Foundation Trust, Manchester.

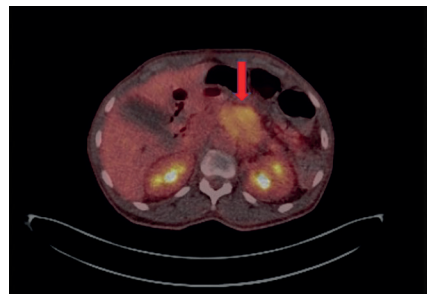


Figure 2b

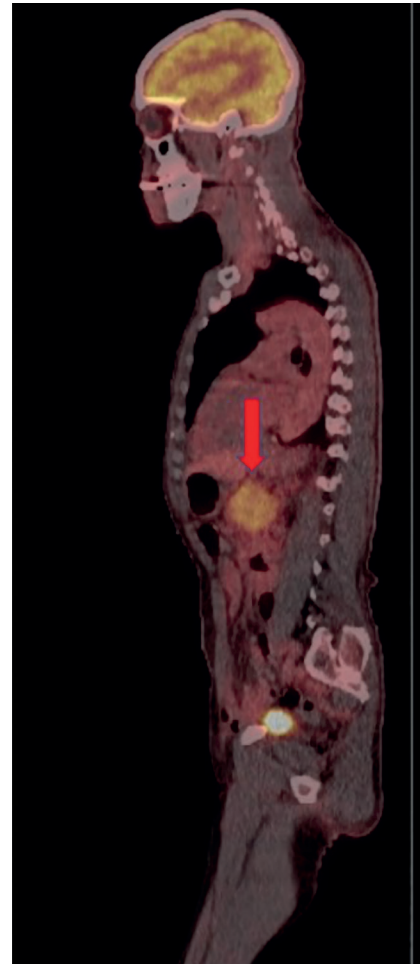


Figure 2c



Figure 2d

appointment, aiming for a minimum 4-hour fasting period, having had a light breakfast and taken their diabetic medication (oral/insulin injection) at breakfast time. However, where high blood sugar levels may be an issue, the appointment should be scheduled around the diabetic patient's routine rather than trying to fit the patient around the scanner schedule.

Individual advice is given to diabetic patients based on the patient's recent blood glucose levels, if known. Diabetic patients are usually asked to attend a late morning

Patients who have undergone bowel surgery and have stomas are required to bring spare stoma bags so that the bag can

be changed immediately before the start of the scan.

For all patients, intense physical activity must be avoided, preferably for 24 hours prior to the appointment.

Information relevant to performance of the scan

On arrival in the department, the patient should be informed that an intravenous injection is needed to perform the scan, that no side effects are expected, and that once the injection is administered, a 60-minute waiting time is required for optimal imaging. During the waiting period, the patient is encouraged to relax by sitting or lying comfortably and to stay hydrated. Additionally, it should be explained that the scan comprises a CT and a PET component and that it has a duration of usually 20 to 25 minutes. The importance of remaining still for the duration of the scan should be stressed.

Following a clear explanation of the procedure, the technologist should confirm the patient's fasting state. A complete medical history should be recorded, including recent surgeries, injuries, vaccinations, current medication, and comorbidities, mainly diabetes mellitus, infection and inflammation. Appropriate timing of the 2-[¹⁸F]FDG PET/CT scan is crucial to ensure optimum accuracy in the assessment of treatment response and to avoid bone marrow uptake. Thus, the dates of the last chemo- and/or radiotherapy treatment should be stated. European

guidelines recommend an interval of at least 10 days after the last chemotherapy dose and of 12 weeks after radiotherapy (3). In cases where this is not possible, the scan should be delayed as long as possible until the next treatment is due (3). Other evidence supports post-therapy assessment being performed with an interval of at least 2 weeks after the end of a specific chemotherapy cycle, and 6 to 8 weeks or longer after radiotherapy (15).

Oral-iodinated contrast allows improved visualisation of the GI mucosa. However, having a CT scan with oral contrast within a 48-hour period prior to the 2-[¹⁸F]FDG PET/CT is normally contraindicated in GI cancer patients. This is because any high-density contrast remaining in the bowel may cause an attenuation correction artefact, which is produced by incorrect scaling of the CT data affected by the contrast agent to the PET attenuation-correction maps. This results in focal overestimation of 2-[¹⁸F]FDG PET/CT activity, possibly leading to a false-positive interpretation (6,16).

Radiopharmaceutical administration and imaging protocol

After obtaining venous access, the patient's plasma glucose level is checked, as uptake of 2-[¹⁸F]FDG in cancer cells is decreased in hyperglycaemic states. Plasma glucose levels ranging from 4.0 to 11.0 mmol/L are usually acceptable (6,15). The line's integrity is then checked with 0.9% sodium chloride solution to reduce

the risk of extravasation. Subsequently, 2-[¹⁸F]FDG is intravenously injected with an activity between 370-740 MBq, depending on patient weight, acquisition time per bed position and bed overlap (3,6). Central venous catheters (CVCs) can be used for 2-[¹⁸F]FDG administration in patients with poor venous access or needle phobia. The exact time at which the injection was administered should be recorded. Residual activity in the syringe and in the administration line should be measured in order to accurately determine net administered 2-[¹⁸F]FDG activity. An uptake time of 60 minutes follows: during this period, the patient should be kept comfortable in a warm and quiet environment to minimise brown fat and physiological muscle uptake. The patient is instructed not to speak or read, explaining that even small muscle activity can affect the uptake of tracer around the larynx and eyes. Bladder voiding immediately prior to image acquisition is encouraged to reduce bladder activity. The patient is then positioned on the scanner table with the arms raised over the head. The correct acquisition protocol should be selected and patient demographic data, plasma glucose levels at the time of injection and administered activity recorded. Image acquisition should begin 60 minutes post injection, with an acceptable range of 55-75 minutes (3). Low-dose CT is generally acquired first, followed by the 2-[¹⁸F]FDG PET acquisition, covering the base of the skull to proximal femur. If

the pelvis is a site of particular concern, the PET acquisition should be initiated from the pelvis to the head to minimise change in bladder volume between the two scans (3,6,15).

Physiological accumulation of 2-[¹⁸F]FDG is visualised in viable tissue, including the brain, myocardium, liver, spleen, bowel, kidneys and urinary tract (3,6,16). At the end of the scan, the overall quality of the scan should be assessed, in particular for the presence of motion misregistration on PET and CT images. If necessary, additional imaging of a localised area should be acquired.

Image processing

The commercially available PET/CT systems are equipped with software that produces aligned CT and 2-[¹⁸F]FDG PET images, fusion images in the axial, coronal and sagittal planes, as well as maximum-intensity projection (MIP) images for review in the 3D cine mode (6,15). Both attenuation-corrected (AC) and non-attenuation-corrected (NAC) 2-[¹⁸F]FDG PET images as well CT images should be available for the reporting radiologist or nuclear medicine specialist.

Imaging with [⁶⁸Ga]Ga-DOTA-somatostatin receptor targeting peptides

Neuroendocrine neoplasms (NENs) are a heterogeneous group of malignancies that mostly arise from the gastro-entero-pancreatic tract (GEP-NETs), including the

stomach, small bowel, appendix, colorectal regions (extra-pancreatic) and the pancreas (pancreatic). These tumours are further classified as non-functioning NENs, which have a higher incidence, and functioning NENs. The latter are caused by the excessive production of peptides that leads to clinical manifestations such as flushing

and diarrhoea in carcinoid syndrome, hypoglycaemia in insulinoma, gastric ulcers in gastrinoma or skin rash in glucagonoma (17,18).

GEP-NETs, especially grade I and grade II tumours, normally express somatostatin cell surface receptors (SSTR), with subtype 2 being the most expressed.

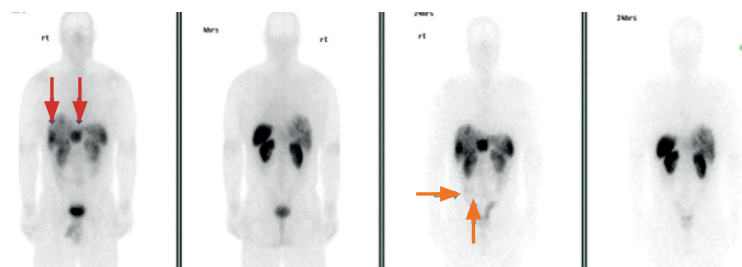


Figure 3a – Patient with GEP-NET (Grade II small bowel). Octreoscan® 4 hours (planar) and 24 hours (planar with SPECT/CT) images (a-planar), (b- axial fused) and (c,d -coronal fused) demonstrating multiple liver metastases (red arrows) with increased uptake of tracer. Small bowel primary (horizontal yellow arrows) and mesenteric node (vertical orange arrows) with lower uptake of tracer. No further sites of abnormal uptake detected. Courtesy of the Department of Nuclear Medicine, The Christie NHS Foundation Trust, Manchester.

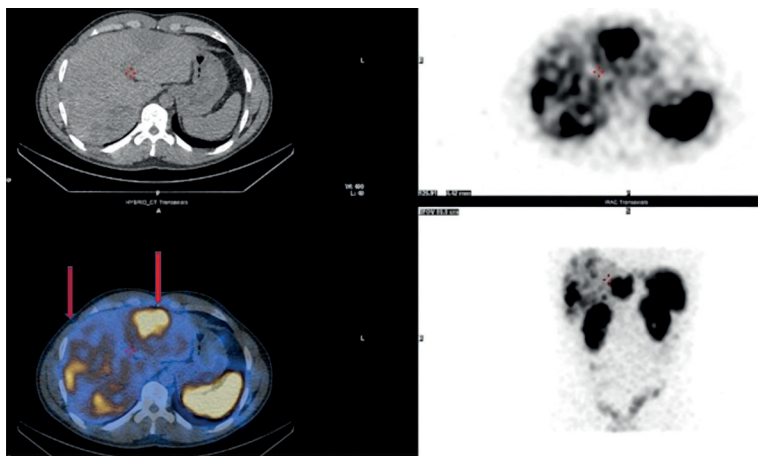


Figure 3b

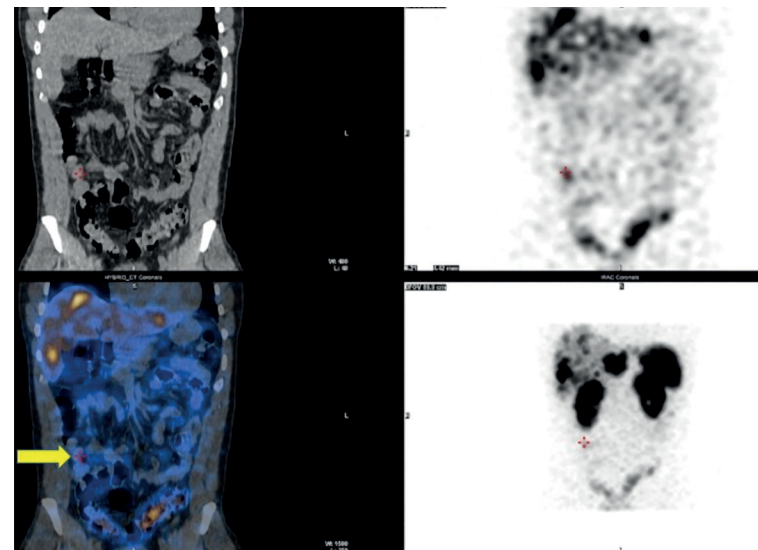


Figure 3c

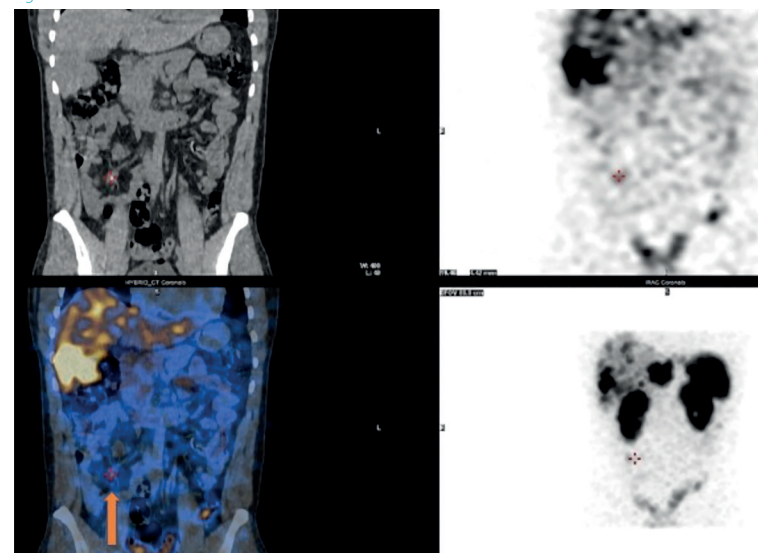


Figure 3d

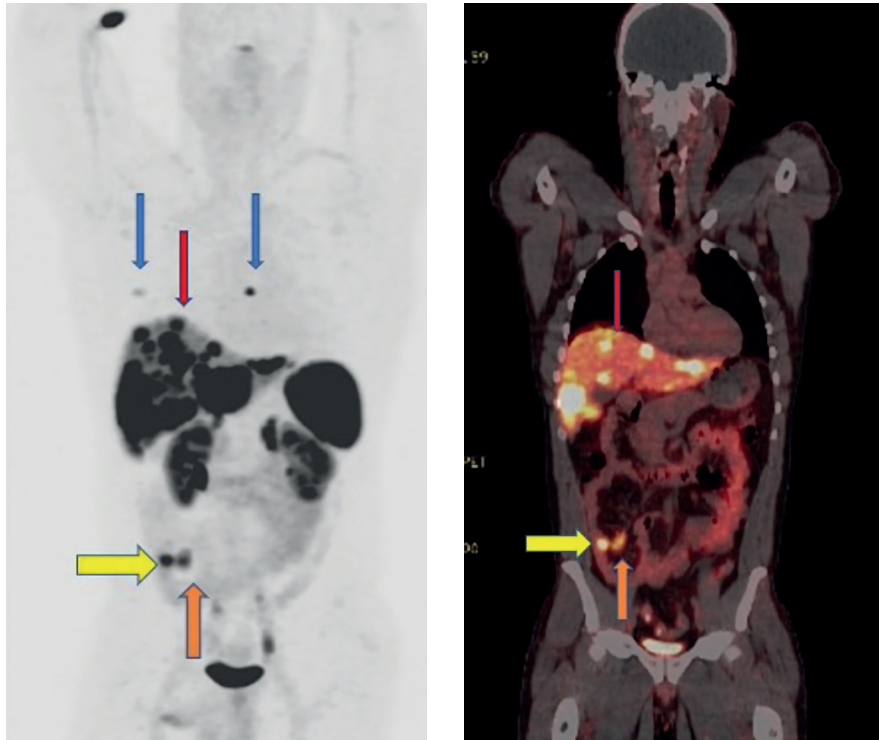


Figure 4a, 4b – Same patient re-staged with $[^{68}\text{Ga}]\text{Ga-DOTA-TOC}$ PET/CT. 90 minutes PET/CT (a- MIP; b-fused coronal, c- fused axial and d- fused sagittal) with areas of increased uptake of tracer $[^{68}\text{Ga}]\text{Ga-DOTA-TOC}$ with higher number of liver metastases (red arrows) identifying primary small bowel tumour (horizontal yellow arrow) with mesenteric node (vertical orange) and bone metastases (vertical blue arrow) that were not detected on the Octreoscan® SPECT/CT, figure 3. Courtesy of the Department of Nuclear Medicine, The Christie NHS Foundation Trust, Manchester.

In the management of NENs, $[^{68}\text{Ga}]\text{Ga-DOTA-SSTR}$ peptide PET/CT imaging is indicated for localisation of primary tumours, detection of metastatic sites and assessment of residual, recurrent or progressive disease. Additionally, it is used to determine SSTR status for the selection of patients who are likely to benefit from peptide receptor

radionuclide therapy (PRRT) (17,19–22). There are three $[^{68}\text{Ga}]\text{Ga-DOTA-SSTR}$ PET radiopharmaceuticals in clinical use: $[^{68}\text{Ga}]\text{Ga-DOTA}^0\text{-Tyr}^3\text{octreotide}$ ($[^{68}\text{Ga}]\text{Ga-DOTA-TOC}$), $[^{68}\text{Ga}]\text{Ga-DOTA}^0\text{-1Na}^3\text{octreotide}$ ($[^{68}\text{Ga}]\text{Ga-DOTA-NOC}$) and $[^{68}\text{Ga}]\text{Ga-DOTA}^0\text{-Tyr}^3\text{octreotate}$ ($[^{68}\text{Ga}]\text{Ga-DOTA-TATE}$).

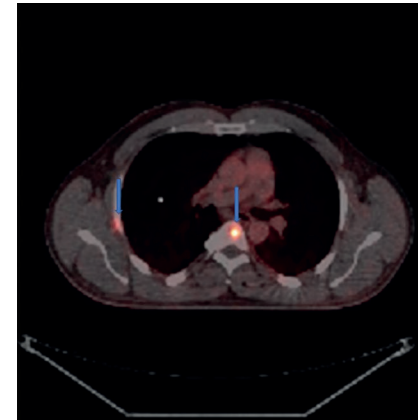


Figure 4c

PET/CT imaging with $[^{68}\text{Ga}]\text{Ga-DOTA-SSTR}$ peptides has shown better diagnostic performance than SSTR scintigraphy (Figures 3 and 4) (23–25), once considered the standard method, with higher sensitivity (90% vs 65%), improved accuracy (88% vs 68%) and similar specificity (80%) (24). Furthermore, in contrast to SSTR scintigraphy, all PET/CT tracer-based imaging is completed on the same day, usually within 180 minutes. This is a major advantage, avoiding an additional journey to the centre that may be detrimental to the patient's well-being and require additional resources in terms of equipment, time and staff. Although $[^{68}\text{Ga}]\text{Ga-DOTA-SSTR}$ PET/CT is considered the 'gold standard' molecular imaging modality, the availability of $[^{68}\text{Ga}]\text{Ga-DOTA-SSTR}$ peptides is limited. Based on the authors' experience, the commercially available germanium-68/



Figure 4d

gallium-68 ($^{68}\text{Ge}/^{68}\text{Ga}$) generators can only be eluted once every 3–4 hours, each elution yielding sufficient ^{68}Ga activity to inject just 1–3 patients (depending on the activity/age of the generator). In addition, there is a high cost associated with $^{68}\text{Ge}/^{68}\text{Ga}$ generators due to the requirement of overlapping purchases throughout the year.

In the context of GEP-NETs, the role of 2- ^{18}F FDG PET/CT is more limited since well-differentiated NETs have a near-normal glucose metabolism. However, the use of 2- ^{18}F FDG PET/CT can be informative in the more histologically aggressive grade III extra-pancreatic GEP-NETs, where higher metabolic turnover and loss of expression of SSTRs occur (17,26). While dual-tracer imaging with 2- ^{18}F FDG and [^{68}Ga]Ga-DOTA-SSTR peptides is a potential strategy for assessing tumour aggressiveness and prognosis, it has an associated cost and limited availability; thus it is best applied in patients with atypical clinical presentation and where there is variable clinical metastatic behaviour.

Patient preparation

As discussed, patients with functioning NENs display distinct clinical symptoms, so they are usually undergoing non-radioactive octreotide therapy with somatostatin analogues (SSAs). These are effective in symptom management and in delaying time-to-tumour progression (27,28). In most centres, patients undergoing [^{68}Ga]Ga-DOTA-SSTR are required to discontinue SSAs

where clinically possible to avoid possible SSTR blockade; this is controversial, however, as there are reported findings of improved tumour-to-background ratios following pre-treatment with SSAs (29,30). A pragmatic approach is therefore recommended, with the patient being booked for a scan just prior to/24 hours before the next long-acting SSAs are administered. If withdrawal of SSAs is required, at the time of scheduling the patient should be instructed to discontinue short-lived molecules for 1 day and long-acting analogues for 3 to 4 weeks. No special dietary preparation or activity restrictions are required.

Information relevant to performance of the scan

A comprehensive explanation of the procedure should be provided to the patient, including the need for an intravenous injection to perform the scan and a 60-minute uptake time for optimal imaging. Additionally, it should be explained that the injection has no pharmacological effect, that the scan is comprised of a CT and a PET component and that it usually lasts 30 minutes, depending on the characteristics of the PET/CT system. The importance of remaining still for the duration of the scan should be stressed.

Prior to radiopharmaceutical administration, the technologist should record the date of last SSA (if applicable), current medication and history of any surgery, recent biopsy and treatment

(chemo-, radiotherapy and/or PRRT). Finally, it is important to ask patients if they are experiencing functional symptoms, as in some cases rescheduling of the scan may be indicated.

Radiopharmaceutical administration and imaging protocol

After obtaining venous access, it is good practice to check the line's integrity with 0.9% sodium chloride solution to reduce the risk of extravasation. Then, [^{68}Ga]Ga-DOTA-SSTR peptide is intravenously injected with an activity normally ranging from 100 to 200 MBq (22). CVCs can be used for radiopharmaceutical administration in patients with poor venous access or needle phobia. The exact time at which the injection was administered should be recorded. Residual activity in the syringe and administration line should be measured in order to accurately determine net administered activity. Following the uptake period, the patient is encouraged to void their bladder immediately prior to scanning to reduce irradiation to the urinary system and background noise. The patient is then positioned on the scanner table with the arms raised over the head. The appropriate acquisition protocol should be selected and patient demographic data, injection time and administered activity should be correctly recorded. Although maximal tumour activity accumulation is reached 70 ± 20 minutes post injection, image acquisition generally begins at 60 minutes

(22,25). Low-dose CT is usually acquired first, followed by the whole-body PET acquisition. Imaging should cover vertex to proximal femur, with PET acquisition being initiated from the pelvis to the head. The acquisition direction may be changed to aid patients with claustrophobia, in order to reduce their anxiety and help them tolerate the scan.

Physiological uptake of [^{68}Ga]Ga-DOTA-SSTR peptides is seen in the pituitary gland, spleen, liver, adrenal glands and urinary system, with thyroid and salivary glands faintly visible. At the end of the scan, the overall quality of the scan should be assessed, in particular for the presence of motion misregistration on PET and CT images. If necessary, additional imaging of a localised area should be acquired.

Image processing

Aligned CT and PET images are automatically produced by the PET/CT system software. The following images should be available for the reporting radiologist or nuclear medicine specialist: AC and NAC PET and CT, as well as MIP and fusion images in axial, coronal and sagittal planes.

Imaging with [^{68}Ga]Ga-FAPI

Fibroblast-activation protein (FAP) is a type II transmembrane protein highly expressed by cancer-associated fibroblasts (CAFs), but minimally expressed by normal fibroblasts in healthy tissue. CAFs are present in the stroma of over 90% of tumours,

suggesting that FAP overexpression is strongly associated with tumour cell invasion, metastatic dissemination, and poor prognosis (31). Similarly to CAFs, FAP expression is upregulated in activated fibroblasts in sites of tissue damage, inflammation and remodelling, as well as in scarring/wound healing (32,33). The differential expression of FAP in normal tissue and tumours makes FAP inhibitor (FAPI)-based radiopharmaceuticals a promising target for cancer imaging and therapy, particularly in GI malignancies (31,34,35). Also, there is growing evidence that high tumour-to-background contrast is achieved with [⁶⁸Ga]Ga-FAPI radiopharmaceuticals, including [⁶⁸Ga]Ga-FAPI-02, [⁶⁸Ga]Ga-FAPI-04 and [⁶⁸Ga]Ga-FAPI-46, and that FAPI PET/CT imaging overcomes limitations associated with FDG PET/CT imaging (31,32,36,37). For example, primary liver tumours that are usually not well visualised with 2-[¹⁸F]FDG, due to their minimal FDG avidity and physiological liver activity, are better demonstrated with [⁶⁸Ga]Ga-FAPI PET/CT imaging (38).

Preliminary findings have recently shown that [⁶⁸Ga]Ga-FAPI PET/CT outperforms 2-[¹⁸F]FDG PET/CT imaging in the diagnosis, clinical staging and target delineation in various GI tumours, including oesophageal, gastric, liver, pancreatic and colorectal cancers (36–43). For instance, [⁶⁸Ga]Ga-FAPI provides more accurate staging than 2-[¹⁸F]FDG in oesophageal cancer by revealing pancreatic metastases and more metastatic

lymph node lesions (40,42). Furthermore, in a pilot study (39) involving patients with primary gastric tumours, the detection rates of [⁶⁸Ga]Ga-FAPI PET/CT and 2-[¹⁸F]FDG PET/CT were 100% and 50%, respectively.

Patient preparation

Adequate pre-hydration is encouraged, but no other special preparation has been reported in the literature to date (32,33,36).

Information relevant to performance of the scan

A thorough explanation of the procedure should be provided to the patient, including the need for an intravenous injection to perform the scan and the uptake time for optimal imaging. Additionally, it should be explained that no side effects are expected and that the scan comprises a CT and a PET component. The importance of remaining still for the duration of the scan should be emphasised.

Prior to radiopharmaceutical administration, and due to FAP overexpression in benign conditions, the technologist should obtain a complete medical history, including recent surgeries, injuries and comorbidities (e.g. cardiovascular disease, chronic inflammatory and destructive processes such as Crohn's disease and rheumatoid arthritis). Although there is evidence of increased [⁶⁸Ga]Ga-FAPI uptake following chemotherapy (44), the appropriate time interval between therapy and scan has not been determined.

Radiopharmaceutical administration and imaging protocol

Currently, no [⁶⁸Ga]Ga-FAPI activity or imaging protocol has been widely established. However, several studies report optimal imaging with an administered activity of 1.8 – 2.2 MBq/kg, usually 60 minutes post-injection (34,37,39,41,45). Early imaging 10 minutes post-injection may also be possible. This allows reduced waiting and scan times, making it particularly beneficial to unwell patients (37). The exact time at which the injection was administered should be recorded and the residual activity in the syringe or administration line should be measured in order to correctly determine net administered activity. During uptake the patient should be encouraged to drink water to stimulate [⁶⁸Ga]Ga-FAPI excretion from the renal calyces and voiding before the scan (45). Sodium chloride (500ml) with 20mg of furosemide may be given as an infusion from 15 minutes before to 30 minutes after [⁶⁸Ga]Ga-FAPI administration. Whole-body image acquisition includes vertex to proximal femur with the patient positioned with the arms raised over the head (36). The appropriate acquisition protocol should be selected and patient data, injection time and administered activity should be correctly recorded. Low-dose CT is usually acquired first, followed by PET acquisition from the pelvis to the head. The acquisition direction can be changed if necessary to enable patients with severe claustrophobia to tolerate the scan.

[⁶⁸Ga]Ga-FAPI is excreted via the urinary and hepatobiliary systems, with the kidneys being the main excretory organs. Moderate physiological uptake is visible within the submandibular gland, thyroid and pancreas, whereas only minimal uptake is seen in the brain, parotid, oral mucosa, lung, myocardium, liver, intestine, fat, spine, and muscle (37,46). At the end of the scan, the technologist should assess the overall quality of the scan to ensure the absence of motion artefacts between the PET and CT images. If necessary, additional imaging of a localised area should be acquired.

Image processing

CT and [⁶⁸Ga]Ga-FAPI PET images are automatically aligned and generated by the system. Appropriate software is used to generate fusion images in axial, coronal and sagittal planes, as well as MIP images. Both AC and NAC [⁶⁸Ga]Ga-FAPI PET images as well as CT images should be available for the reporting radiologist or nuclear medicine specialist.

SPECT/CT IMAGING OF GASTROINTESTINAL CANCERS

SPECT/CT imaging systems combine functional and metabolic information from SPECT with the high spatial resolution and anatomical localisation provided by CT. SPECT relies on physical collimation to direct the gamma-ray photons that result from the decay of gamma-emitting radionuclides towards the large

scintillation crystal on the detector. A series of planar images are acquired at different angles around the patient, followed by CT acquisition. As a result, the radiopharmaceutical distribution within the patient is displayed in 3D.

SPECT/CT imaging plays an important role in the detection of GEP-NET, showing higher sensitivity, specificity and accuracy than traditional stand-alone SPECT (47). However, when compared to [⁶⁸Ga]Ga-DOTA-SSTR PET/CT, SSTR-based SPECT/CT imaging has several limitations, namely poorer image quality, significant physiological uptake in the abdomen that may lead to false-positive interpretation of small abdominal lesions, prolonged acquisition time, and the relatively high radiation dose to patients. Notwithstanding, GEP-NET imaging with SPECT/CT remains the most prevalent molecular imaging modality worldwide due to the limited availability and high cost of [⁶⁸Ga]Ga-DOTA-SSTR PET/CT imaging (24,48–50).

This section focuses on SSTR-based imaging tracers that are routinely used for SPECT/CT imaging of GEP-NET (Table 2), including [¹¹¹In]In-DTPA-pentetreotide (Octreoscan®) and ^{99m}Tc-EDDA/HYNIC-TOC (Tektrotyd). GEP-NET imaging with [¹²³I]I-meta-iodobenzylguanidine ([¹²³I]I-mIBG) has lower sensitivity and specificity, and is therefore not recommended for routine use (51). For this reason, it is not included in this chapter.

Imaging with [¹¹¹In]In-DTPA-pentetreotide (Octreoscan®)

Imaging with [¹¹¹In]In-DTPA-pentetreotide, commercially known as Octreoscan®, is a well-established diagnostic tool for the management of NENs containing SSTR, predominantly subtypes 2 and 5. [¹¹¹In]In-DTPA-pentetreotide SPECT/CT imaging is indicated for localisation of primary tumours, detection of metastatic disease and monitoring of therapy response. In addition, it is also recommended to assess for residual disease, recurrence or progression in patients with known disease and to determine patient eligibility for PRRT. The diagnostic sensitivity is generally high (>67%) for most grade I and II pancreatic GEP-NETs; however, the sensitivity for insulinoma is significantly reduced (25–60%) due to poorer expression of SSTR (48,52).

Patient preparation

Patients undergoing imaging with [¹¹¹In]In-DTPA-pentetreotide are required to follow the same preparation procedure as for [⁶⁸Ga]Ga-DOTA-SSTR (please refer to the relevant section above). In addition, when abdominal lesions are suspected patients are required to start a mild oral laxative the evening before and to continue for the duration of the study to reduce physiological uptake in the intestine. Bowel preparation is not required in patients with insulinoma or active diarrhoea.

Imaging of gastrointestinal cancer with SPECT/CT.

Radiopharmaceutical	Patient Preparation	Recommended Activity	Imaging Protocol
[¹¹¹ In]In-DTPA-pentetreotide (Octreoscan®)	Adequate pre-hydration. Withdrawal of SSAs for 1 day for short-lived analogues and 3–4 weeks for long-acting analogues. Bowel preparation with a mild oral laxative the evening before, continuing for the duration of the study.	200 MBq (53).	Early imaging at 4 hours, whole-body planar of both anterior and posterior of head, neck, thorax, abdomen and pelvis. Patient in supine position with arms alongside the body. Delayed imaging at 24 hours, whole-body planar and SPECT/CT of the abdomen and thorax. Patient in supine position with arms raised over the head. Delayed images may be acquired at 48, 72 and/or 96 hours post-injection
^{99m} Tc-EDDA/HYNIC-TOC (Tektrotyd)		170 to 740 MBq (59).	Early imaging at 1 to 2 hours, whole-body planar of both anterior and posterior of head, neck, thorax, abdomen and pelvis. Patient in supine position with arms alongside the body. Delayed imaging at 4 hours, whole-body planar and SPECT/CT of the abdomen and thorax. Patient in supine position with arms raised over the head.

Table 2 – Imaging of gastrointestinal cancer with SPECT/CT.

Patients are encouraged to stay well hydrated before and after radiopharmaceutical administration to minimise radiation exposure to the urinary tract and reduce background noise.

Information relevant to performance of the scan

A comprehensive explanation of the procedure should be provided to the patient, including the need for an intravenous injection and multiple scans (typically whole-body planar images and SPECT/CT at 4 and 24 hours or 24 and 48 hours post-administration). Delayed images may be acquired at 72 and/or 96 hours post-injection to allow clearance of interfering bowel uptake (52,53). The patient's booking should take account of these possible variations in the day's schedule. It should be explained that the scan comprises a SPECT acquisition, whereby two detector heads will rotate around the patient's body, followed by a CT acquisition. The importance of remaining still during the scan should be stressed. The total duration of the scan varies according to the protocol used (SPECT/CT with or without whole-body planar images).

Prior to radiopharmaceutical administration, the technologist should record the date of last SSA (if applicable), whether bowel preparation was carried out, current medication and history of any surgery, recent biopsy and treatment (chemo-, radiotherapy and/or PRRT). Finally, it is important to ask patients if they are experiencing functional symptoms, as in some cases rescheduling of the scan may be indicated.

Patients with insulinoma or insulin-dependent diabetes mellitus may

experience a hypoglycaemic episode due to a temporary inhibition of glucagon secretion following [¹¹¹In]In-DTPA-pentetreotide. The administration of an intravenous solution containing glucose immediately before and during radiopharmaceutical administration may therefore be advised (52,53).

Radiopharmaceutical administration and imaging protocol

After obtaining venous access, it is good practice to check the line's integrity with 0.9% sodium chloride solution to reduce the risk of extravasation. Then, [¹¹¹In]In-DTPA-pentetreotide is intravenously administered with a recommended activity of 200 MBq (53). A copper filter should be used for the measurement of indium-111 to minimise variations in measurement as a function of geometry (54). The exact time at which the injection was administered should be recorded. Residual activity in the syringe should be measured in order to accurately determine net administered activity.

Image acquisition requires a gamma camera fitted with a medium-energy, parallel-hole collimator, with window setting over both indium-111 peaks at 172 and 245 keV. Whole-body planar imaging and SPECT/CT should be performed at 24 hours post-injection, as the best target-to-background ratio is achieved at that point. By contrast, the target-to-background ratio is low at 4 hours, so imaging at that point is optional. However, since bowel

uptake is absent at 4 hours but visible on 24-hour imaging, comparison between early and delayed imaging may be useful to differentiate physiological bowel uptake from pathological lesions.

At centres where imaging is performed at 4 hours, acquisition at this point is of whole-body planar images only. This is then repeated at 24 hours, followed by SPECT/CT of the pelvis and abdomen (e.g. with 45 seconds per projection and 120 projections in total) as per Figure 3. For whole-body planar imaging, the patient is positioned supine on the scanner table with the arms alongside the body. Planar images are acquired of both anterior and posterior of head, neck, thorax, abdomen and pelvis, each image with a duration of 15 minutes. For SPECT/CT imaging, the patient is positioned supine on the scanner table with the arms raised over the head. The SPECT study is usually acquired first, followed by low-dose CT acquisition in which the field of view should be limited to the area of interest. Imaging of the pelvis (planar or SPECT/CT) should be performed first and immediately after bladder voiding. Head SPECT/CT may need to be performed when abnormal uptake is suspected or identified on the static image. In this case, the patient is positioned with the arms alongside the body.

Physiological uptake of [¹¹¹In]In-DTPA-pentetreotide is seen in the pituitary and thyroid glands, spleen, liver and renal parenchyma. Adrenal glands may be

faintly seen. Visualisation of gallbladder, bowel, renal collecting systems, ureters and bladder are associated with hepatobiliary and renal excretion (52,53). At the end of the scan, the overall quality of the scan should be assessed, in particular for the presence of motion misregistration on SPECT and CT images. If necessary, additional imaging of a localised area should be acquired.

Image processing

Imaging processing varies according to the gamma-camera system and software used. Whole-body planar images should be adjusted for appropriate interpretation and according to local procedures. Modern SPECT/CT systems have integrated software that automatically produces registered and aligned SPECT images, CT images, MIP and fusion images (axial, coronal and sagittal planes). Both AC and NAC [¹¹¹In]In-DTPA-pentetreotide SPECT images and CT images should be available for the reporting radiologist or nuclear medicine specialist.

Imaging with ^{99m}Tc-EDDA/HYNIC-TOC (Tektrotyd)

^{99m}Tc-EDDA/HYNIC-TOC, commercially known as Tektrotyd, has been utilised as an alternative to indium-111 in the diagnosis, staging and follow-up of patients with GEP-NETs. When compared to [¹¹¹In]In-DTPA-pentetreotide, SPECT/CT imaging with ^{99m}Tc-EDDA/HYNIC-TOC has several advantages, namely lower physiological liver and bowel uptake, improved image resolution,

reduced costs and ready availability from departmental molybdenum-99/technetium-99m generators (49,55,56). Moreover, given the shorter half-life of Tc-99m (approximately 6 hours vs 2.8 days for In-111), single-day imaging with ^{99m}Tc -EDDA/HYNIC-TOC SPECT/CT is possible with a lower radiation burden (57,58).

Patient preparation

Patients undergoing imaging with ^{99m}Tc -EDDA/HYNIC-TOC are required to follow the same preparation procedure as for [^{68}Ga]Ga-DOTA-SSTR (please refer to the relevant section above). Good hydration, a liquid diet and bowel preparation with a mild oral laxative are recommended before the scan. Bowel preparation is not required in patients with insulinoma or active diarrhoea (56,59).

Information relevant to performance of the scan

A clear explanation of the procedure should be provided to the patient, including the need for an intravenous injection and scans at different time points (typically early imaging at 1 to 2 hours and 4 hours post-injection with whole-body planar images and SPECT/CT). It should be explained that the scan comprises a SPECT acquisition, whereby two detector heads will rotate around the patient's body, followed by a CT acquisition. The importance of remaining still during the scan should be stressed.

Prior to radiopharmaceutical administration, the technologist should

record the date of last SSA (if applicable), whether bowel preparation was carried out, current medication and history of any surgery, recent biopsy and treatment (chemo-, radiotherapy and/or PRRT). Finally, it is important to ask patients if they are experiencing functional symptoms, as in some cases rescheduling of the scan may be indicated.

Radiopharmaceutical administration and imaging protocol

After gaining venous access, the line's integrity should be checked with 0.9% sodium chloride solution to reduce the risk of radiopharmaceutical extravasation. Then, ^{99m}Tc -EDDA/HYNIC-TOC is administered with a recommended activity ranging from 170 to 740 MBq (59). The exact time at which the injection was administered should be recorded. Residual activity in the syringe should be measured in order to accurately determine net administered activity. As with [^{111}In]In-DTPA-pentetreotide, caution should be applied in patients with insulinoma or insulin-dependent diabetes mellitus following ^{99m}Tc -EDDA/HYNIC-TOC injection (59).

Image acquisition requires a gamma camera equipped with a low-energy, high-resolution collimator. Standard imaging protocols for ^{99m}Tc -EDDA/HYNIC-TOC consist of one-day acquisition 1 to 2 hours post-injection with whole-body planar imaging, followed by 4-hour imaging with whole-body planar imaging supplemented

by SPECT/CT of the abdomen and thorax (56,60). Performing double acquisition reduces the risk of false findings in the abdomen as a result of physiological uptake. For whole-body planar imaging (both anterior and posterior of head, neck, thorax, abdomen and pelvis), the patient is positioned supine on the scanner table with the arms alongside the body. For SPECT/CT imaging, the patient is positioned supine on the scanner table with the arms raised over the head. The SPECT study is usually acquired first, followed by low-dose CT acquisition in which the field of view should be limited to the area of interest. Imaging of the pelvis (planar or SPECT/CT) should be performed first and immediately after bladder voiding. Head SPECT/CT may need to be performed when abnormal uptake is suspected on the static image. In this case, the patient is positioned with the arms alongside the body.

Physiological uptake of ^{99m}Tc -EDDA/HYNIC-TOC occurs in the spleen, liver and kidneys. Pituitary, salivary and thyroid glands may be faintly seen. ^{99m}Tc -EDDA/HYNIC-TOC is excreted mainly via the urinary system with a small amount of hepatic excretion. At the end of the scan, the overall quality of the scan should be assessed, in particular for the presence of motion misregistration on SPECT and CT images. If necessary, additional imaging of a localised area should be acquired.

Image processing

Imaging processing varies according to gamma-camera system and software used. Whole-body planar images should be adjusted for appropriate interpretation and according to local procedures. Modern SPECT/CT systems have integrated software that automatically produces registered and aligned SPECT images, CT images, MIP and fusion images (axial, coronal and sagittal planes). Both AC and NAC ^{99m}Tc -EDDA/HYNIC-TOC SPECT images and CT images should be available for the reporting radiologist or nuclear medicine specialist.

REFERENCES

- Arnold M, Abnet CC, Neale RE, Vignat J, Giovannucci EL, McGlynn KA, et al. Global Burden of 5 Major Types of Gastrointestinal Cancer. *Gastroenterology* [Internet]. 2020 [cited 2023 Jan 2];159:335-349. e15. Available from: <https://doi.org/10.1053/j.gastro.2020.02.068>
- Dizdar Ö, Kılıçkap S. Global Epidemiology of Gastrointestinal Cancers. *Textbook of Gastrointestinal Oncology* [Internet]. 2019 [cited 2023 Jan 2];1-12. Available from: https://link.springer.com/chapter/10.1007/978-3-030-18890-0_1
- Boellaard R, Delgado-Bolton R, Oyen WJG, Giammarile F, Tatsch K, Eschner W, et al. FDG PET/CT: EANM procedure guidelines for tumour imaging: version 2.0. *Eur J Nucl Med Mol Imaging*. 2015;42:328-54.
- Notes for guidance on the clinical administration of radiopharmaceuticals and use of sealed radioactive sources. [Internet]. Administration of Radioactive Substances Advisory Committee. 2022 [cited 2023 Jan 6]. Available from: www.gov.uk/arsac
- The Ionising Radiation (Medical Exposure) Regulations 2017 [Internet]. Department of Health and Social Care. 2017 [cited 2023 Jan 8]. Available from: <https://www.legislation.gov.uk/uksi/2017/1322/made/data.pdf>
- Delbeke D, Coleman RE, Guiberteau MJ, Brown ML, Royal HD, Siegel BA, et al. Procedure Guideline for Tumor Imaging with 18F-FDG PET/CT 1.0. *Journal of Nuclear Medicine*. 2006;47(5):885-95.
- Coleman RE. Single Photon Emission Computed Tomography and Positron Emission Tomography in Cancer Imaging. 1990.
- Herrero Álvarez N, Bauer D, Hernández-Gil J, Lewis JS. Recent Advances in Radiometals for Combined Imaging and Therapy in Cancer. Vol. 16, *ChemMedChem*. John Wiley and Sons Ltd; 2021. p. 2909-41.
- Kluetz PG, Meltzer CC, Villemagne VL, Kinahan PE, Chander S, Martinelli MA, et al. Combined PET/CT Imaging in Oncology: Impact on Patient Management. *Clinical Positron Imaging*. 2000 Nov 1;3(6):223-30.
- Boellaard R. Standards for PET Image Acquisition and Quantitative Data Analysis. *J Nucl Med*. 2009;50:11-20.
- Kitajima K, Murakami K, Yamasaki E, Kaji Y, Shimoda M, Kubota K, et al. Performance of integrated FDG-PET/contrast-enhanced CT in the diagnosis of recurrent pancreatic cancer: comparison with integrated FDG-PET/non-contrast-enhanced CT and enhanced CT. *Mol Imaging Biol* [Internet]. 2010 Aug [cited 2023 Jan 8];12(4):452-9. Available from: <https://pubmed.ncbi.nlm.nih.gov/19949988/>
- Maffione AM, Lopci E, Bluemel C, Giammarile F, Herrmann K, Rubello D. Diagnostic accuracy and impact on management of (18)F-FDG PET and PET/CT in colorectal liver metastasis: a meta-analysis and systematic review. *Eur J Nucl Med Mol Imaging* [Internet]. 2015 Nov 26 [cited 2023 Jan 8];42(11):152-63. Available from: <https://pubmed.ncbi.nlm.nih.gov/25319712/>
- Salaün PY, Abgral R, Malard O, Querellou-Lefranc S, Quere G, Wartski M, et al. Good clinical practice recommendations for the use of PET/CT in oncology. *Eur J Nucl Med Mol Imaging*. 2020 Jan 1;47(1):28-50.
- Menon N, Mandelkern · Mark. Utility of PET Scans in the Diagnosis and Management of Gastrointestinal Tumors. *Dig Dis Sci* [Internet]. 2022 [cited 2023 Jan 8];67:4633-53. Available from: <https://doi.org/10.1007/s10620-022-07616-3>
- Shankar LK, Hoffman JM, Bacharach S, Graham MM, Karp J, Lammertsma AA, et al. Consensus Recommendations for the Use of 18 F-FDG PET as an Indicator of Therapeutic Response in Patients in National Cancer Institute Trials. *Journal of Nuclear Medicine*. 2006 Jul;47(6):1059-66.
- Vangu MDT, Momodu JI. F-18 FDG PET/CT Imaging in Normal Variants, Pitfalls and Artifacts in the Abdomen and Pelvis. *Frontiers in Nuclear Medicine*. 2022 Jan 17;1:11.
- Ilett EE, Langer SW, Olsen IH, Federspiel B, Kjær A, Knigge U. Neuroendocrine Carcinomas of the Gastroenteropancreatic System: A Comprehensive Review. *Diagnostics (Basel)* [Internet]. 2015 [cited 2023 Jan 14];5(2):119-76. Available from: <https://pubmed.ncbi.nlm.nih.gov/26854147/>
- Yao JC, Hassan M, Phan A, Dagohoy C, Leary C, Mares JE, et al. One hundred years after 'carcinoid': epidemiology of and prognostic factors for neuroendocrine tumors in 35,825 cases in the United States. *J Clin Oncol* [Internet]. 2008 [cited 2023 Jan 14];26(18):3063-72. Available from: <https://pubmed.ncbi.nlm.nih.gov/18565894/>
- Prasad V, Ambrosini V, Hommann M, Hoersch D, Fanti S, Baum RP. Detection of unknown primary neuroendocrine tumours (CUP-NET) using (68) Ga-DOTA-NOC receptor PET/CT. *Eur J Nucl Med Mol Imaging* [Internet]. 2010 Jan [cited 2023 Jan 15];37(1):67-77. Available from: <https://pubmed.ncbi.nlm.nih.gov/19618183/>
- Fani Bozkurt M, Virgolini I, Balogova S, Beheshti M, Rubello D, Decristoforo C, et al. Guideline for PET/CT imaging of neuroendocrine neoplasms with 68 Ga-DOTA-conjugated somatostatin receptor targeting peptides and 18 F-DOPA Background information and definitions.
- Gabriel M, Oberauer A, Dobrozemsky G, Decristoforo C, Putzer D, Kendler D, et al. 68 Ga-DOTA-Tyr 3-Octreotide PET for Assessing Response to Somatostatin-Receptor-Mediated Radionuclide Therapy. *J Nucl Med* [Internet]. 2009 [cited 2023 Jan 15];50:1427-34. Available from: <http://jnm.snmjournals.org>
- Virgolini I, Ambrosini V, Bomanji JB, Baum RP, Fanti S, Gabriel M, et al. Procedure guidelines for PET/CT tumour imaging with 68Ga-DOTA-conjugated peptides: 68Ga-DOTA-TOC, 68Ga-DOTA-NOC, 68Ga-DOTA-TATE. *Eur J Nucl Med Mol Imaging* [Internet]. 2010 Oct 2 [cited 2023 Jan 15];37(10):2004-10. Available from: <http://link.springer.com/10.1007/s00259-010-1512-3>
- Deppen SA, Liu E, Blume JD, Clanton J, Shi C, Jones-Jackson LB, et al. Safety and Efficacy of 68Ga-DOTATATE PET/CT for Diagnosis, Staging, and Treatment Management of Neuroendocrine Tumors. *J Nucl Med* [Internet]. 2016 May 1 [cited 2023 Jan 15];57(5):708-14. Available from: <https://pubmed.ncbi.nlm.nih.gov/26769865/>
- Fallahi B, Manafi-Farid R, Eftekhari M, Fard-Esfahani A, Emami-Ardekani A, Geramifard P, et al. Diagnostic Efficiency of 68Ga-DOTATATE PET/CT as Compared to 99mTc-Octreotide SPECT/CT and Conventional Morphologic Modalities in Neuroendocrine Tumors. *Asia Ocean J Nucl Med Biol* [Internet]. 2019 [cited 2023 Jan 14];7(2):129. Available from: <https://pubmed.ncbi.nlm.nih.gov/11734911/>
- Hofmann M, Maecke H, Börner AR, Weckesser E, Schöffski P, Oei ML, et al. Biokinetics and imaging with the somatostatin receptor PET radioligand (68)Ga-DOTATOC: preliminary data. *Eur J Nucl Med* [Internet]. 2001 [cited 2023 Jan 15];28(12):1751-7. Available from: <https://pubmed.ncbi.nlm.nih.gov/11734911/>
- Kayani I, Bomanji JB, Groves A, Conway G, Gacinovic S, Win T, et al. Functional imaging of neuroendocrine tumors with combined PET/CT using 68Ga-DOTATATE (DOTA-DPhe1,Tyr3-octreotate) and 18F-FDG. *Cancer* [Internet]. 2008 Jun 1 [cited 2023 Jan 15];112(11):2447-55. Available from: <https://pubmed.ncbi.nlm.nih.gov/18383518/>
- Caplin ME, Pavel M, Ćwikła JB, Phan AT, Raderer M, Sedláčková E, et al. Anti-tumour effects of lanreotide for pancreatic and intestinal neuroendocrine tumours: the CLARINET open-label extension study. *Endocr Relat Cancer* [Internet]. 2016 Mar [cited 2023 Jan 15];23(3):191-9. Available from: <https://erc.bioscientifica.com/view/journals/erc/23/3/191.xml>
- Rinke A, Wittenberg M, Schade-Brittinger C, Aminossadati B, Ronicke E, Gress TM, et al. Placebo-Controlled, Double-Blind, Prospective, Randomized Study on the Effect of Octreotide LAR in the Control of Tumor Growth in Patients with Metastatic Neuroendocrine Midgut Tumors (PROMID): Results of Long-Term Survival. *Neuroendocrinology* [Internet]. 2017 [cited 2023 Jan 15];104(1):26-32. Available from: <https://www.karger.com/Article/FullText/443612>
- Haug AR, Rominger A, Mustafa M, Auernhammer C, Goke B, Schmidt GP, et al. Treatment with octreotide does not reduce tumor uptake of (68)Ga-DOTATATE as measured by PET/CT in patients with neuroendocrine tumors. *J Nucl Med* [Internet]. 2011 Nov 1 [cited 2023 Jan 15];52(11):1679-83. Available from: <https://pubmed.ncbi.nlm.nih.gov/21976529/>

30. Yilmaz F, Öner H, Kara Gedik G, Şahin Ö, Çelik AV, Erol Ç. Does Treatment with Somatostatin Analogs Affect the Radioactive Uptake of Normal Target Organs and Malignant Lesions on 68Ga-DOTATATE PET/CT imaging? *Genel Tıp Dergisi* [Internet]. 2022 Aug 22 [cited 2023 Jan 15]; Available from: <https://dergipark.org.tr/en/doi/10.54005/geneltip.1157941>
31. Peng D, He J, Liu H, Cao J, Wang Y, Chen Y. FAPI PET/CT research progress in digestive system tumours. *Vol. 54, Digestive and Liver Disease*. Elsevier B.V.; 2022. p. 164–9.
32. Kessler L, Ferdinandus J, Hirmas N, Zarrad F, Nader M, Kersting D, et al. Pitfalls and Common Findings in 68Ga-FAPI PET: A Pictorial Analysis. *Journal of Nuclear Medicine* [Internet]. 2022 Jun [cited 2023 Jan 8];63(6):890–6. Available from: <http://jnm.snmjournals.org/lookup/doi/10.2967/jnumed.121.262808>
33. Mori Y, Dendl K, Cardinale J, Kratochwil C, Giesel FL, Haberkorn U. FAPI PET: Fibroblast Activation Protein Inhibitor Use in Oncologic and Nononcologic Disease. *Radiology* [Internet]. 2023 Jan 3 [cited 2023 Jan 18];220749. Available from: <http://www.ncbi.nlm.nih.gov/pubmed/36594838>
34. Koerber SA, Staudinger F, Kratochwil C, Adeberg S, Haefner MF, Ungerechts G, et al. The role of 68ga-fapi pet/ct for patients with malignancies of the lower gastrointestinal tract: First clinical experience. *Journal of Nuclear Medicine*. 2020 Sep 1;61(9):1331–6.
35. Assadi M, Rekabpour SJ, Jafari E, Divband GA, Nikkholgh B, Amini H, et al. Feasibility and Therapeutic Potential of 177Lu-Fibroblast Activation Protein Inhibitor-46 for Patients With Relapsed or Refractory Cancers: A Preliminary Study. *Clin Nucl Med*. 2021 Nov 1;46(11):e523–30.
36. Kratochwil C, Flechsig P, Lindner T, Abderrahim L, Altmann A, Mier W, et al. 68Ga-FAPI PET/CT: Tracer Uptake in 28 Different Kinds of Cancer. *Journal of Nuclear Medicine* [Internet]. 2019 Jun;60(6):801–5. Available from: <http://jnm.snmjournals.org/lookup/doi/10.2967/jnumed.119.227967>
37. Giesel FL, Kratochwil C, Lindner T, Marschalek MM, Loktev A, Lehnert W, et al. 68 Ga-FAPI PET/CT: Biodistribution and preliminary dosimetry estimate of 2 DOTA-containing FAP-targeting agents in patients with various cancers. *Journal of Nuclear Medicine*. 2019;60(3).
38. Shi X, Xing H, Yang X, Li F, Yao S, Congwei J, et al. Comparison of PET imaging of activated fibroblasts and 18F-FDG for diagnosis of primary hepatic tumours: a prospective pilot study. *Eur J Nucl Med Mol Imaging* [Internet]. 2021 May 1 [cited 2023 Jan 16];48(5):1593–603. Available from: <https://pubmed.ncbi.nlm.nih.gov/33097975/>
39. Kuten J, Levine C, Shamni O, Pelles S, Wolf I, Lahat G, et al. Head-to-head comparison of [68Ga]Ga-FAPI-04 and [18F]-FDG PET/CT in evaluating the extent of disease in gastric adenocarcinoma. *Eur J Nucl Med Mol Imaging*. 2022 Jan 1;49(2):743–50.
40. Zhao L, Chen S, Lin L, Sun L, Wu H, Lin Q, et al. [68Ga] Ga-DOTA-FAPI-04 improves tumor staging and monitors early response to chemoradiotherapy in a patient with esophageal cancer. *Eur J Nucl Med Mol Imaging* [Internet]. 2020 Dec 24;47(13):3188–9. Available from: <https://link.springer.com/10.1007/s00259-020-04818-7>
41. Pang Y, Zhao L, Luo S, Hao B, Wu H, Lin Q, et al. Comparison of 68Ga-FAPI and 18F-FDG Uptake in Gastric, Duodenal, and Colorectal Cancers. *Radiology*. 2021 Feb 1;298(2):393–402.
42. Liu Q, Shi S, Xu X, Yu X, Song S. The superiority of [68Ga]-FAPI-04 over [18F]-FDG PET/CT in imaging metastatic esophageal squamous cell carcinoma. *Eur J Nucl Med Mol Imaging* [Internet]. 2021 Apr 28;48(4):1248–9. Available from: <https://link.springer.com/10.1007/s00259-020-04997-3>
43. Şahin E, Elboğa U, Çelen YZ, Sever ÖN, Çayırılı YB, Çimen U. Comparison of 68Ga-DOTA-FAPI and 18FDG PET/CT imaging modalities in the detection of liver metastases in patients with gastrointestinal system cancer. *Eur J Radiol*. 2021;142.
44. Af Burén S, Tran TA, Klevebro F, Holstenson M, Axelsson R. A 68Ga-FAPI-46 PET/CT Imaging Pitfall in Assessing Residual Gastric Cancer Early After Chemotherapy. *Clin Nucl Med* [Internet]. 2022 Jul 1 [cited 2023 Jan 18];47(7):644–5. Available from: https://journals.lww.com/nuclearmed/Fulltext/2022/07000/A_68Ga_FAPI_46_PET_CT_Imaging_Pitfall_in_Assessing.15.aspx
45. Chen H, Pang Y, Wu J, Zhao L, Hao B, Wu J, et al. Comparison of [68Ga]Ga-DOTA-FAPI-04 and [18F] FDG PET/CT for the diagnosis of primary and metastatic lesions in patients with various types of cancer. *Eur J Nucl Med Mol Imaging*. 2020 Jul 1;47(8):1820–32.
46. Gilardi L, Farulla LSA, Demirci E, Clerici I, Salè EO, Ceci F. Imaging Cancer-Associated Fibroblasts (CAFs) with FAPI PET. *Vol. 10, Biomedicines*. MDPI; 2022.
47. Perri M, Erba P, Volterrani D, Lazzeri E, Boni G, Grosso M, et al. Octreo-SPECT/CT imaging for accurate detection and localization of suspected neuroendocrine tumors. *The quarterly journal of nuclear medicine and molecular imaging: official publication of the Italian Association of Nuclear Medicine (AIMN) [and] the International Association of Radiopharmacology (IAR), [and] Section of the Society of*. [Internet]. 2008 Dec [cited 2023 Jan 18];52(4):323–33. Available from: <https://pubmed.ncbi.nlm.nih.gov/18480741/>
48. Sanli Y, Garg I, Kandathil A, Kendi T, Zanetti MJB, Kuyumcu S, et al. Neuroendocrine Tumor Diagnosis and Management: ⁶⁸Ga-DOTATATE PET/CT. *American Journal of Roentgenology* [Internet]. 2018 Aug [cited 2023 Jan 15];211(2):267–77. Available from: <https://www.ajronline.org/doi/10.2214/AJR.18.19881>
49. Opalinska M, Hubalewska-Dydejczyk A, Sowa-Staszczak A, Stefanska A. NEN - The role of somatostatin receptor scintigraphy in clinical setting. *Vol. 19, Nuclear Medicine Review*. Via Medica; 2016. p. 118–25.
50. Decristoforo C, Mather SJ, Cholewinski W, Donnemiller E, Riccabona G, Moncayo R. (99m)Tc-EDDA/HYNIC-TOC: A new (99m)Tc-labelled radiopharmaceutical for imaging somatostatin receptor-positive tumours: First clinical results and intra-patient comparison with ¹¹¹In-labelled octreotide derivatives. *Eur J Nucl Med* [Internet]. 2000 Jun 17 [cited 2023 Jan 22];27(9):1318–25. Available from: <https://link.springer.com/article/10.1007/s002590000289>
51. Ramage JK, Ahmed A, Ardill J, Bax N, Breen DJ, Caplin ME, et al. Guidelines for the management of gastroenteropancreatic neuroendocrine (including carcinoid) tumours (NETs). *Gut* [Internet]. 2012 Jan 1 [cited 2023 Jan 21];61(1):6–32. Available from: <https://gut.bmj.com/content/61/1/6>
52. Balon HR, Brown TLY, Goldsmith SJ, Silberstein EB, Krenning EP, Lang O, et al. The SNM Practice Guideline for Somatostatin Receptor Scintigraphy 2.0. *J Nucl Med Technol* [Internet]. 2011 Dec 1 [cited 2023 Jan 18];39(4):317–24. Available from: <http://tech.snmjournals.org/cgi/doi/10.2967/jnmt.111.098277>
53. Bombardieri E, Ambrosini V, Aktolun C, Baum RP, Bishof-Delaloye A, Vecchio S del, et al. In-pentetreotide scintigraphy: procedure guidelines for tumour imaging. *Eur J Nucl Med Mol Imaging*. 2010;37:1441–8.
54. Kowalsky RJ, Johnston RE. Dose Calibrator Assay of Iodine-123 and Indium-111 with a Copper Filter. *J Nucl Med Technol*. 1998;26(2):94–8.
55. Gabriel M, Decristoforo C, Donnemiller E, Ulmer H, Christine ; Rychlinski W, et al. An Inpatient Comparison of 99m Tc-EDDA/ HYNIC-TOC with 111 In-DTPA-Octreotide for Diagnosis of Somatostatin Receptor-Expressing Tumors.
56. Garai I, Barna S, Nagy G, Forgács A. Limitations and pitfalls of 99mTc-EDDA/HYNIC-TOC (Tekrotyd) scintigraphy. *Nuclear Medicine Review* [Internet]. 2016 Jul 29 [cited 2023 Jan 18];19(2):93–8. Available from: https://journals.viamedica.pl/nuclear_medicine_review/article/view/NMR.2016.0019/38026
57. Grimes J, Celler A, Birkenfeld B, Shcherbinin S, Listewnik MH, Piwowarska-Bilska H, et al. Patient-Specific Radiation Dosimetry of 99m Tc-HYNIC-Tyr 3-Octreotide in Neuroendocrine Tumors. *J Nucl Med* [Internet]. 2011 [cited 2023 Jan 22];52:1474–81. Available from: <http://jnm.snmjournals.org>
58. Krenning EP, Kwekkeboom DJ, Bakker WH, Breeman WAP, Kooij PPM, Oei HY, et al. Somatostatin receptor scintigraphy with [¹¹¹In-DTPA-d-Phe1]- and [123I-Tyr3]-octreotide: the Rotterdam experience with more than 1000 patients. *Eur J Nucl Med*. 1993 Aug;20(8):716–31.
59. Tekrotyd, summary of product characteristics.
60. Al-Chalabi H, Cook A, Ellis C, Patel CN, Scarsbrook AF. Feasibility of a streamlined imaging protocol in technetium-99m-Tekrotyd somatostatin receptor SPECT/CT. *Clin Radiol*. 2018 Jun 1;73(6):527–34.

DOI: <https://doi.org/10.52717/IJDW6277>

Publisher:

European Association of Nuclear Medicine
Schmalzhofgasse 26, 1060 Vienna, Austria
Phone: +43 1 890 44 27 | +43 1 890 44 27-9
Email: office@eanm.org | URL: www.eanm.org

Main Editor:

Andrea Santos

Co-Editors:

Luisa Pereira
Paolo Turco

English Language Editing:

Angela Parker

Project Management:

Núria Serra Serra, EANM Executive Office
Sophie Karsai, EANM Executive Office

Layout & Design:

Olga Dogadina, EANM Executive Office
Nikolaus Schmidt, EANM Executive Office

Content:

*No responsibility is taken for the correctness of this information.
Information as per date of printing September 2023.*

FIND MORE EANM TECHNOLOGISTS' GUIDES HERE
<http://www.eanm.org/publications/technologists-guide/>